Involvements of the Plant 3'-5' Exonuclease ERL1 in Chloroplast Ribosomal RNA Biogenesis and RNA Silencing Pathways

Dissertation zur

Erlangung des akademischen Grades eines

Doktors der Naturwissenschaften (Dr. rer. nat.)

im Fachbereich 18 - Naturwissenschaften

der Universität Kassel

vorgelegt von: **Heiko Tobias Schumacher**

Kassel im Mai 2009

Datum der Disputation: 16. Juli 2009

Die Natur
ist aller Meister Meister,
sie zeigt uns erst
den Geist
der Geister

Johann Wolfgang v. Goethe

Erklärung

Hiermit versichere ich, dass ich die vorliegende Dissertation selbständig und ohne unerlaubte Hilfe angefertigt und andere als die in der Dissertation angegebenen Hilfsmittel nicht benutzt habe. Alle Stellen, die wörtlich oder sinngemäß aus veröffentlichten oder unveröffentlichten Schriften entnommen sind, habe ich als solche kenntlich gemacht. Kein Teil dieser Arbeit ist in einem anderen Promotions- oder Habilitationsverfahren verwendet worden.

Kassel, den 03. Mai 2009

_____

Heiko Tobias Schumacher

Zusätzliche Erklärung über kooperative Arbeiten und Publikation

Teile der in dieser Dissertation präsentierten Resultate sind das Ergebnis kooperativer Arbeiten von Heiko Tobias Schumacher (Universität Kassel) und Jutta Maria Helm (Universität für Bodenkultur Wien) am Institut für Molekularbiologie und Biotechnologie in Heraklion, Griechenland.
Die folgenden Arbeiten wurden von Jutta Maria Helm durchgeführt:

- Herstellung transgener *Nicotiana benthamiana*-Pflanzen zur Überexpression bzw. Suppression von *ERL1* (vergl. Abschnitt 2.2.6.).
- Herstellung doppelt-homozygoter Kreuzungen zwischen der *GFP*-exprimierenden *Nicotiana benthamiana*-Linie *GFP* 6.4 mit *ERL1*-überexprimierenden Pflanzen (vergl. Abschnitt 3.3.2.).
- Chlorophyll *a* Fluoreszenz-Messungen zur Charakterisierung grundlegender bioenergetischer Parameter in *ERL1*-überexprimierenden Pflanzen (vergl. Abschnitt 3.4.3.).
- Klonierung kleiner ribosomaler RNAs zur Analyse der 3'-Enden pflanzlicher 5.8S, 5S und 4.5S rRNAs (vergl. Abschnitte 2.2.11. und 3.6.1.).

Der Elektronenmikroskop-Service wurde von Eva Papadogiorgaki geleitet. Alle weiteren Arbeiten wurden von Heiko Tobias Schumacher, teilweise mit Unterstützung von Jutta Maria Helm, durchgeführt.

Die folgend aufgeführten Abbildungen oder Teile derselben könnten in dieser oder veränderter Form auch in der Dissertation „RNA Silencing in Plants" (Arbeitstitel) von Jutta Maria Helm verwendet werden, die voraussichtlich Ende 2009 an der Universität für Bodenkultur Wien eingereicht werden wird: 1.6, 3.1-3.11, 4.1.

Teile dieser Arbeit werden unter dem Titel „The Plant Homologue of Enhanced RNAi 1 (ERI-1) is Involved in Chloroplast Ribosomal RNA Biogenesis" zur Publikation im Fachjournal The Plant Cell vorbereitet. Die Veröffentlichung dieser Publikation wird für Ende 2009 erwartet.

Abstract

Throughout evolution eukaryotes have developed systems of repressive gene regulation by means of small RNA regulators that are collectively referred to as RNA silencing pathways. Since one of the primary functions for small interfering RNA (siRNA)-mediated RNA silencing is the defence against invading pathogens (*i.e.* viruses and viroids) it is not surprising that viruses developed means to counteract their hosts's antiviral RNA silencing pathways during virus-host co-evolution. Viral suppressors of silencing (VSRs) employ diverse strategies to suppress the hosts's RNA silencing responses, with repressive siRNA binding being a common strategy.

Extensive research has been undertaken to indentify endogenous factors that may act analogously to VSRs by negatively modulating RNA silencing pathways in order to prevent overreactions or off-target effects. To date only a single protein has been described that may be annotated as a *bona fide* endogenous suppressor of silencing based on its abilities to bind and degrade siRNAs, thereby having a negative impact on RNA silencing efficiency. *Caenorhabditis elegans* ERI-1 (Enhanced RNAi 1) is a 3'-5' exonuclease with a conserved ERI-1_3'hExo_like EXOIII domain that binds and degrades siRNAs *in vitro* and whose loss of function results in an enhanced RNAi phenotype. ERI-1 is phylogenetically conserved, and ERI-1 homologues have been identified and characterised for RNA silencing-repressing activites in a variety of model organisms across kingdoms. These activities include, but are not limited to, *cis*-restriction of siRNA-mediated heterochromatin formation in the fission yeast *Schizosaccharomyces pombe*, suppression of RNA interference in *C. elegans* moto-neurons, and passenger strand degradation after siRNA incorporation into the *Neurospora crassa* Argonaute protein QDE-2. In addition to their involvements in RNA silencing regulation a number of ERI-1 homologues have been shown to exert conserved functions in the biogenesis of 5.8S ribosomal RNA, *i.e.* catalysing the final step in 5.8S rRNA 3' end maturation. This dual function of ERI-1 homologues constitutes an interesting bridge between two evolutionary very distant non-coding RNA mechanisms.

This work presents data regarding characteristics of the plant ERI-1 homologue ERI-1-LIKE 1 (ERL1) in RNA silencing regulation and ribosomal RNA biogenesis. ERL1 was found to localise to chloroplasts, which are regarded an RNA silencing-free compartment. Correspondingly ERL1 fails to exert *bona fide* RNA silencing suppressor activities in *Nicotiana benthmiana*, exemplified by the inability of ERL1 to influence patterns of

Abstract

GFP silencing, even under conditions of constitutive *ERL1* overexpression. These findings support results from phylogenetic analyses that place ERL1 in evolutionary relation with a subset of ERI-1 homologues whose joint characteristic is the lack of a discernable SAP domain. These Group II ERI-1 homologues could thus far not be shown to facilitate RNA silencing regulation and hence stand in contrast to the SAP domain-containing Group I ERI-1 homologues (*e.g. C. elegans* ERI-1, fission yeast Eri1, *N. crassa* QIP, and mouse Eri1) for which diverse functionalities in the regulation of RNA silencing pathways have been verified.

It was observed that *ERL1*-overexpressing transgenic *N. benthamiana* plants exhibit frequent and severe variegation phenotypes that manifest as distinct formation of pale green, yellow, or even white leaf sectors neighbouring to wildtype-like green sectors. White sector formation in these cases is dependent on high *ERL1* expression levels, and variegated *ERL1* overexpressor plants show defects in growth and fertility as well as characteristic histological and ultrastructural alterations that are reminiscent of reported variegation phenotypes caused in different plant species as results of mutation- or infection-induced arrested plastid differentiation. In a majority of cases white sector formation in variegated mutants has been appointed to defective biogenesis of chloroplastic ribosomal RNAs, which ultimately leads to a general breakdown of plastid transcription and translation, rendering thus affected plastids unable to differentiate. Hence, an involvement of ERL1 in plastid rRNA biogenesis was investigated.

Indeed the steady-state levels of the chloroplastic 5S rRNA were found to be negatively affected upon transient and constitutive *ERL1* misexpression. Correspondingly, 2 nt 3'-elongated 5S rRNA molecules were found to accumulate in *ERL1*-misexpressing samples. 5S rRNA maturation has long been known to be a multistep process employing several endonucleolytic cleavages and exonucleolytic recessions. The full complement of exonucleases responsible for the final step of 5S rRNA 3' end maturation, however, remained undefined as yet. 5S rRNA 3' end maturation is in part facilitated by RIBONUCLEOTIDE REDUCTASE 1 (RNR1) in *Arabidopsis thaliana*. Yet, mature 5S rRNA accumulates even in variegated *rnr1* null mutants, leading to the proposition that RNR1 may act cooperatively and redundantly with a second as yet unidentified exonucleolytic activity.

Based on the results presented in this work, ERL1 may constitute this activity.

Zusammenfassung

Die RNA-Welt und der Ursprung des Lebens

Unser Wissen grundlegender zellulärer Regulationsmechanismen erfuhr in der letzten Dekade eine beispiellose Revolution, die der Entdeckung einer bis dato unvorstellbaren Fülle auf nicht-codierender RNA (ncRNA) basierender Signalwege geschuldet ist. Innerhalb nur weniger Jahre hat sich die RNA-Forschung damit von einer ausgereiften Disziplin traditioneller Molekularbiologie zu einem der innovativsten und sich am schnellsten entwickelnden Forschungsgebiete unserer Zeit gewandelt.

Seit ihrer Entdeckung und molekularen Charakterisierung wurde RNA traditionell als Klasse von Hilfsmolekülen angesehen, deren primäre Aufgaben aus Struktur gebenden (ribosomale RNA; rRNA) und Adapter-Funktionen (Transfer-RNA; tRNA) sowie dem Transfer von Information (messengerRNA; mRNA) bestehen. Im „Zentralen Dogma" der Molekularbiologie, demzufolge Proteine die entscheidenden Endprodukte genetischer Information darstellen, nimmt RNA lediglich eine intermediäre Stellung ein, da ihr sowohl die chemische Stabilität als auch die katalytische Vielseitigkeit und Effizienz fehlen, derenthalben DNA und Proteine ihre fundamentalen Rollen zu Speicherung genetischer Information und zur Ausübung katalytischer Prozesse im Laufe der Evolution angenommen haben. Unter diesen Gesichtspunkten waren RNA-abhängige Mechanismen, die in ihrer Tragweite über simple Hilfsfunktionen hinausgehen, traditionell nicht vorstellbar. Mit der Entdeckung katalytisch aktiver RNA in den frühen 1980er Jahren setzte sich indes die Realisation durch, dass die funktionellen Implikationen von RNA womöglich unterschätzt worden waren. Seitdem wurde erkannt, dass RNA essenzielle Aufgaben in praktisch allen Aspekten zellulärer Regulation ausübt. Die regulatorische sowie evolutionäre Komplexität dieser RNA-Netzwerke rückt RNA darüber hinaus in den Fokus der Forschung über den Ursprung des Lebens.

Eines der grundlegenden Dilemmata der Molekularbiologie im Zusammenhang mit der Entstehung des Lebens besteht in dem Paradoxon, dass in einem auf DNA und Protein basierenden Konzept von Leben Nukleinsäuren für die Produktion von Proteinen notwendig sind, während Proteine ihrerseits als Voraussetzung für die Produktion von Nukleinsäuren gelten. Zentrale Säule dieser Betrachtungsweise ist das Ribosom, das als die fundamentale Entwicklung in der Evolution zellulären Lebens angesehen werden

kann. Das Ribosom stellt eine der stammesgeschichtlich ältesten makromolekularen Maschinen dar und ist integraler Bestandteil aller lebenden Organismen. Erst nachdem sich der auf dem Ribosom basierende Fluss genetischer Information von DNA zu Protein etabliert gehabt hatte, konnten die Urahnen der drei Domänen des Lebens entstehen. Ungeachtet wichtiger Unterschiede in den Translations-Systemen von Archaeen, Bakterien und Eukaryoten, stellen die hochgradige Konservierung des Ribosoms, der universale genetische Code sowie der universale Gebrauch von DNA zur Speicherung genetischer Information weitreichende Indizien für die Existenz eines Letzten Universalen Gemeinsamen Vorfahren (LUGV) dar. Der LUGV selbst muss wiederum als das Produkt einer langen evolutionären Entwicklung angesehen werden, die die Etablierung eines Ribosom-basierten Translations-Systems zur Folge hatte, das effizient und präzise genug war, um die nachfolgende Entwicklung der drei Domänen des Lebens bedingen zu können. Diese Ableitung enthält jedoch eine Zwickmühle. Nach traditioneller Sichtweise konnte das Ribosom erst zu einem Zeitpunkt entstehen, nachdem sich ein funktionales Translations-System bereits entwickelt gehabt hatte. Schließlich wären proteinöse Enzyme notwendig gewesen, um die anspruchsvollen katalytischen Aufgaben durchzuführen, die für die Schaffung einer solch komplexen makromolekularen Maschine wie des Ribosoms erforderlich gewesen wären. Die röntgenkristallografische Aufklärung der Struktur des Ribosoms war ohne Zweifel der Schlüssel zur Lösung dieses Dilemmas, denn im diametralen Gegensatz zu Jahrzehnte lang etablierter Lehrmeinung sind es die ribosomalen Proteine, die an der Peripherie des Ribosoms positioniert sind und Struktur gebende Aufgaben erfüllen. Der katalytische Kern des Ribosoms hingegen besteht ausschließlich aus ribosomaler RNA. Im Jahr 2000 wurde so die Biologie revolutioniert, als unzweifelhaft festgestellt wurde, dass die stammesgeschichtlich älteste und fundamentalste makromolekulare Maschine nicht etwa ein proteinöses Enzym ist, sondern ein Ribozym.

Diese Realisation birgt weit reichende Konsequenzen in sich. Die Ribozym-Natur des Ribosoms impliziert die Möglichkeit früher Formen von Leben basierend auf RNA, die in der Lage waren zu replizieren, primitive Stoffwechsel aufrecht zu erhalten und sich in Darwinischer Evolution den Selektionsdrücken auf der frühen Erde anzupassen. Der Höhepunkt dieser „RNA-Welt“ existierte vor etwa 3,8 Milliarden Jahren, in deren Zenit die Entwicklung eines Proto-Ribosoms stand, das vollständig aus RNA bestand; eine

Entwicklung, die im Auftreten des LUGV kulminierte. 3,6 Milliarden Jahre später haben wir erkannt, dass die RNA-Welt von einst nicht etwa im Zuge der Entwicklung von DNA und Proteinen verschwand, sondern im Gegenteil eine weit reichende Evolution durchmachte, so dass die heutigen DNA/Protein-basierten Organismen von Grund auf von hochkomplexen Netzwerken regulatorischer RNA-Systeme kontrolliert werden.

Genregulation durch ncRNA und die moderne RNA-Welt

Die am besten verstandenen auf ncRNA basierenden Signalwege beinhalten transkriptionelle und posttranskriptionelle repressive Genregulationsmechanismen (zusammenfassend: RNA-Silencing), die durch unterschiedliche Klassen kurzer RNA-Moleküle vermittelt werden. Drei individuelle, jedoch teilweise überlappende Signalwege werden hierbei unterschieden: Spaltung spezifischer mRNAs und viraler RNA durch small interfering RNAs (siRNAs), (reversible) translationelle Inhibition von mRNAs durch microRNAs (miRNAs), sowie Spaltung von RNA-Intermediaten egoistischer genetischer Elemente und Transposons durch Piwi-interagierende RNAs (piRNAs). All diese Klassen kurzer RNA-Moleküle sind zwischen 20 und 33 Nukleotiden lang und stellen die Spezifizitätsfaktoren proteinöser Effektorkomplexe dar, indem sie spezifische, auf komplementärer Basenpaarung basierende physische Interaktionen zwischen den katalytischen Effektorkomplexen und den Ziel-RNAs vermitteln.
Auf siRNAs basierendes RNA-Silencing gehört hierbei zu den am besten erforschten Signalwegen kurzer RNAs. Die Hauptaufgabe dieses Mechanismus besteht in der Abwehr exogener Pathogene wie zum Beispiel Viren. Die meisten Viren durchlaufen während einer Infektion Replikations-Intermediate, die aus doppelsträngiger RNA (dsRNA) bestehen. dsRNA wird von der RNA-Silencing-Maschinerie spezifisch erkannt und in siRNAs umgewandelt, die daraufhin die ursprünglichen Virus-RNAs sequenzspezifisch erkennen und abbauen. Auf diese Weise können Viren auf molekularer Ebene bekämpft werden, und nahezu alle eukaryotischen Organismen haben in ihrer Evolution homologe Verteidigungsstrategien entwickelt. Während der Ko-Evolution von Viren und ihren entsprechenden Wirten haben Viren wiederum Strategien entwickelt, um die RNA-Silencing-basierte Immunreaktion ihrer Wirte zu

bekämpfen. Virale Suppressoren von RNA-Silencing verwenden unterschiedliche Mechanismen, um RNA-Silencing zu unterdrücken. Eine weit verbreitete Strategie besteht in der repressiven Bindung von siRNAs, die nachfolgend nicht für den RNA-Silencing-Signalweg zur Verfügung stehen, was die siRNA-basierte Immunantwort schwächt.

Da siRNA-basiertes RNA-Silencing Ziel-RNAs einzig aufgrund derer Sequenzen erkennt, muss gewährleistet werden, dass RNA-Silencing nicht außer Kontrolle gerät und im Zuge dessen RNAs zerstört, die essenziell für den jeweiligen Organismus sind. Große Anstrengungen wurden daher unternommen, endogene RNA-Silencing-Suppressoren zu identifizieren, die für die negative Modulation bestimmter RNA-Silencing-Signalwege verantwortlich sind.

Endogene Suppressoren von RNA-Silencing und die Rollen von ERI-1 in der Degradation von siRNAs und der Biogenese ribosomaler RNA

Bislang wurde ein einziges Protein identifiziert, das als echter endogener Suppressor von RNA-Silencing angesehen werden kann. Das Protein Enhanced RNAi 1 (ERI-1) des Fadenwurms *Caenorhabditis elegans* degradiert siRNAs *in vitro* und übt durch diese Fähigkeit einen repressiven Effekt auf die Effizienz von RNA-Silencing in Neuronen von *C. elegans* aus. ERI-1 ist ein evolutionär konserviertes Protein und ERI-1-homologe Proteine wurden in einer Vielzahl von Modellorganismen erkannt und charakterisiert. Allen gemein ist die Präsenz einer EXOIII-Domäne des Subtyps ERI-1_3'hExo_like. EXOIII-Proteine erkennen und prozessieren bevorzugt dsRNA-Substrate mit 3'-Überhängen, was die Spezifität für siRNAs erklärt, die kurze dsRNA-Duplexe mit 3'-Überhängen von 2 Nukleotiden darstellen. Eine weitere konservierte Funktion mancher ERI-1-homologer Proteine ist die Prozessierung des unreifen 3'-Endes der kleinen 5.8S ribosomalen RNA. In *C. elegans*, der Spalthefe *Schizosaccharomyces pombe* und der Maus *Mus musculus* wurde gezeigt, dass die entsprechenden ERI-1-homologen Proteine den finalen Prozessierungs-Schritt in der Biogenese der 5.8S rRNA katalysieren, indem sie 2 Nukleotide an deren 3'-Ende entfernen. Diese doppelte Funktion von ERI-1

(Degradation von siRNAs sowie Prozessierung der 5.8S rRNA) schlägt eine interessante Brücke zwischen evolutionär weit entfernten auf ncRNA basierenden Prozessen.

Beteiligung der pflanzlichen 3'-5'-Exonuclease ERL1 in der Biogenese plastidärer ribosomaler RNA und in RNA-Silencing-Signalwegen

In der vorliegenden Dissertation werden Resultate präsentiert, die die funktionelle Charakterisierung des pflanzlichen ERI-1-Homologs ERI-1-LIKE 1 (ERL1) in der Regulation von RNA-Silencing sowie der Biogenese ribosomaler RNA zum Gegenstand haben. ERL1 lokalisiert in Chloroplasten, die als Kompartiment frei von RNA-Silencing gelten. Dementsprechend konnte eine Aktivität von ERL1 in der Regulation von RNA-Silencing in *Nicotiana benthamiana* nicht festgestellt werden. Dies wird durch die Unfähigkeit ERL1s zur Beeinflussung von *GFP* Silencing-Phänotypen selbst bei konstitutioneller *ERL1*-Überexpression verdeutlicht. Diese Resultate stehen im Einklang mit der evolutionären Verwandtschaft von ERL1 mit anderen ERI-1-homologen Proteinen der Gruppe II, die durch das Nichtvorhandensein einer SAP-Domäne charakterisiert sind. Diese ERI-1-homologen Proteine der Gruppe II konnten bis dato nicht mit der Regulation von RNA-Silencing in Verbindung gebracht werden und stehen damit im Gegensatz zu ERI-1-homologen Proteinen der Gruppe I. Proteine der Gruppe I (beispielsweise *C. elegans* ERI-1, *S. pombe* Eri1, *Neurospora crassa* QIP und *M. musculus* Eri1) enthalten eine dsRNA-bindende SAP-Domäne und gelten als echte endogene Suppressoren von RNA-Silencing. Auffallender Weise entwickeln transgene *ERL1*-überexprimierende Exemplare von *N. benthamiana* charakteristische phänotypische Aberrationen, die sich als Ausbildung benachbarter weißer und wildtyp-artiger grüner Blattsektoren manifestieren. Die Ausbildung weißer Sektoren ist abhängig von hoher *ERL1*-Expression und ist reversibel, sofern die Überexpression von *ERL1* spontan oder nach exogener Stimulation per RNA-Silencing gehemmt wird. Solch beeinträchtigte Pflanzen akkumulieren Wachstums- und Fertilitäts-Defekte sowie histologische und ultrastrukturelle Veränderungen, die in ähnlicher Form auch von anderen Pflanzen-Mutanten in der wissenschaftlichen Literatur beschrieben worden sind. In der Mehrzahl der Fälle ist eine solche „Vielfarbigkeit" das Resultat geschädigter Plastid-

Zusammenfassung

Differenzierung, was zur Folge hat, dass sich keine reifen Chloroplasten bilden können. Die grundlegende Schädigung, die zur Blockade der Plastid-Differenzierung führt, ist in solchen Fällen häufig in einer gestörten Biogenese plastidärer ribosomaler RNAs zu suchen, woraufhin es zu einem allgemeinen Zusammenbruch plastidärer Translation und Transkription kommt. Solch geschädigte Plastiden kommen in ihrer Differenzierung nicht über ein frühes Proplastid-Stadium hinaus und können sich in der Folge nicht in die für die Pflanze lebenswichtigen unterschiedlichen Formen reifer Plastiden (z. B. Chloroplasten) entwickeln. Dementsprechend wurde untersucht, ob ERL1 eine Funktion in der Biogenese plastidärer ribosomaler RNA ausübt.

In der Tat konnte beobachtet werden, dass das Fließgleichgewicht der kleinen plastidären 5S rRNA durch *ERL1*-Fehlexpression negativ beeinflusst wird, während sich 4.5S rRNA (plastidär) und 5.8S rRNA (zytosolisch) unbeeinflusst zeigen. Die Klonierung von 5S rRNA aus transient sowie konstitutionell *ERL1*-überexprimierenden und -inhibierenden Proben förderte in der Folge inkorrekt prozessierte 5S rRNA-Moleküle zu Tage, die an ihren 3‘-Enden Verlängerungen von 2 Nukleotiden aufweisen. Die Reifung plastidärer 5S rRNA ist seit langem als Prozess bekannt, der in vielen präzise geregelten Stufen abläuft. Verschiedene konzertierte endo- und exonukleolytische Aktivitäten sind notwendig, um reife 5S rRNA herzustellen. Die Gesamtheit der Exonuklease-Proteine, die für die Reifung des 3‘-Endes der 5S rRNA verantwortlich sind, konnte bislang jedoch nicht bestimmt werden. Die exonukleolytische Prozessierung des 5S rRNA 3‘-Endes wird zum Teil von dem Protein RIBONUCLEOTIDE REDUCTASE 1 (RNR1) bewerkstelligt. Dennoch akkumulieren auch in *rnr1*-Nullmutanten reife 5S rRNA 3‘-Enden, so dass postuliert wurde, dass RNR1 redundant und in Kooperation mit einer weiteren, bis dato nicht identifizierten Exonuklease-Aktivität wirkt.

Basierend auf den Ergebnissen, die in der vorliegenden Arbeit präsentiert werden, stellt ERL1 mit hoher Wahrscheinlichkeit diese Aktivität dar.

Acknowledgements

This work would not have been possible without the help and the support of many people who I would like to acknowledge herewith.

I wish to express my sincere gratitudes to **Dr Kriton Kalantidis** for his trust and encouragements to undertake this Ph. D. project in his laboratory at emotionally difficult times, and for his enduring support and invaluable guidance without which the success of this work would not have been possible.

***

I would like to thank **Prof Dr Wolfgang Nellen** for almost 10 years of continuing support and uncountable good advice that have made walking this path worthwhile and always enjoyable and inspiring.

***

I am grateful to all the members of the **Plant Molecular Biology Laboratory** at the Institute of Molecular Biology & Biotechnology for inspiring discussions, a great deal of good times, and creative donkey fun.

***

Very special thanks I owe to **Jutta Helm**, not only for being a reliable collegue in professional terms, but more importantly for being a trusted friend in difficult times. Furthermore it was your selfless devotion that presented me with an incredibly black and overwhelmingly enjoyable companion.

***

Last but not least I wish to thank **Tamar Shahal** for joyful times and continuing encouragement and support, **my friends** for thinking about me in a distance, and **my parents** for being there for me at all times.

This work was funded by the European Union through a Marie Curie Fellowship to H.T.S. under contract MEST-CT-2004-007295 FAMED.

Abbreviations

aa	Amino acid(s)
APS	Ammonium persulfate
Asp	Aspartic acid
BLAST	Basic Local Alignment Search Tool
bp	Base pair(s)
cDNA	complementary DNA
CTAB	Cetrimonium bromide
dGTP	Deoxyguanosine triphosphate
DMSO	Dimethylsulfoxide
DNA	Deoxyribonucleic acid
dNTP	Deoxynucleoside triphosphate
dpi	Days postinfection; days postinfiltration
dsDNA	Double-stranded DNA
dsRNA	Double-stranded RNA
DTT	Dithiothreitol
dTTP	Deoxythymidine triphosphate
e.g.	Exempli gratia
EDTA	(Ethylenedinitrilo)tetraacetic acid
ELSS	Extensive local silencing spread
EST	Expressed sequence tag
et al.	And others
EtBr	Ethidium bromide
hcRNA	Heterochromatic RNA
HeLa	Helen Lane
HEPES	2(4(2-Hydroxyethyl)-1-piperazinyl)-ethanesulfonic acid
His	Histidine
i.e.	Id est
IPTG	Isopropyl β-D-1-thiogalactopyranoside
JMH	Jutta Maria Helm
kb	kilobase(s)
LB	Lysogeny broth
LUCA	Last Universal Common Ancestor
MES	2-(N-morpholino)ethanesulfonic acid
miRNA	microRNA
MMA	MS/MES/acetosyringone
MOPS	3-(N-morpholino)propanesulfonic acid

Abbreviations

mRNA	messenger RNA
MS	Murashige & Skoog
nat-siRNA	Natural antisense transcript-derived siRNA
NCBI	National Center for Biotechnology Information
ncRNA	Non-coding RNA
Ni-NTA	Nickel-nitriloacetic acid
nt	Nucleotide(s)
OD_{600}	Optical density at 600 nm
P	Phosphorus
PAA	Polyacrylamide
PAGE	Polyacrylamide gel electrophoresis
PAZ	Piwi/Argonaute/Zwille
PCR	Polymerase chain reaction
PIPES	Piperazine-N,N'-bis(2-ethanesulfonic acid)
piRNA	Piwi-interacting RNA
Pol.	Polymerase
pre-miRNA	Precursor miRNA
pri-miRNA	Primary miRNA
PTGS	Posttranscriptional gene silencing
ra-siRNA	Repeat-associated siRNA
RdRP	RNA-dependent RNA polymerase
RISC	RNA-induced silencing complex
RITS	RNA-induced transcriptional silencing
RNA	Ribonucleic acid
RNAi	RNA interference
RNase	Ribonuclease
RNP	Ribonucleoprotein
rpm	Rotations per minute
rRNA	Ribosomal RNA
RT	Reverse transcription
SAP	SAF-A/B, Acinus, and PIAS
scnRNA	scanRNA
SDS	Sodium dodecyl sulfate
siRNA	Small interfering RNA
SLSS	Short-range local silencing spread
SOB	Super optimal broth

Abbreviations

SSC	Sodium chloride/sodium citrate buffer
ssRNA	Single-stranded RNA
TAE	Tris-acetate-EDTA
TBE	Tris-borate-EDTA
TE	Tris-EDTA
TEM	Transmission electron microscopy
TEMED	Tetramethylethylenediamine
TGS	Transcriptional gene silencing
T_m	Melting temperature
tncRNA	Tiny non-coding RNA
Tris	Tris(hydroxymethyl)aminoethane
tRNA	Transfer RNA
UTR	Untranslated region
UV	Ultraviolet
VSR	Viral suppressor of silencing
w/v	Weight per volume
X-Gal	5-Bromo-4-chloro-3-indolyl-β-galactopyranoside

Organisms

A. thaliana	*Arabidopsis thaliana*
A. tumefaciens	*Agrobacterium tumefaciens*
Agrobacterium	*Agrobacterium tumefaciens*
Arabidopsis	*Arabidopsis thaliana*
At	*Arabidopsis thaliana*
C. elegans	*Caenorhabditis elegans*
C. reinhardtii	*Chlamydomonas reinhardtii*
D. melanogaster	*Drosophila melanogaster*
D. rerio	*Danio rerio*
Dictyostelium	*Dictyostelium discoideum*
Drosophila	*Drosophila melanogaster*
E. coli	*Escherichia coli*
M. musculus	*Mus musculus*
N. benthamiana	*Nicotiana benthamiana*
N. crassa	*Neurospora crassa*

Abbreviations

N. tabacum	*Nicotiana tabacum*
Nt	*Nicotiana tabacum*
O. sativa	*Oryza sativa*
Os	*Oryza sativa*
P. trichocarpa	*Populus trichocarpa*
PLMVd	*Peach latent mosaic viroid*
PPV	*Plum pox virus*
PSTVd	*Potato spindle tuber viroid*
Pt	*Populus trichocarpa*
S. bicolor	*Sorghum bicolor*
S. pombe	*Schizosaccharomyces pombe*
S. purpuratus	*Strongylocentrotus purpuratus*
T. brucei	*Trypanosoma brucei*
Tribolium	*Tribolium castaneum*
V. vinifera	*Vitis vinifera*
Zm	*Zea mays*

Chemical formulas

Ca^{2+}	Divalent calcium ion
$CaCl_2$	Calcium chloride
H_2O	Water
HCl	Hydrochloric acid
K_2HPO_4	Potassium phosphate, dibasic
KCl	Potassium chloride
$MgCl_2$	Magnesium chloride
$MnCl_2$	Manganese chloride
NaCl	Sodium chloride
NaOH	Sodium hydroxide
OsO_4	Osmiumtetraoxide

Units of meaure

°C	Degrees Celsius

Abbreviations

Å	Ångström(s)
Ci	Curie(s)
cm	Centimetre(s)
cm^2	Square centimetre(s)
g	Gramme(s); relative centrifugal force
h	Hour(s)
kDa	Kilodalton(s)
kV	Kilovolt(s)
M	Molar
mA	Milliampere(s)
mg	Milligramme(s)
mJ	Millijoule(s)
mL	Millilitre(s)
mM	Millimolar
mmol	Millimole(s)
µg	Microgramme(s)
µL	Microlitre(s)
µm	Micrometre(s)
µM	Micromolar
N	Normal
ng	Nanogramme(s)
nm	Nanometre(s)
pmol	Picomole(s)
S	Svedberg (sedimentation coefficient)
u	Unit(s)
V	Volt(s)
W	Watt(s)

Genes and proteins

Ago/AGO	Argonaute/ARGONAUTE
ATRLI2	RNASE L INHIBITOR 2
Aub	Aubergine
BSA	Bovine serum albumin
CHS	CHALCONE SYNTHASE

Abbreviations

CLP	CASEINOLYTIC PROTEASE
CLPP	CASEINOLYTIC PROTEASE P 1
CLSY1	CLASSY 1
DCL1-4	DICER-LIKE1-4
DCR-1	DiCer Related 1
DRB4	DOUBLE-STRANDED RNA-BINDING PROTEIN 4
EGO-1	Enhancer of Glp-One 1
eIF4E/F	Eukaryotic initiation factor 4E/F
eIF6	Eukaryotic initiation factor 6
ERI-1/Eri1	Enhanced RNAi 1
eriA	Enhancer of RNAi A
ERL1	ERI-1-LIKE 1
FRY1	3'(2'), 5'-BISPHOSPHATE NUCLEOTIDASE/INOSITOL POLYPHOSPHATE 1-PHOSPHATASE
GFP	Green Fluorescent Protein
HC-Pro	Helper component-proteinase
HEN1	HUA ENHANCER 1
HST	HASTY
HYL1	HYPONASTIC LEAVES 1
lin-4	abnormal cell-LINeage-4
let-7	LEThal-7
NEP	Nucleus-encoded polymerase
NRPD1a/b	NUCLEAR RNA POLYMERASE D 1A/B
PEP	Plastid-encoded polymerase
Piwi	*P* element-induced whimpy testes
PNK	Polynucleotide kinase
Pol II	RNA polymerase II
Pol IV	RNA polymerase IV
Pol V	RNA polymerase V
QDE-2	Quelling-deficient 2
QIP	QDE-2-interacting protein
RBCL	Ribulose bisphosphate carboxylase, large chain
RDR1-6	RNA-DEPENDENT RNA POLYMERASE 1-6
rgs-CaM	REGULATOR OF GENE SILENCING – CALMODULIN-LIKE
RNR1	RIBONUCLEOTIDE REDUCTASE 1
RPL23	RIBOSOMAL PROTEIN L23

Abbreviations

RPOB	RNA POLYMERASE SUBUNIT BETA
RRF-1	RNA-dependent RNA polymerase Family 1
RRF-3	RNA-dependent RNA polymerase Family 3
RuBisCo	Ribulose-1,5-bisphosphate carboxylase/oxygenase
SGS3	SUPPRESSOR OF GENE SILENCING 3
SDE5	SILENCING-DEFICIENT 5
SE	SERRATE
TAS3	TRANS-ACTING SIRNA 3
Thex1/3'hExo	3' histone exonuclease
Tnc-Snp	*Tribolium castaneum* Snipper
VDL1	VARIEGATED AND DISTORTED LEAVES 1
XRN2-4	EXORIBONUCLEASE 2-4

Table of Contents

Table of Contents

Table of Contents

Table of Contents

1

Introduction

1.1. RNA makes a stand

In the past decade our knowledge of fundamental regulatory processes in the cell have been revolutionised by unravelling a thus far unimagined plethora of non-coding RNA pathways. In only a couple of years RNA research has made a transition from a mature field of traditional molecular biology to one of the most cutting-edge and fastest growing areas of contemporary research.

Historically RNA had been regarded as an auxiliary molecule class with the primary purposes to provide structural scaffolding (ribosomal RNA; rRNA), adapter function (transfer RNA; tRNA), and transfer of information (messenger RNA; mRNA). In light of the 'Central Dogma' of molecular biology, according to which protein is the crucial end-product of genetic information, RNA lacks both DNA's stability as well as protein's catalytic versatility to qualify for more than assisting functions. While this view holds true in many respects, it in the same breath altogether disregards the possibility for RNA to act in diverse key functions. The discovery of catalytically active RNA (Kruger et al., 1982; Guerrier-Takada et al., 1983), however, started stirring up the discussion, whether RNA may have been underestimated in its abilities.

Today non-coding RNAs have been demonstrated to fulfill essential tasks in virtually every aspect of cellular regulation. The complexity of these RNA networks, in regulatory as well as evolutionary terms, additionally fueled extensive debate about the role of RNA in the origin of life (Joyce and Orgel, 1999).

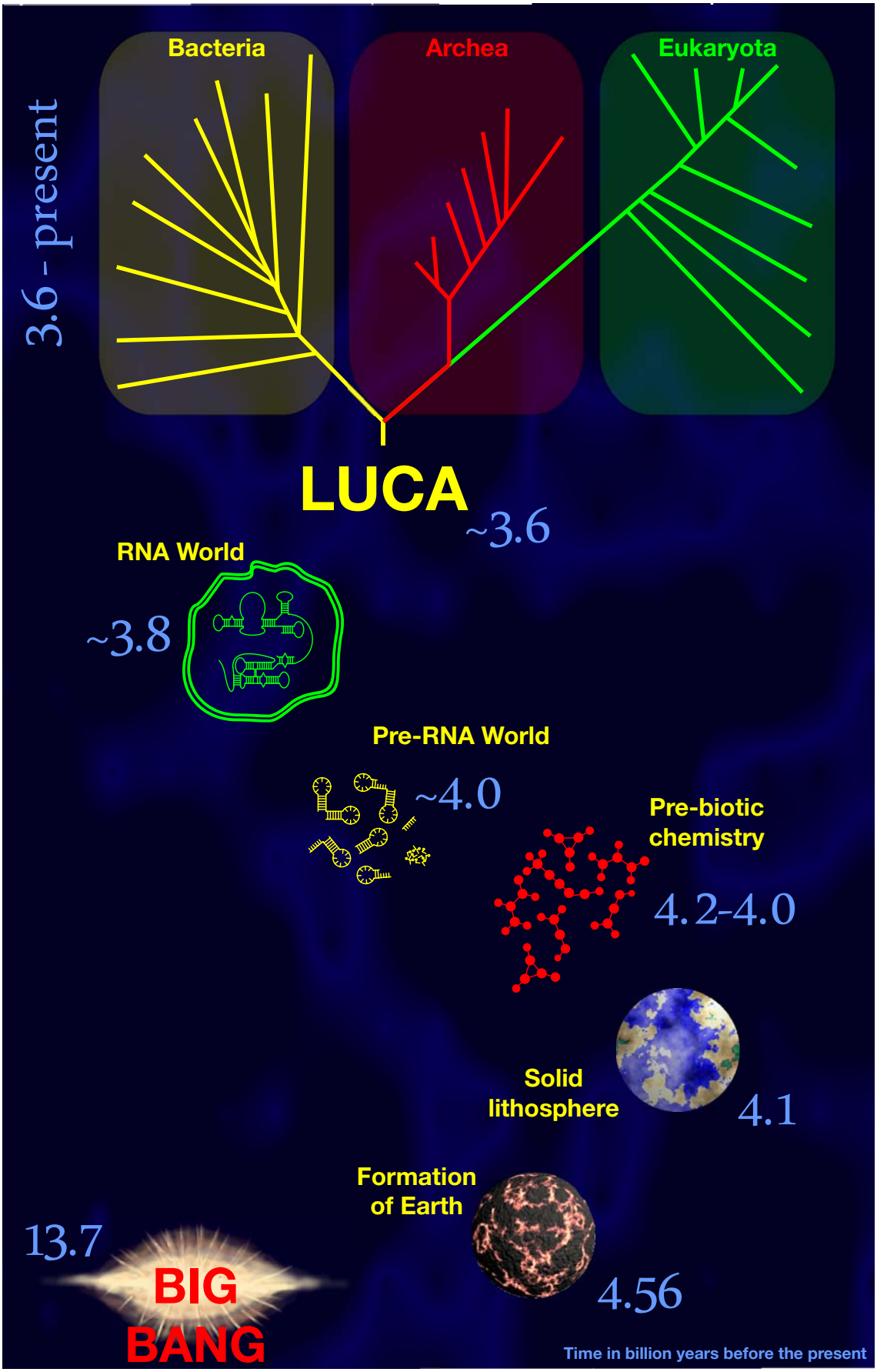

Figure 1.1 Evolution of life, the universe, and everything. Based on Gesteland et al., 1999.

1. Introduction

1.2. Let there be RNA

The overwhelming complexity of contemporary life naturally raises the question, how the transition from the primordial early Earth to the advent of cellular life may have come to pass. Although the debate about the mechanisms for the actual conversion from prebiotic chemistry to the first biomolecules is still highly speculative, the existence of an 'RNA World' (Gilbert, 1986) preceding the emergence of DNA/protein-based life is widely accepted today (Chen et al., 2006).

A fundamental dilemma of molecular biology is defined by the paradox that in a DNA/protein-based concept of life nucleic acids are required for the production of proteins, while proteins are in turn a prerequisite for the generation of nucleic acids (Chen et al., 2006). The ribosome stands in the centre of this view, seen by many as the fundamental denouement in the evolution of cellular life (Benner et al., 2006). The ribosome constitutes one of the evolutionary most conserved macromolecular machines and is a joint feature of all living organisms. Only after establishing the ribosome-based flow of genetic information from DNA to protein, providing the means for stable genetic inheritance along with efficient, versatile, and highly adaptive catalysis, the forebears of the three domains of life could accrue (Wolf and Koonin, 2007). Notwithstanding crucial differences between the translation systems in archaea, bacteria, and eukaryota the high conservation of the ribosome's core, the universality of the genetic code, and the universal use of DNA to store genetic information are compelling evidence for the existence of a Last Universal Common Ancestor (LUCA) of all extant life forms (Wolf and Koonin, 2007). The LUCA itself must have been the outcome of a long evolutionary process resulting in a ribosome-based translation system that was precise and efficient enough to allow for the subsequent development of the three domains of life (Benner et al., 2006). This deduction, however, carries a catch-22 aspect. From a habitual point of view, the ribosome could only have been developed, once a functional translation system had already been established. After all, protein enzymes would have been necessary to exert the sophisticated catalytic functions associated with the generation of a macromolecular machine as complex as the ribosome. In this respect, solving the crystal structure of the ribosome (Ban et al., 2000; Wimberly et al., 2000; Yusupov et al., 2001) was, *a fortiori*, the key scientific

Table 1.1 Examples of chemical reactions by *in vitro*-selected ribozymes

Bond formed*		
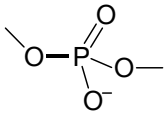	RNA cleavage	
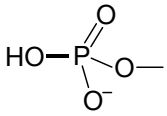	2',3'-Cyclic-phosphate hydrolysis	
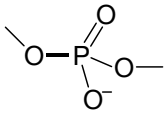	5'-3' RNA ligation (leaving group = pyrophosphate)	7×10^6
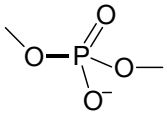	5'-5' RNA ligation (leaving group = imidazole)	10^3-10^4 (over templated reaction)
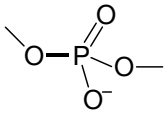	AMP-capped 5'-3' ligation (leaving group = 5' phosphate of AMP)	
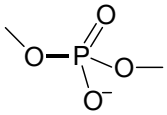	RNA phosphorylation	
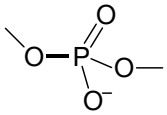	5'-5' self-capping (leaving group = pyrophosphate moiety)	
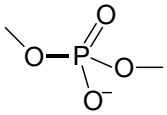	Acyl activation (leaving group = pyrophosphate)	
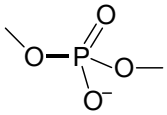	Polymerisation (leaving group = pyrophosphate)	
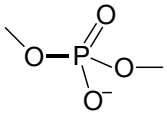	RNA branching	
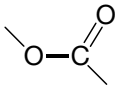	Aminoacyl-RNA synthesis (leaving group = 5' phosphate of AMP)	$\geq 10^5$

Table 1.1 *continued*

Bond formed*	Reaction	Rate enhancement
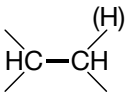	Aldol reaction	4300
	Redox reaction	$>10^7$
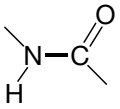	Amide bond formation (leaving group = 3' OH group of RNA)	
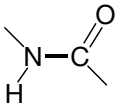	Amide bond formation (leaving group = 5' phosphate of AMP)	10^4
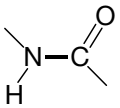	Peptide bond formation (leaving group = 5' phosphate of AMP)	10^6
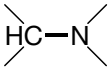	Glycosidic bond formation	10^7
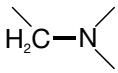	RNA alkylation	3×10^6
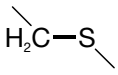	Thio alkylation	2400
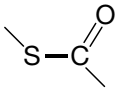	Thiol ester formation	>3400
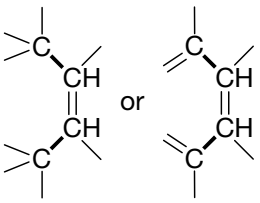	*Diels-Alder*	800

* Newly formed bonds are shown in bold. Modified from Chen et al., 2007.

breakthrough for resolving this predicament. Diametrical to traditional textbook knowledge, it is the ribosome's protein components that are arranged on the surface to provide structural scaffolding, while the core of the ribosome is composed exclusively of its RNA moiety (Nissen et al., 2000; Steitz and Moore, 2003). No amino acid chain comes within 18 Å of the active site of the peptidyl transferase centre (Nissen et al., 2000), showing beyond doubt that the ribosome is in fact a ribozyme. It is therefore realistic to presume early forms of life based solely on RNA that were able to replicate, sustain primitive metabolisms, and evolve in a Darwinian fashion based on selective pressures on the primordial Earth. The apogee of this RNA World existed roughly 3.8 billion years ago (Figure 1.1), only few hundred million years after the formation of a solid crust on the early Earth. Even though the indications for this scenario are most persuasive, science is still faced with the problem that contemporary ribozymes exhibit a very limited scope of catalytic activities (Strobel and Cochrane, 2007) that by far lack the sophistication and versatility that would be necessary to sustain a functional 'RNA ecosystem'. To address this constraint researchers have used directed *in vitro* evolution to explore the repertoire of chemical mechanisms that may have been catalysed by ancient ribozymes (Chen et al., 2007). A large number of artificial ribozymes have thus been generated, exerting functions including RNA ligation, peptide bond formation, and RNA polymerisation (Table 1.1), demonstrating that RNA-based metabolisms as proposed in the RNA World hypothesis may conceivably have existed [(Chen et al., 2007) and references therein]. At the zenith of the RNA World stood the development of the primitive ribosome that was composed entirely of RNA (Crick, 1968) and paved the way for the emergence of catalysis based on protein enzymes; a development that culminated in the appearance of the LUCA 3.6 billion years before the present.

1.3. The contemporary RNA World

Life has indeed come a long way since the times of the LUCA, both in terms of variability between and complexity within organisms. Yet, the eukaryotic lineage underwent a much more dramatic increase in complexity than the bacterial and archeal

domains. Divergent strategies in genomic and regulatory landscapes between the three domains of life may provide clues to understanding these differences.

Extensive research has been undertaken *e.g.* in the nematode *C. elegans* to decipher the developmental programmes responsible for the precise coordinations during its ontogeny, including invariable cell divisions, apoptosis, and differentiation. It can be assumed that the ontogeny of higher organisms including mammals is under similar, yet significantly more complex, control by developmental programmes. It came as a big surprise, however, that mammalian genomes do not contain significantly more protein-coding genes than nematodes or sea urchins (Mattick, 2007). Apparently, the amounts of protein-coding genes do not scale consistently with morphological and developmental complexity [(Mattick, 2007) and Figure 1.2]. Even though extensive alternative splicing provides a means to increase the proportion of protein isoforms from similar amounts of protein-coding genomic loci, this alone could not suffice to account for the increase in developmental complexity between nematodes and mammals (Mattick, 2007). It is therefore plausible to presume a connection between the increasing non-protein-coding portions of genomes and the evolution of higher organisms.

Prokaryotic genomes are typically very compact and comprise 80-95 % protein-coding loci (Waters and Storz, 2009). Although non-coding RNAs (ncRNAs) contribute to prokaryotic cell regulation (Waters and Storz, 2009), the regulatory architecture of bacteria is primarily protein-based. It has been shown that the amounts of genes encoding regulatory proteins in prokaryotic genomes increase exponentially with total gene number and genome size (Mattick, 2007). From these data it may be inferred that prokaryotic genomes have reached a point, where further increase in complexity based on additional non-regulatory proteins would require concomitant additions of regulatory genes, which may constitute an evolutionary barrier for further prokaryotic development due to the exponential costs for each newly introduced gene (Mattick, 2007). Eukaryotic genomes, conversely, have extended exponentially beyond protein-coding genes (Figure 1.2), allowing for the co-development of ncRNA regulators and a protein machinery able to recognise, integrate, and act on the signals communicated through RNA sequence and structure (Mattick, 2007). RNA lends itself to regulatory functions, as relatively short nucleotide sequences are already sufficient for precise target identification *via* base pairing interactions. At the same time RNA's ability to

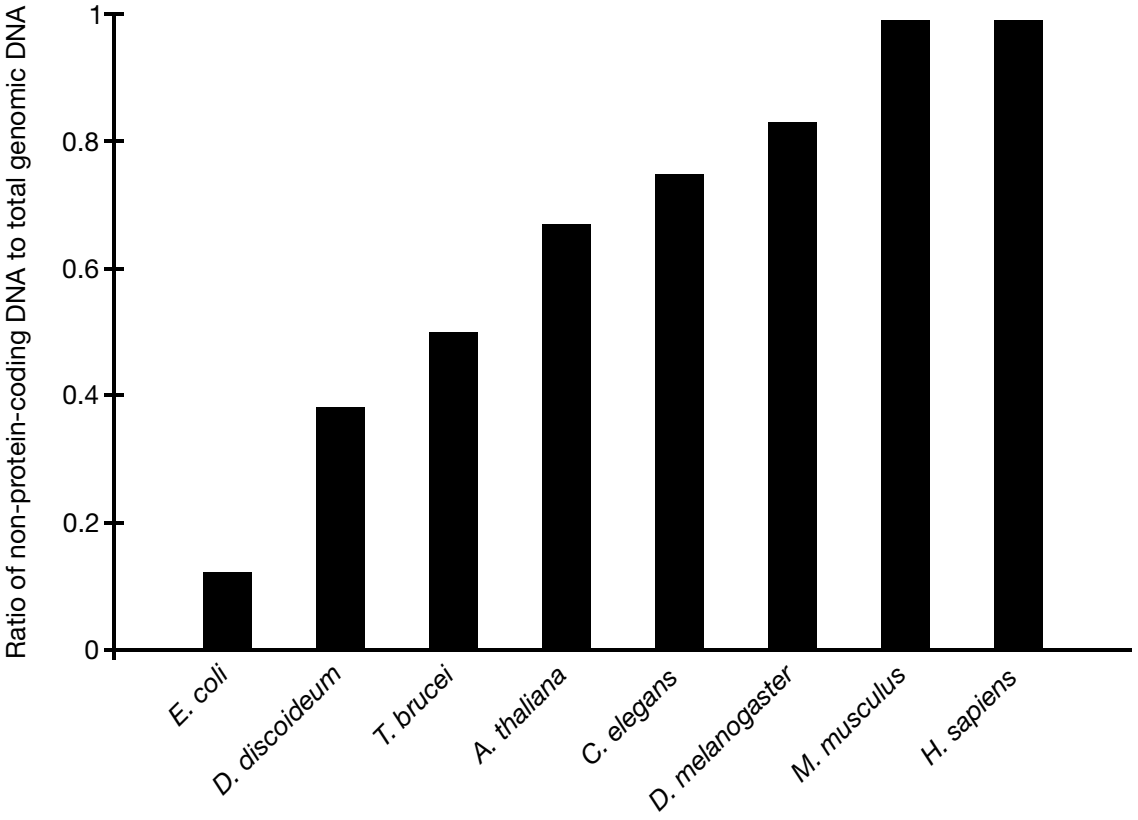

Figure 1.2 The fraction of non-protein-coding DNA per haploid genome in different species. The ratio of protein-coding loci reduces significantly with increasing complexity during phylogeny. In mammalian genomes protein-coding genes account for only about 1 % of the genome. Based on Mattick, 2007.

allow for mismatches and non-Watson-Crick base pairing provides ample flexibility for RNA-target interactions. Compared to proteins, RNA is easy and quick to produce and to turn over, which are important prerequisites for spatiotemporal control of regulatory molecules. In addition, RNA sequences can evolve quickly, and potentially deleterious mutations can comparably easily be corrected by compensatory mutations.

Recent advances in transcriptome analysis revealed that functional ncRNAs appear to be even more omnipresent than originally imagined (Mattick, 2007; Ponting et al., 2009). 5-10 % of mammalian genomes are stably transcribed at all times and in all cell types. Yet, only 10 % of these transcripts account for productive mRNAs, whereas 90 % of this transcriptional output constitutes ncRNAs of largely unknown function (Ponting et al., 2009). This alone would be an impressive example for the pervasive production of ncRNAs. But recent studies moreover firmly establish that the classical view of genome architecture with distinct transcript-generating loci does not appear to be accurate (Birney et al., 2007). Quite the contrary, it appears that the complete human euchro-

matic genome gives rise to transcripts from one or both strands, very often in a regulated manner, surpassing protein-coding transcripts >100fold (Ponting et al., 2009). Unspecific transcription evidently exists in several forms (Ebisuya et al., 2008; Ponting et al., 2009) and must be taken into consideration when analysing the repertoire of ncRNAs. Yet, vast numbers of non-protein-coding loci show fewer nucleotide substitutions than expected according to a neutral evolution, indicating that these ncRNAs have been under selective pressures, which suggests functional importance (Ponjavic et al., 2007). This notion is underscored by spatiotemporally controlled expression and specific subcellular localisations of many of these ncRNAs, which are characteristics not to be expected from 'transcriptional noise' (Mattick, 2007; Ponting et al., 2009). Most ncRNAs are expressed at very low levels compared to mRNAs, which complicates functional analyses of individual ncRNAs. Reverse genetics approaches are likely not to yield strong developmental or morphological defects when single ncRNAs are studied, since each individual ncRNA supposedly contributes only slightly to an organism's fitness (Ponting et al., 2009). In concert, however, ncRNA networks are essential for an organism's ontology (Ponting et al., 2009).

Almost 4 billion years of evolution stand between the ancestral RNA World and its derivatives in form of the unfathomable diversity of contemporary organisms. The realisation of today's life's descent from RNA brought with it the task to understand the nature of the contemporary RNA World and its implications as they are being uncovered.

1.4. Gene regulation by small RNAs

The best studied non-coding RNA pathways include transcriptional and post-transcriptional gene silencing mechanisms mediated by sundry classes of small RNA molecules. In the most basic sense RNA silencing constitutes the repressive actions of effector complexes on target transcripts or genomic loci to which they are guided sequence-specifically by ~20-33 nt antisense RNAs. The mediated silencing actions most commonly involve cleavage of target mRNAs, transcriptional silencing of genomic loci through chromatin remodelling, and (reversible) translational arrest of mRNAs. The

catalogue of identified and characterised small silencing-related RNAs comprises three major categories: small interfering RNAs (siRNAs), microRNAs (miRNAs), and Piwi-interacting RNAs (piRNAs), each mediating distinct but partially overlapping regulatory pathways (Table 1.2).

The main protein components of small RNA-associated RNPs are members of the Argonaute/Piwi (Ago/Piwi) family that form functional effector complexes when loaded with siRNAs/miRNAs/piRNAs (Farazi et al., 2008). Ago/Piwi proteins are present in all

Table 1.2 Characeristics of small silencing-related RNA families

Small RNA class	Size	Mechanism	Organism
siRNA-type:			
siRNA	20-24	mRNA cleavage Chromatin regulation	*C. reinhardtii* *D. rerio* Insects Mammals *N. crassa* Nematodes Plants *S. pombe* *T. brucei*
ta-siRNA	21-22	mRNA cleavage	Plants
nat-siRNA	21-22	mRNA cleavage	Plants
Secondary siRNA	20-25	mRNA cleavage	Nematodes Plants
hcRNA	24	Chromatin regulation	Plants *S. pombe* *T. brucei*
tncRNA	22	Unknown	Nematodes
miRNA-type:			
miRNA	20-23	Translational repression mRNA cleavage	*C. reinhardtii* *D. rerio* Insects Mammals Nematodes Plants Viruses
piRNA-type:			
piRNA	28-33	mRNA cleavage	*D. rerio* Insects Mammals
21U RNA	21	Unknown	Nematodes
ra-siRNA	23-28	Chromatin regulation	*D. rerio* Insects
scnRNA	26-30	Chromatin regulation	Protozoa

Modified from Farazi et al., 2008. See text for references.

organisms exerting RNA silencing and are often expressed in a tissue- and developmental stage-specific manner. Ago/Piwi proteins are composed of four conserved domains. The PAZ domain (for Piwi/Argonaute/Zwille) conveys RNA binding specificity in a sequence-independent manner and binds the 3' end of the small RNA guide (Faehnle and Joshua-Tor, 2007; Hutvagner and Simard, 2008). The PIWI domain adopts an RNase H-like fold and constitutes the slicer domain of catalytically active small RNA-loaded Ago/Piwi proteins through a conserved Asp-Asp-His motif (Faehnle and Joshua-Tor, 2007). A supposedly cap-binding MC motif is present in the Mid domain and may play an important role in miRNA-mediated translational repression (Hutvagner and Simard, 2008). Additionally, the Mid domain binds the 5' end of the associated small RNA (Faehnle and Joshua-Tor, 2007; Hutvagner and Simard, 2008). Finally, the N-terminal domain was shown to interact with heterochromatin protein-1a in *Drosophila melanogaster* and may therefore be involved in chromatin regulation (Hutvagner and Simard, 2008).

The different RNA silencing pathways exhibit partial redundancies and functional overlaps, as well as organism-specific idiosyncrasies, but may in general be classified according to the type of small RNA in combination with specific Ago/Piwi proteins binding it.

1.4.1. siRNA-mediated transcriptional and posttranscriptional gene silencing

Posttranscriptional gene silencing (PTGS) mediated by siRNAs in the context of antiviral defence was the first RNA silencing mechanism to be discovered. The supposedly earliest description of antiviral RNA silencing dates back as long as 1928, when S. A. Wingard described the gradual disappearance of *Tobacco ringspot virus* symptoms in upper, freshly emerging leaves of infected *Nicotiana tabacum* plants (Wingard, 1928). The underlying mechanism of this phenomenon, however, remained unresolved at the time. More than 60 years later an unknown mechanism was reported in petunia, by which transgenic plants suppressed not only the introduced transgene, but simultaneously the corresponding endogene (Napoli et al., 1990; van der Krol et al.,

1990). The researchers originally aimed to increase anthocyanin production by overexpressing the allegedly rate-limiting protein CHALCONE SYNTHASE (CHS). To their surprise, 25-42 % of plants with the introduced *CHS* gene produced fully and/or partially white flowers, caused by posttranscriptional co-suppression of both transgene and endogene and a resulting downregulation in anthocyanin production (Napoli et al., 1990; van der Krol et al., 1990). In the years to follow it was realised that co-suppression/gene silencing and antiviral defence are parts of the same RNA-targeting mechanism (Covey et al., 1997; Ratcliff et al., 1997). The existence of small RNAs conveying sequence specificity to such a suppression mechanism for both gene and virus silencing was posited already in 1993 (Lindbo et al., 1993), and subsequently ~21-25 nt siRNAs were discovered to constitute the specificity determinants in RNA silencing (Hamilton and Baulcombe, 1999). Studies in *C. elegans* identified double-stranded RNA (dsRNA) as the main inducer of posttranscriptional gene silencing (in animals referred to as RNA interference; RNAi) (Fire et al., 1998), and the discovery that siRNAs are produced from dsRNA precursors by the RNase III-type protein Dicer lastly allowed for the development of a general working model of RNA silencing [(Bernstein et al., 2001) and Figure 1.3 a].

Dicer is evolutionary conserved, with different numbers of Dicer homologues present in all organisms that possess RNA silencing pathways. Dicer initiates RNA silencing by binding and processing dsRNA into phased ~21 nt siRNA duplexes with 2 nt 3' overhangs. Dicer substrates comprise double-stranded virus RNA, dsRNA produced by the actions of RNA-dependent RNA polymerases (RdRPs), or transcripts that fold into perfectly or near-perfectly complementary hairpin structures. Single siRNAs are subsequently loaded into an RNA-induced effector complex, whose catalytic component is a member of the Ago family (Liu et al., 2004; Meister et al., 2004; Rand et al., 2004). The identity of the Ago protein and the class of siRNA bound by it define whether an active RNA-induced silencing complex (RISC) or RNA-induced transcriptional silencing (RITS) complex is formed. Upon binding to Ago the sense-oriented passenger strand of an siRNA duplex is cleaved and displaced (Rand et al., 2005), and the thus activated effector complex is guided to targets perfectly complementary to the bound single-stranded antisense siRNA. In the case of posttranscriptional gene silencing, the Ago protein contained in RISC slices the targeted mRNA between nucleotides 10 and 11

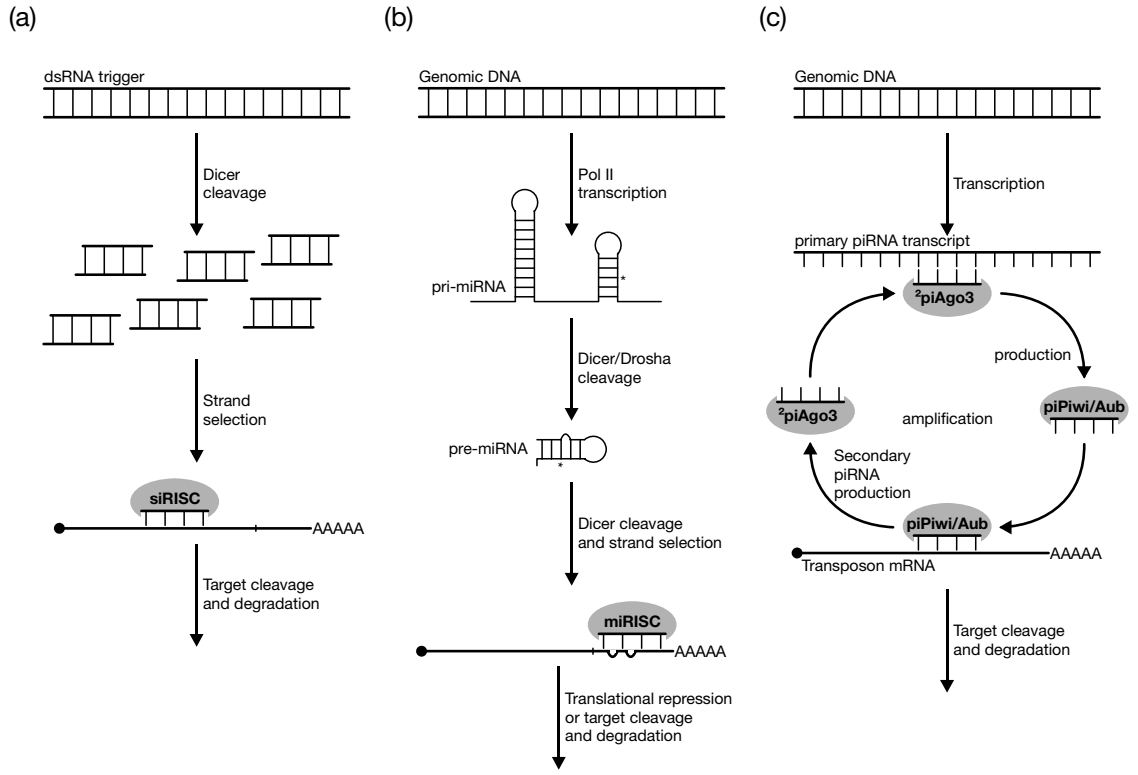

Figure 1.3 Simplified flow-chart models of the three major small RNA-mediated RNA silencing pathways. **(a)** In siRNA-mediated posttranscriptional gene silencing a dsRNA trigger is converted into siRNAs by Dicer cleavage. siRNA duplexes are incorporated into RISC (siRISC), and after separation of the siRNA's passenger strand cognate target mRNAs are cleaved and degraded. **(b)** miRNA precursors are transcribed from genomic loci and converted to mature miRNAs in a Dicer-dependent multistep process. The miRNA* is displaced upon loading into miRNA-RISC (miRISC). miRISC binds to the 3' UTR of target mRNAs and mediates translation repression or mRNA degradation. **(c)** piRNAs are produced in a unique, albeit not yet fully understood, Dicer-independent manner that may involve a so-called Ping-Pong amplification cycle. Mature primary piRNAs are bound by Piwi proteins to mediate cleavage of target transposon mRNAs.

of the guide RNA with its RNase H-like PIWI domain (Rivas et al., 2005). The mRNA cleavage products are either degraded exonucleolytically or may serve as templates for RdRP-mediated formation of dsRNA that will in turn constitute a template for Dicer to produce secondary siRNAs feeding back into the pathway and amplifying the original silencing response. Thus, PTGS-targeted mRNAs are efficiently silenced/degraded in a sequence-specific manner. When forming an active RITS complex, the siRNA-programmed Ago protein will in contrast be guided to genomic loci to which the Ago-siRNA complex will recruit different chromatin-modifying enzymes. RITS-targeted loci often comprise repetitive elements or transposon sequences that need to be silenced at the transcriptional level in order to maintain genome integrity. The precise catalytic activities in RITS-dependent chromatin remodelling and their regulations that lead to

DNA methylation and heterochromatin formation are, however, not fully understood (Chan, 2008).

With few exceptions the described core mechanisms of siRNA-mediated RNA silencing (Figure 1.3 a) are common to all eukaryotes. Species-specific distinctions are primarily, but not exclusively, seen in the evolutionary diversifications of Ago and Dicer proteins [reviewed in (Farazi et al., 2008; Jaskiewicz and Filipowicz, 2008)]. In addition, many projects aimed to characterise the small RNA transcriptomes of different model species have uncovered previously unknown endogenous siRNA families mediating a variety of RNA silencing actions. The plant-specific *trans*-acting siRNAs (ta-siRNAs) are produced in a unique way distinct from siRNA and miRNA biogenesis but utilising components of both pathways (Kalantidis et al., 2008; Felippes and Weigel, 2009). ta-siRNA production is a multistep process that is initiated by the miRNA-mediated cleavage of non-protein-coding ta-siRNA precursor transcripts. The cleavage products are protected from unspecific degradation (Felippes and Weigel, 2009) and serve as templates for an RdRP to produce dsRNA substrates that are processed into phased 21 nt ta-siRNAs by DICER-LIKE 4 (DCL4). Mature ta-siRNAs guide Ago-containing complexes to cleave complementary targets. Five distinct ta-siRNA-producing loci have thus far been discovered in the *Arabidopsis thaliana* genome that give rise to specific sets of mature ta-siRNAs (Allen et al., 2005) targeting transcripts different from the sequences generating the ta-siRNAs (Adenot et al., 2006). Known ta-siRNA targets are genes involved in auxin response and plant development (Ramachandran and Chen, 2008). Since site-specific cleavage of ta-siRNA target transcripts could potentially be accomplished by respective plant miRNAs, it might in the future be interesting to determine the selective pressures that rather lead to the development of the ta-siRNA pathway for the posttranscriptional regulation of the respective genes in plants. Natural antisense transcript-derived siRNAs (nat-siRNAs) represent another plant-specific family of small RNAs that are produced from dsRNA as a result of overlapping transcripts (Kalantidis et al., 2008; Xie and Qi, 2008). Two characterised nat-siRNAs are stress-induced and downregulate the transcripts from which they originate (Ramachandran and Chen, 2008). Since the overlapping of genes is a common phenomenon in eukaryotic genomes, nat-siRNAs may very well constitute a more widely prevalent small RNA family than currently realised. A large number of Ago-

associated small RNAs from repetitive sequences were found in plants, *Schizosaccharomyces pombe*, and *Trypanosoma brucei*. These heterochromatic siRNAs (hcRNAs) guide RITS complexes to repeat-containing chromosomal sectors and associate with nascent transcripts from heterochromatic regions, where they reinforce and sustain transcriptional gene silencing (TGS) through methylation and chromatin remodelling. Targets of hcRNA-directed TGS comprise transposons and centromeric loci (Djikeng et al., 2001; Reinhart and Bartel, 2002). Hence, hcRNAs may function analogously to piRNAs, which represent a different class of heterochromatin- and repeat-associated small RNAs in animals that are bound by Piwi proteins and serve as regulators of transposon activity (discussed below). Endogenously encoded siRNAs termed tiny non-coding RNAs (tncRNAs) are found in *C. elegans*, but not in mammals or insects (Farazi et al., 2008). Their functions in *C. elegans* have not been fully understood because they derive from non-conserved sequences, and no obvious targets could be unequivocally identified as yet (Ambros et al., 2003; Ruby et al., 2006; Farazi et al., 2008). Secondary siRNAs in *C. elegans* originate from RdRP-synthesised dsRNA using products of primary siRNA-mediated cleavage as unprimed templates (Sijen et al., 2007). Such secondary siRNAs associate with nematode-specific Class 3 Ago/Piwi proteins and positively feed back into the primary siRNA-dependent silencing activities (Yigit et al., 2006; Pak and Fire, 2007). Hence, they function similarly to RdRP-dependent secondary siRNAs in plant RNA silencing that are involved in antiviral PTGS, as well as TGS and the phenomenon of transitive RNA silencing. Lastly, siRNAs derived from viruses and viroids are readily identified in plants infected with the respective pathogens (Voinnet, 2005a). They guide cleavage of virus/viroid transcripts and are crucial to antiviral defence mechanisms including unique systems of local and systemic RNA silencing spread, as well as for protection from agrobacterial genetic colonisation (Dunoyer et al., 2006).

Since siRNA-mediated PTGS can be induced externally by introduction of dsRNA containing the sequences of selected target transcripts, RNA silencing has become a standard tool in molecular biology, allowing for rapid and specific knockdown of genes of interest in reverse genetics studies (Dykxhoorn and Lieberman, 2005). In addition, siRNA-based therapeutics are promising candidates to control genetic disorders caused by the overexpression of particular genes (Haasnoot and Berkhout, 2009), despite

pronounced difficulties in the spatiotemporally controlled delivery of such siRNA-based drugs.

1.4.2. miRNAs represent a divergent class of endogenous small RNAs mediating pervasive PTGS

A second major class of small silencing-mediating RNAs is known as miRNAs, which can be distinguished from siRNAs in terms of biogenesis and regulatory actions.
In 1981 the heterochronic gene *lin-4* was shown to repress cell proliferation in certain *C. elegans* cell lineages (Chalfie et al., 1981). 12 years later it was realised that *lin-4* does not encode a protein but rather a short non-coding RNA with complementarity to sequence motifs in the 3' untranslated region (UTR) of the *lin-14* mRNA, leading to translational downregulation *via* RNA-RNA interactions (Lee et al., 1993). It took another 7 years until a second small RNA was reported that acted in a fashion comparable to *lin-4*. The 21 nt RNA *let-7* is temporally regulated and mediates translational repression of mRNAs by targeting complementary regions in their 3' UTRs (Reinhart et al., 2000). Subsequent studies established *lin-4* and *let-7* as members of an abundant class of genomically encoded small RNA regulators that were termed miRNAs (Ambros, 2001; Lagos-Quintana et al., 2001; Lau et al., 2001; Lee and Ambros, 2001).
miRNAs are endogenously encoded, and many miRNA genes reside in introns, exons, or intergenic regions. While intronic and exonic miRNA genes may be controlled through their host genes's regulatory elements, intergenic miRNA genes likely represent individual transcriptional units with specific promoter elements (Bartel, 2004). Primary miRNA transcripts (pri-miRNA) are products of RNA polymerase II (Pol II) several hundred nucleotides in length that undergo a multistep maturation pathway before binding to respective Ago proteins (Figure 1.3 b). A nuclear cleavage event releases a ~60-70 nt precursor molecule (pre-miRNA) that adopts a hairpin structure due to extensive self-complementarity. This first stage in miRNA biogenesis may be circumvented by a special class of intron-residing miRNAs (mirtrons) that fold into a pre-miRNA structure after the splicing event and hence do not go through a pri-miRNA stage (Shabalina and Koonin, 2008). The pre-miRNA is a substrate for Dicer that

generates a single ~21 nt miRNA/miRNA* duplex with 2 nt 3' overhangs reminiscent of siRNA duplexes, but with imperfect complementarity. The miRNA* is degraded upon loading into RISC, and the mature single-stranded miRNA remains to guide the respective Ago protein to target mRNAs (Bartel, 2004). At this stage miRNA and siRNA pathways exhibit significant similarities. One of the main differences lies in the degree of complementarity between the small RNA guide and the target transcript. While siRNAs are commonly perfectly complementary to their targets, miRNA binding allows for numerous mismatches and non-Watson-Crick base pairing. Therefore it has proven difficult to confidently predict miRNA targets, even though miRNA target prediction algorithms have been significantly improved in recent years (discussed below). Since the degree of complementarity between a small RNA and its target seems to dictate the action of RISC, it has been shown that siRNAs may function as miRNAs if introduced in the appropriate cellular context (Doench et al., 2003). It is, however, unclear if this principle is notably biologically relevant.

Animal miRNAs are usually well conserved, even between evolutionary distant species. In contrast, very little inter-kingdom conservation is observed between plant and animal miRNAs. Coupled with distinct modes of miRNA actions in the two kingdoms, plant and animal miRNAs may have originated independently during evolution (Axtell and Bowman, 2008). Nevertheless, the extensive functional similarities between the RNA silencing core machineries allow for the interpretation that an archaic miRNA-like pathway had already been developed in the last common ancestor of plants and animals. Presumably, siRNA-mediated gene silencing was already established at this point since it appears to be the best conserved small RNA-mediated gene silencing mechanism between the plant and animal kingdoms. This may derive from an early necessity to protect organisms against viruses or selfish genetic elements (Shabalina and Koonin, 2008). The primary function of miRNAs on the other hand is to regulate endogenous gene expression. If proto-miRNAs were already present in the last common ancestor of plants and animals, these may have undergone rapid and far-reaching diversifications in order to meet the regulatory needs of the different ecologies connected with plant or animal evolution. In this model, the miRNA system could be of archaic origin, but today's plant and animal miRNAs may have diverged to a point, where ancestral sequence conservation may not be detectable anymore. Current knowledge permits for

both hypotheses, and future deep sequencing projects of ancestral organisms are likely to shed more light on this question. As yet, miRNAs and miRNA candidates have been identified in the single-cell alga *Chlamydomonas reinhardtii* and in the unicellular slime-mold *Dictyostelium discoideum* that both evolved only shortly after the divergence of the plant and animal kingdoms (Hinas et al., 2007; Hong et al., 2007; Molnár et al., 2007). A significant increase in miRNA repertoires is seen in bilaterians, whereas early-branching animals like *Amphimedon queenslandica* contain only few miRNAs (Grimson et al., 2008). This may reflect an increased necessesity for miRNA-mediated gene regulation in higher organisms and could also indicate that the diversification of miRNAs directly contributed to the emergence of more complex animal body plans (Shabalina and Koonin, 2008).

In the early stages of miRNA research new miRNAs were identified mainly bioinformatically based on their interspecies conservation and predicted precursor structures, or by large-scale Sanger sequencing of small RNA cDNA libraries. Thus, several hundred individual miRNA genes were discovered, biased towards highly expressed and evolutionary conserved miRNA species (Kim and Nam, 2006). Newly developed deep sequencing techniques later allowed for high-throughput analyses of small RNA transcriptomes and helped to verify many bioinformatically predicted miRNAs as well as to find new non-conserved miRNAs that had not been predicted at the time (Hafner et al., 2008; Chellappan and Jin, 2009). At present the numbers of confidently identified miRNA genes are in the range of 100-200 in plants, *C. elegans* and *Drosophila*, while the human genome may contain up to 500 individual miRNA genes (Bartel, 2009). Despite the large numbers of verified miRNAs, reliable information about the regulatory functions of individual miRNAs are still relatively sparse in comparison, due to difficulties in the identification of *bona fide* miRNA targets. Computational miRNA target prediction is reasonably straightforward in plants, where miRNAs bind to the coding regions of mRNAs with near-perfect complementarity to induce Ago-mediated cleavage (Axtell and Bowman, 2008). Plant miRNA-mediated translational repression has also been reported (Cheng et al., 2004; Brodersen et al., 2008), but still needs to be experimentally verified as a widespread phenomenon. Animal miRNA-target interactions are very flexible in contrast, which makes their prediction more cumbersome due to an increased potential for false-positive results (Bartel, 2009). A

large number of miRNA target prediction algorithms have been developed and constantly improved over the years [reviewed in (Chaudhuri and Chatterjee, 2007; Watanabe et al., 2007; Bartel, 2009)], so that animal miRNA-target interactions are relatively well defined today. Perfect pairing of nucleotides 2-7 of a miRNA (called the 'seed') is considered to be essential for productive miRNA binding (Bartel, 2009). Perfect seed pairing along with flexible complementarity of a miRNA's 3' portion to the target mRNA's 3' UTR constitute strong indications for productive miRNA-target interactions (Bartel, 2009), but experimental verifications are still necessary for each individual miRNA binding prediction. Yet, recent results based on the most comprehensive miRNA target prediction algorithms estimate a total of >45000 miRNA target sites within 3' UTRs of human mRNAs (Friedman et al., 2009). Furthermore, over 60 % of human protein-coding genes appear to have been under selective pressures to maintain pairing to miRNAs, underscoring the regulatory importance of this class of small RNA regulators (Friedman et al., 2009).

The precise mechanisms by which miRNAs direct posttranscriptional repression of target mRNAs are still under intense investigation and a number of possible models currently exist in parallel. A common feature of all these models is the imperfect binding of animal miRNAs to the 3' UTRs of their target mRNAs, even though miRNA binding has occasionally been observed in the coding regions or the 5' UTRs of specific mRNAs (Carthew and Sontheimer, 2009). Central bulges and mismatches in miRNA-mRNA duplexes exclude Ago-catalysed cleavage and rather promote suppression of target mRNA translation (Carthew and Sontheimer, 2009). The discussion about miRNA function is centred on the question, whether the miRNA-mediated translational repression occurs at translation initiation or postinitiation. Numerous studies presented incongruent data in favour of one or the other hypothesis, underlining the need for additional research in order to fully understand the scope of miRNA-directed gene regulation (Carthew and Sontheimer, 2009). Presently at least three competing and highly divergent models have been formulated to explain miRNA-mediated translational repression. The Mid domains of Ago proteins share homology with the cap-binding domain of eIF4E, so that eIF4E and miRNA-loaded Ago may compete for binding to the mRNA 5' cap structure (Carthew and Sontheimer, 2009). eIF4E is part of the eIF4F complex that recruits the 40S ribosomal subunit to an mRNA's 5' end. Hence,

if miRNA-Ago blocks the cap structure, ribosome assembly and translation initiation may be disturbed, resulting in reduced translational efficiency. In an alternative model, miRNA-Ago binding is proposed to stimulate deadenylation of the target mRNA, which may lead to mRNA decay or decreased translation efficiency by inhibiting mRNA circularisation (Carthew and Sontheimer, 2009). This model is supported by the fact that many miRNA-regulated mRNAs are found to be deadenylated *in vivo* (Carthew and Sontheimer, 2009). miRNA-mediated mRNA decay in animals is likely not a result of cleavage by miRNA-Ago, but of unspecific decapping and exonucleolytic degradation induced by deadenylation (Carthew and Sontheimer, 2009). It remains unclear, however, why some miRNA targets are degraded while others are stable, but quite possibly a combination of both pathways may account for the observed results. A third model for miRNA-mediated repression proposes that joining of the 60S ribosomal subunit to the 40S-mRNA complex may be blocked by an observed binding affinity of miRNA-Ago to the 60S ribosomal subunit and to eIF6, which is involved in the biogenesis and maturation of the 60S subunit (Carthew and Sontheimer, 2009). Many studies have provided evidence in favour and against each of the proposed models, underscoring that our understanding of miRNA-directed regulation is still rather poor (Carthew and Sontheimer, 2009). Complex patterns of spatiotemporally differential miRNA expres-sion in different cellular contexts make the finding of definite answers in these matters an intricate task.

1.4.3. piRNAs bind to Piwi proteins and act as master regulators of transposon silencing in animals

The latest addition to the catalogue of small silencing-associated RNAs are called Piwi-interacting RNAs (piRNAs), which have been identified in large numbers by deep sequencing of diverse animal model species.

We know today that the first example for piRNA-mediated transposon silencing was described in the early 1990s, when two papers reported on the *Drosophila* locus X-TAS at cytological position 1A as conferring the ability to silence the *P* element in the germline (Malone and Hannon, 2009). Similarly, regulation of several retrotransposons

of the *gypsy* family was appointed to the *flamenco* locus near the centromere of the X chromosome (Malone and Hannon, 2009). Unknown at the time, both loci correspond to piRNA clusters, pointing out a critical role for piRNAs in transposon silencing.

Transposons of various types inhabit eukaryotic genomes to varying extents. About 5 % of the *Drosophila* genome are composed of mobile genetic elements, whereas in mammals up to 50 % of the genome may be burdened with DNA transposons and retrotransposons (Kazazian, 2004; Malone and Hannon, 2009). Their ability to shape the contents of genomes implies transposons to constitute a critical driving force in eukaryotic evolution (Kazazian, 2004; Malone and Hannon, 2009). Nevertheless, tight control of transposon movement is essential for an organism's survival, thus preventing active transposons from destroying open reading frames and regulatory elements upon transposition. Therefore, eukaryotes have developed diverse strategies to silence transposable elements, including small RNA-mediated pathways. In plants, 24 nt siRNAs are the main regulators of the heterochromatic state of repetitive elements and exert their functions through association with ARGONAUTE 4 (AGO4). In *Drosophila* and *Danio rerio* repeat-associated siRNAs (ra-siRNAs) of 23-28 nt have been found in large numbers that exhibit a particular bias for germline expression (Farazi et al., 2008; Malone and Hannon, 2009). Like miRNAs, ra-siRNAs are genomically encoded, but their biogenesis and maturation are independent of Dicer, suggesting that they may derive from single-stranded precursors (Farazi et al., 2008). While the exact transcriptional mode of ra-siRNAs still needs to be determined, ra-siRNA production is dependent on members of the Piwi clade of the Ago/Piwi family. Those Ago/Piwi proteins most similar to *Arabidopsis* ARGONAUTE 1 (AGO1) constitute the Ago clade, whereas those Ago/Piwi proteins with highest similarities to *Drosophila* Piwi belong to the Piwi clade. Both clades share extensive structural homologies but differ greatly in their expression patterns and small RNA binding partners. Ago proteins are expressed ubiquitously and bind dsRNA-derived small RNAs (siRNAs and miRNAs), while Piwi proteins are exclusively expressed in the germline and have an affinity for single-stranded small RNAs (piRNAs) (Malone and Hannon, 2009). It was soon realised that *Drosophila* and zebrafish ra-siRNAs share germline-specific expression and Piwi association with other classes of small RNAs (*i.e.* 21U RNAs and scanRNAs), prompting to jointly refer to these Piwi-interacting small RNA families as piRNAs. The *C. elegans*

1. Introduction

21U RNAs are a startlingly diverse class of germline-specific 21 nt small RNAs that are produced from close to 16000 unique genomic loci in two broad regions on chromosome IV (Ruby et al., 2006; Batista et al., 2008). Common to all 21U RNAs are the presence of a 5' uridine residue, a methylated 3'-terminal ribose, and a conserved CTGTTTCA motif upstream of 21U RNA loci, but their sequences are highly divergent with no significant similarities between individual 21U RNA species (Ruby et al., 2006; Batista et al., 2008; Das et al., 2008). 21U RNAs associate with the *C. elegans* Piwi protein Piwi-Related Gene 1 (PRG-1), which is developmentally regulated and germline-specifically expressed. *prg-1* mutants accumulate a broad spectrum of germline defects that can be attributed to activation of mobile genetic elements and increased destructive transposition (Ruby et al., 2006; Batista et al., 2008; Das et al., 2008). Hence, the 21U RNAs may be regarded as the *C. elegans* piRNAs. A related family of small Piwi-associated RNAs was identified in *Tetrahymena thermophilia* (Farazi et al., 2008). The biogenesis of these scanRNAs (scnRNAs) is independent of Dicer, and they are involved in chromatin modification (Farazi et al., 2008).

The strong bias for a 5' uridine in many piRNA families is thought to be connected to a unique pathway of secondary piRNA biogenesis that shares certain analogies with transitivity of RNA silencing in plants. In the 'Ping-Pong' model (Figure 1.3 c) primary piRNAs of antisense orientation associate with *Drosophila* Piwi or the related Piwi-clade protein Aubergine (Aub) to target and cleave transposon mRNAs. The Piwi/Aub-piRNA complex cleaves targets at position 10 from the piRNAs's 5' ends. A second cleavage of the targets by a yet unkown endonuclease produces 21 nt sense piRNAs that are bound by Argonaute 3 (Ago3) (Brennecke et al., 2007). Ago3-piRNA can subsequently cleave a cognate putative primary antisense piRNA precursor transcript at position 10 of its bound secondary piRNA. Additional endonucleolytic cleavages, supposedly by the same predicted endonuclease responsible for secondary piRNA 3' end formation, would then in turn produce the 3' ends of *bona fide* primary piRNAs to be incorporated into Piwi/Aub (Brennecke et al., 2007). The Ping-Pong model accounts for several piRNA characteristics. In *Drosophila* antisense piRNAs are strongly biased to contain 5'-terminal uridines, which is not the case for secondary sense piRNAs. Instead, sense piRNAs commonly contain a conserved adenine at position 10 and overlap with antisense piRNA sequences by 10 nt (Brennecke et al., 2007). Co-immunoprecipitations

of Piwi, Aub, and Ago3 complexes furthermore showed distinct binding affinities of Piwi and Aub for antisense piRNAs, whereas Ago3 was found to preferentially bind secondary sense piRNAs (Brennecke et al., 2007). Functionally, the Ping-Pong system may serve to amplify an original piRNA response to transposon activation in order to ensure rapid downregulation of transposon mRNA. Nevertheless, Ping-Pong amplification has only been demonstrated in *Drosophila* and zebrafish (Brennecke et al., 2007; Houwing et al., 2008) and may hence not constitute a general feature of piRNA-mediated regulation.

Even though functions for piRNAs as regulators of transposon silencing and germline maintenance have been shown in many studies [(Malone and Hannon, 2009) and references therein], additional yet uncharacterised piRNA functions are expected, since large numbers of identified piRNAs do not map to known repetitive elements or transposons (Malone and Hannon, 2009). Identifying targets for these orphan piRNAs is likely to yield further fascinating insights into regulatory small RNA networks.

1.4.4. Common themes, daunting differences

Small RNA-mediated gene silencing has been revealed as a common eukaryotic strategy for transcriptional and posttranscriptional gene regulation, even though the RNA silencing machinery was partially or completely lost in certain eukaryotic lineages (Shabalina and Koonin, 2008). The core machinery of RNA silencing pathways shows many conserved features, like the involvement of Dicer homologues in the production of most small RNA species and the association of thus generated small RNAs with specific Ago/Piwi proteins to form active effector complexes. Nevertheless, many organisms developed unique variations of the RNA silencing theme. A number of excellent review articles on these topics have recently been published and some of them are herewith referred to for further reading (Pikaard et al., 2008; Vaucheret, 2008; Voinnet, 2008; Carthew and Sontheimer, 2009; Malone and Hannon, 2009; Ponting et al., 2009; Sonenberg and Hinnebusch, 2009; Voinnet, 2009; Waters and Storz, 2009).

1. Introduction

1.5. RNA silencing in plants

Plant RNA silencing pathways are among the best understood small RNA-mediated mechanisms of repressive gene regulation. Three distinct silencing pathways are discerned in plants, all with their own unique distinctions from respective homologous RNA silencing mechanisms in animals. In classical RNAi-like posttranscriptional gene silencing 21-24 nt siRNAs generated from dsRNA mediate target RNA cleavage through AGO1 actions. Plant PTGS has the ability to spread from cell to cell as well as from metabolic source to metabolic sink and can thus provide a flexible response to viral infection (Voinnet, 2005b; Xie and Guo, 2006; Kalantidis et al., 2008). Plant miRNAs associate with AGO1 or ARGONAUTE 10 (AGO10) and typically direct cleavage of target mRNAs. AGO4 is implicated in RITS-mediated chromatin regulation guided by 24 nt siRNAs (Qi and Hannon, 2005; Voinnet, 2009). The *Arabidopsis* genome contains four Dicer paralogues (DICER-LIKE 1-4) and 10 Ago paralogues (ARGONAUTE 1-10) that act cooperatively and/or distinctly in the different RNA silencing systems, while exhibiting significant functional redundancies. In addition, a variety of RNA-binding proteins as well as plant-specific RNA polymerases fulfill essential tasks in the establishment and maintenance of the three RNA silencing pathways (Margis et al., 2006; Vaucheret, 2008; Voinnet, 2008; Xie and Qi, 2008).

1.5.1. The four *Arabidopsis* DICER-LIKE proteins produce distinct species of plant siRNAs

Similar to other eukaryotes plant DICER-LIKE proteins constitute central players in diverse RNA silencing pathways that produce sundry species of small silencing-related RNAs. *Arabidopsis* DCL1-4 fulfill distinct, albeit partially redundant, functions and share a common domain composition (Figure 1.4 a). Phylogenetic analysis indicates that all higher plants contain multiple DICER-LIKE paralogues that can be grouped according to their similarities to *Arabidopsis* DCL1-4 (Margis et al., 2006; Casas-Mollano et al., 2008), which is exemplified for the 8 rice DICER-LIKE proteins in Figure 1.5 c. Early metazoans contained multiple Dicer genes that presumably acted in

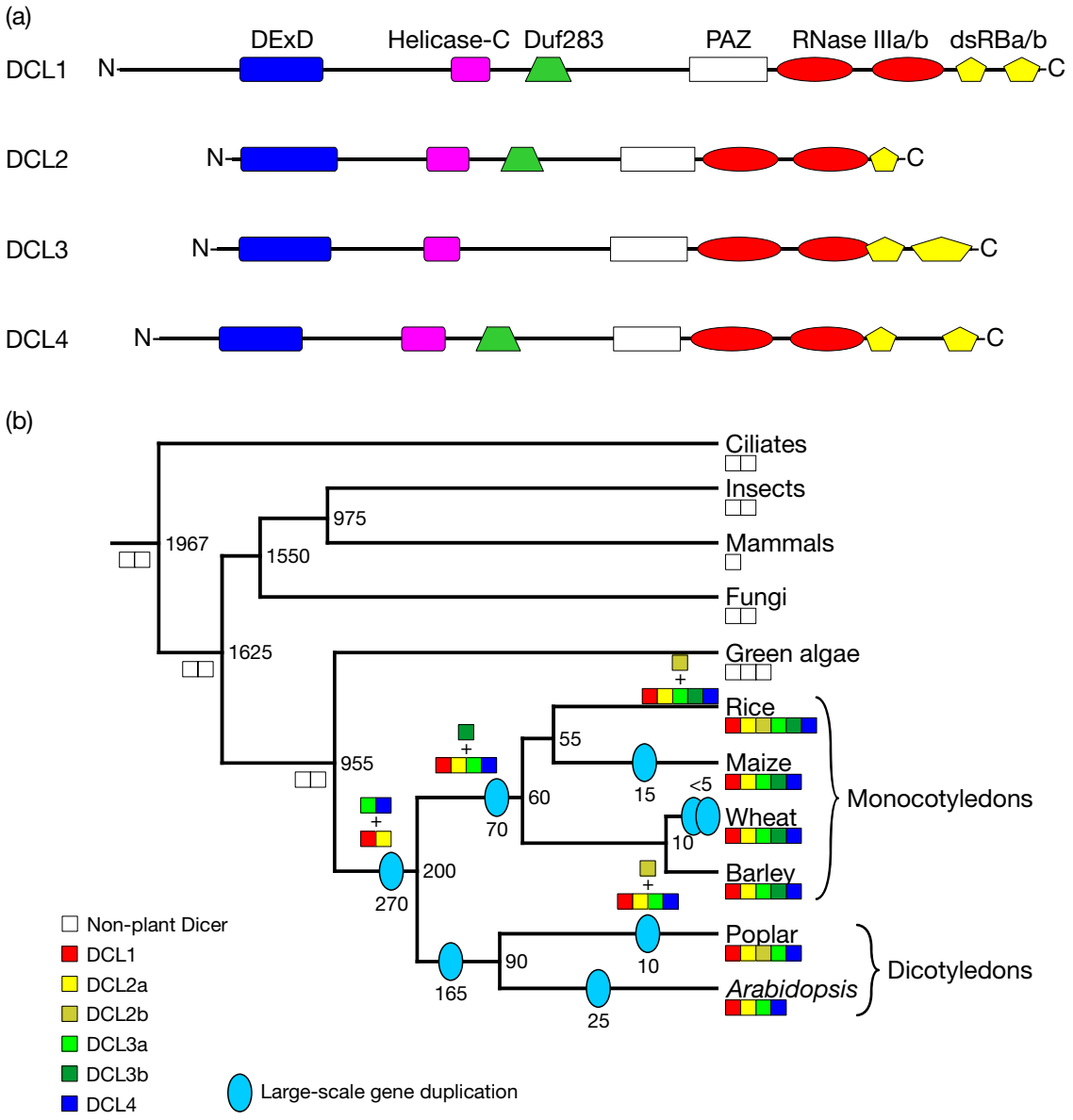

Figure 1.4 Domain structure of *Arabidopsis* DICER-LIKE proteins and evolution of Dicer enzymes in eukaryotes. **(a)** Schematic representation of the domain structures of the four *Arabidopsis* DICER-LIKE paralogues. Drawn to scale with respect to secondary protein structure. **(b)** Phylogenetic tree of Dicer genes, with emphasis on plant Dicer homologues. Numbers at the nodes and at the ellipses indicate time in million years before the present. Branch lengths are not drawn to scale. Plant DCL proteins are colour-coded, while non-plant Dicer homologues are depicted as white boxes. Blue ellipses stand for estimated large-scale gene duplication events during plant evolution.
(a) Based on data from Margis et al., 2006. (b) Modified from Margis et al., 2006.

diverse antiviral defence mechanisms (de Jong et al., 2009). During evolution, however, most of these Dicers were lost, and the last common ancestor of plants and animals probably contained two proto-Dicers of which one was lost in most animals and in the plant lineage (Margis et al., 2006). *C. reinhardtii* contains three *DICER-LIKE* genes that are not closely related to the plant DCL proteins and are presumably the results of

recent duplications. Hence, the plant DCLs diversified only after the split between higher plants and green algae (Casas-Mollano et al., 2008), but before the divergence of monocotyledons and dicotyledons [(Margis et al., 2006) and Figure 1.4 b]. Animal Dicers are mostly, but not exclusively, implicated in the production of miRNAs, while cellular defence mechanisms are exerted by specialised pathways like the interferon response or the adaptive antibody-based immune system in mammals. Since comparable systems are absent in plants, Dicer diversification may have been an evolutionary necessity to protect plants from diverse exogenous threats (Margis et al., 2006).

Arabidopsis DCL proteins have been studied in detail to elucidate their functional niches in the different RNA silencing pathways that operate in plants. DCL1 excises miRNAs from stem-loop-forming miRNA precursor transcripts. miRNA production is DCL1's primary role that cannot be compensated for by other DCL proteins (Blevins et al., 2006). DCL2 is responsible for nat-siRNA generation and produces 22 nt siRNAs from viruses (Blevins et al., 2006). The main biological role of DCL3 is the production of 24 nt ra-siRNAs derived from repetitive heterochromatinised DNA loci, but may also assist in antiviral defence (Blevins et al., 2006). Upon viral infection DCL4 is the primary *Arabidopsis* Dicer paralogue to bind virus-derived dsRNA for the production of 21 nt siRNAs in classical antiviral PTGS (Blevins et al., 2006). The DCL4-dependent 21 nt siRNAs also constitute the mobile signal in passive local RNA silencing spread, underscoring their importance in antiviral actions (Kalantidis et al., 2008). In addition, production of the endogenous ta-siRNAs is catalysed by DCL4 (Yoshikawa et al., 2005), and, exceptionally, miRNAs 822 and 839 are dependent on DCL4 rather than DCL1 (Ramachandran and Chen, 2008). While DCL proteins work specifically in the production of distinct families of endogenous small RNAs, their actions upon viral infections are cooperative and redundant. All DCLs participate in the generation of 21, 22, and 24 nt virus-derived siRNAs in the hierarchical order DCL4>DCL2>DCL3>DCL1 (Blevins et al., 2006). This, in combination with the observation that different subsets of DCL proteins fulfill primary roles in the defence against distinct viruses, underlines the necessity of plants to harbour multiple DICER-LIKE proteins in order to ensure an adequate protection against diverse exogenous threats (Blevins et al., 2006).

1.5.2. A multitude of ARGONAUTE proteins as integral players in RNA-directed regulatory pathways

Arabidopsis AGO1, the founding member of the Ago protein family, was first identified as a factor controlling leaf development, with *ago1* mutants exhibiting defects in general plant architecture as well as distinct leaf malformations reminding of the tentacles of the squid genus *Argonauta* (Bohmert et al., 1998). Not known at the time, the observed phenotypic alterations in *ago1* mutants reflect disturbed miRNA-mediated gene regulation (Vaucheret et al., 2004). Today we know that Ago/Piwi proteins are at the heart of all RNA silencing pathways involving small RNAs (Vaucheret, 2008). Numbers and diversity of Ago/Piwi proteins vary greatly between organisms, reflecting specialisations and adaptions of RNA silencing systems throughout evolution. The budding yeast *Saccharomyces cerevisiae* appears to have completely lost Ago/Piwi proteins and consequently does not bear functional RNA silencing systems. *S. pombe* contains a single Ago protein conveying transcriptional and posttranscriptional gene silencing (Gobeil et al., 2008; Vaucheret, 2008). Several Ago/Piwi proteins are present in animals, including 18 *C. elegans*-specific Class 3 Ago proteins (Vaucheret, 2008). Plants do not contain any member of the Piwi clade, but instead encode multiple *AGO* paralogues that can be phylogenetically subdivided into four distinct clades, based on full protein alignments of the 10 *Arabidopsis* and the 19 *O. sativa* Ago proteins [Figure 1.5 a and (Kapoor et al., 2008)]. The different phylogenetic clades reflect related functional characteristics of the respective *Arabidopsis* Ago proteins.

AGO1 is considered to be the primary silencing-related Ago protein in *Arabidopsis*, since it was found to associate with transgene-derived siRNAs, virus-derived siRNAs, ta-siRNAs, and miRNAs. Biochemically AGO1 shows a preference for a 5' uridine in small RNAs and is therefore mostly found to be associated with miRNAs, which in plants are significantly enriched for 5' uridine residues (Vaucheret, 2008). AGO1 homeostasis is, at least partially, directed by miRNA 168 that regulates the *AGO1* mRNA, thus providing tight control of *AGO1* expression levels; an important factor for properly balanced miRNA steady-state levels (Vaucheret, 2008). AGO10 is the closest AGO1 paralogue providing partial functional redundancies. It was reported that the expression levels of miRNA 165/166 are increased in *ago10* mutants, suggesting that

AGO10 may play a role in the repression of these miRNAs (Liu et al., 2008). The actual molecular functions of AGO10 have, however, not been determined yet (Vaucheret, 2008). AGO5 is closely related to both AGO1 and AGO10, but its precise role in RNA silencing remains unclear. No obvious developmental phenotypes have been found in *ago5* mutants, but biochemically AGO5 appears to have a preference for small RNAs with a 5' cytidine. miRNA 169 is one of the few miRNAs containing such a 5' cytidine, but a biologically productive interaction between AGO5 and miRNA 169 has not been reported so far (Vaucheret, 2008). AGO7 plays an important role in *Arabidopsis* developmental timing, *i.e.* correct temporal regulation of the transitions from juvenile to adult and from adult to vegetative states (Hunter et al., 2003). Loss-of-function *ago7* mutants exhibit a precocious juvenile to adult state transition caused by the loss of the ta-siRNAs generated from the *TAS3* locus (Vaucheret, 2008). This connection is explained by the specific interaction of AGO7 with miRNA 390, which guides the initial cleavage of the *TAS3* ta-siRNA precursor transcript (Montgomery et al., 2008). *TAS3*-derived ta-siRNAs target genes temporally controlling the juvenile/adult state transition. Functions for AGO2 and AGO3 have not been reported to date. Both proteins are highly similar and encoded in a close tandem, suggesting that they are the result of an evolutionary recent duplication and supposedly elicit related functions (Vaucheret, 2008). Similarly, AGO8 and AGO9 may also be the result of a recent duplication event. Loss-of-function mutants of *ago2*, *ago3*, *ago8*, and *ago9* all fail to exhibit obvious developmental phenotypes (Vaucheret, 2008). AGO4 is the primary *Arabidopsis* Ago protein mediating TGS. AGO4 localises to nuclear structures called Cajal Bodies along with the large subunit of NUCLEAR RNA POLYMERASE D 1A (Pol IV), RNA-DEPENDENT RNA POLYMERASE 2 (RDR2), DCL3, and endogenous 24 nt siRNAs that are the hallmarks of transcriptional gene silencing. 24 nt siRNA-loaded AGO4 cleaves heterochromatin-derived nascent transcripts and recruits chromatin remodelling proteins to heterochromatic loci (Vaucheret, 2008). Even though AGO4 was found to bind miRNAs 172 and 390 in immunoprecipitation studies, this association is likely not biologically productive, since *ago4* mutants do not exhibit the miRNA 172/390-associated phenotypic alterations (Vaucheret, 2008). Interestingly, AGO4 was found to be required for resistance to *Pseudomonas syringae* in *Arabidopsis* (Agorio and Vera, 2007), suggesting additional functions of AGO4 that have yet to be determined. AGO6

1. Introduction

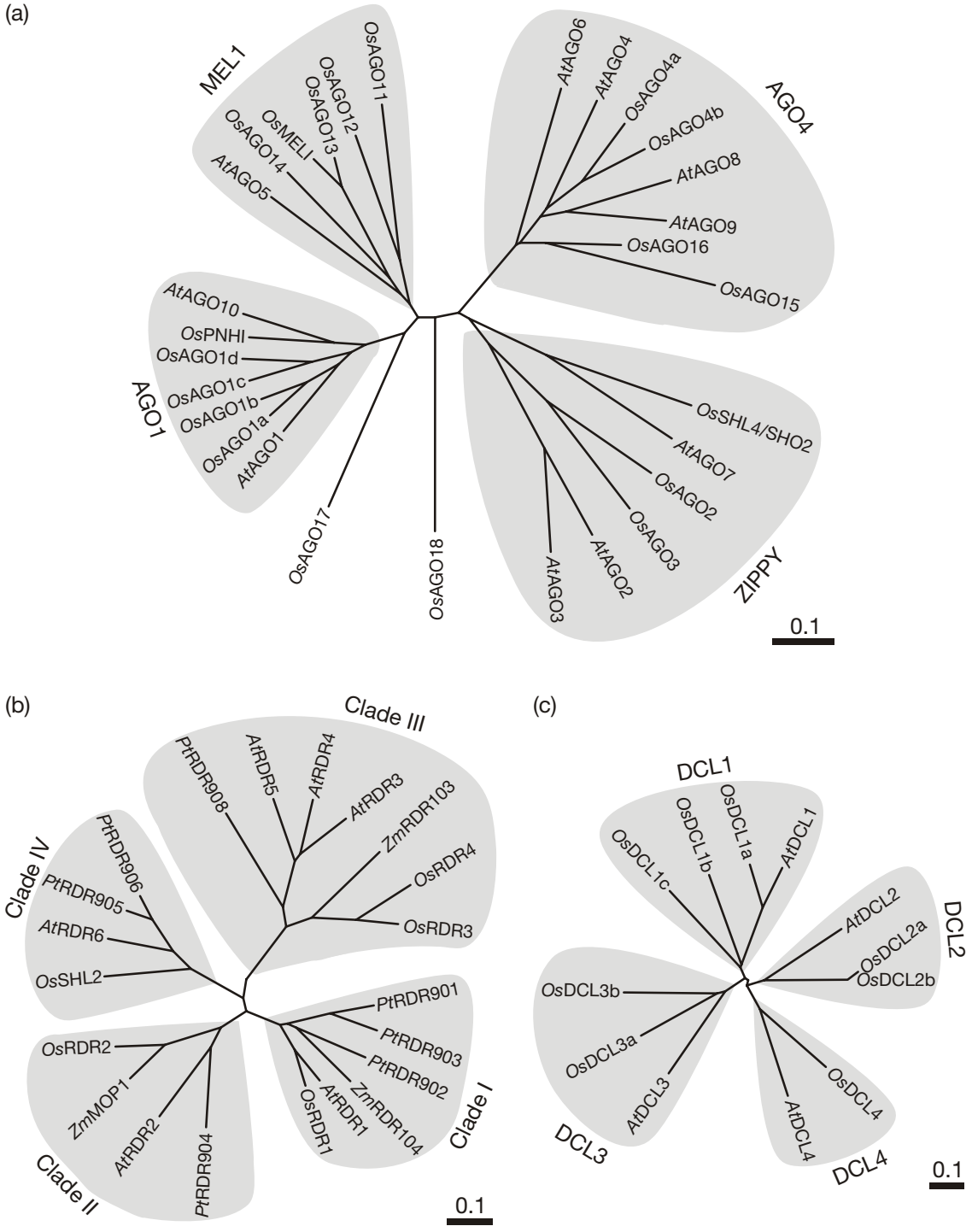

Figure 1.5 Phylogenetic analysis of plant AGO, DCL, and RDR proteins. Unrooted trees constructed by alignment of full-length protein sequences. **(a)** Phylogenetic relationships between rice (*Os*) and *Arabidopsis* (*At*) AGO proteins, divided into four clades. Three clades are defined by similarities with *Arabidopsis* AGO1, AGO4, and ZIPPY (AGO7). The fourth clade contains AGO members most similar to rice MEL1. **(b)** Evolutionary relations between rice, *Arabidopsis*, maize (*Zm*), and poplar (*Pt*) RDR proteins in four distinct clades. **(c)** Phylogenetic tree of rice and *Arabidopsis* DCL proteins. DCL proteins can be divided into four clades based on their similarities to *Arabidopsis* DCL1-4. Scale bars in each panel represent 0.1 amino acid substitutions per site.
Modified from Kapoor et al., 2008.

has been reported to be important for the accumulation of specific heterochromatin-related siRNAs and to be functionally redundant to AGO4 (Zheng et al., 2007). Even though exhaustive functional analyses of Ago proteins in other plant species have not been reported yet, it can be expected that many of them will show functionalities analogous to their *Arabidopsis* homologues.

1.5.3. Additional factors involved in small RNA production, modification, and stability as well as amplified RNA silencing

Small RNA production and functionality depend on a variety of co-factors additional to DCL and AGO proteins. Plant small RNAs can be differentiated from most animal and fungal small RNAs by the presence of a 2'-*O*-methylated ribose at their 3' ends. Originally discovered as a modification of plant miRNAs (Yu et al., 2005) it was later realised that methylation of the 3' end is a joint feature of all plant silencing-related small RNAs (Li et al., 2005; Yang et al., 2006c). The modification is mediated by the methyltransferase HUA ENHANCER 1 (HEN1) in *Arabidopsis* and occurs downstream of DCL-mediated small RNA production. Loss-of-function *hen1* mutants are characterised by a reduction in small RNA steady-state levels. The remaining small RNAs are frequently heterogeneously elongated due to polyadenylation (Li et al., 2005). It was inferred from these results that 3' end 2'-*O*-methylation may protect plant small RNAs from being targeted for degradation by polyadenlyation (Li et al., 2005). It was subsequently shown that animal HEN1 orthologues catalyse the same 3' end modification in the case of piRNAs (Horwich et al., 2007; Kirino and Mourelatos, 2007; Saito et al., 2007; Kurth and Mochizuki, 2009). The dsRNA-binding protein HYPONASTIC LEAVES 1 (HYL1) is an important factor in *Arabidopsis* development, with *hyl1* mutants exhibiting widespread pleiotropic defects (Lu and Fedoroff, 2000). The observed defects in *hyl1* mutants are likely the results of disturbed miRNA-mediated regulation (Han et al., 2004; Vazquez et al., 2004), and HYL1 was accordingly shown to specifically interact with DCL1 and assist in the precise processing of pri-miRNAs (Hiraguri et al., 2005; Kurihara et al., 2006). The HYL1-DCL1 complex localises to nuclear Dicing Bodies that are distinct from Cajal Bodies and constitute the

sites of primary miRNA processing (Fang and Spector, 2007; Song et al., 2007). Productive pri-miRNA processing is also dependent on interaction of the HYL1-DCL1 complex with SERRATE (SE), a zinc finger protein that physically interacts with HYL1 (Lobbes et al., 2006; Yang et al., 2006a; Dong et al., 2008; Laubinger et al., 2008). Mature plant miRNAs are exported to the cytoplasm by the Exportin-5 orthologue HASTY (HST), whose loss of function leads to premature shoot maturation in *Arabidopsis* and hence connects it with developmental timing like AGO7 in the ta-siRNA pathway (Telfer and Poethig, 1998; Peragine et al., 2004; Park et al., 2005). In the cytoplasm RISC cleavage products are typically degraded sequence-independently by EXORIBONUCLEASE 2-4 (XRN2-4) as part of the regular cellular RNA turnover pathways. XRN2-4 compete with RNA-DEPENDENT RNA POLYMERASE 6 (RDR6) for binding to these cleavage products and thus prevent uncontrolled amplification of the respective silencing responses (Voinnet, 2008).

Arabidopsis encodes six RdRPs that can be phylogenetically grouped into four distinct clades in comparison to their homologues in other plant species (Figure 1.5 b). RNA-DEPENDENT RNA POLYMERASE 3-5 (RDR3-5), also known as RDR3a-c, have not been functionally characterised yet (Herr, 2005). *Arabidopsis* RDR6 and RNA-DEPENDENT RNA POLYMERASE 1 (RDR1) are critical components in PTGS-mediated antiviral defence and transgene silencing, whereas RDR2 acts predominantly during TGS (Herr, 2005; Voinnet, 2008). In general, RDRs facilitate RNA silencing by amplifying the silencing response initiated by small amounts of trigger RNAs like transposon- and virus-derived small RNAs. This amplification is accomplished by RNA-primed or unprimed synthesis of dsRNA that can serve as additional DCL substrate for the production of secondary small RNAs (Voinnet, 2008). RDR substrates can be the cleavage products of siRNA- and miRNA-mediated RISC and RITS complex actions, as well as aberrant RNAs of unknown identities that may occur during transgene silencing. RDR-dependent dsRNA production from RISC cleavage products is an important factor in the phenomenon of transitivity, in which the sequence specificity of RNA silencing spreads from the originally targeted primary siRNA-complementary sites to upstream and downstream regions that are not recognised by the original silencing triggers (Voinnet, 2008). Typically, the different RDRs are functionally coupled to specific DCL/AGO proteins, reflecting their roles in distinct pathways. DCL3

and AGO4 mediate transcriptional silencing of transposons and repetitive elements, and this regulation depends on RDR2. The DCL1-dependent miRNA pathway has not been found to be associated with RDR functions. The functions of RDR6 in transgene- and virus-induced PTGS are associated with downstream activities of DCL4 and AGO1 (Voinnet, 2008). Important additional functions of RDR6 comprise ta-siRNA and nat-siRNA production (discussed above) as well as systemic RNA silencing (discussed below). Generation of dsRNA from ta-siRNA precursor transcripts requires the coiled-coil protein SUPPRESSOR OF GENE SILENCING 3 (SGS3) and possibly SILENCING-DEFICIENT 5 (SDE5) (Mallory and Bouché, 2008). DCL4 interacts with DOUBLE-STRANDED RNA-BINDING PROTEIN 4 (DRB4) during the subsequent production of mature ta-siRNAs (Mallory and Bouché, 2008), and DRB4 is also critical for the accumulation of viral or hairpin-derived DCL4-dependent 21 nt siRNAs (Curtin et al., 2008). The exact modes of operation of SGS3, SDE5, and DRB4 have yet to be determined to define their roles in small RNA production. RDR2 is required for the production of 24 nt siRNAs in *Arabidopsis* and is thus mainly involved in TGS amplification (Herr, 2005). AGO4/6-cleaved nascent heterochromatin-derived transcripts are believed to constitute the substrates for RDR2 actions, and methylation of the respective genomic loci is dependent on the putative chromosome architecture protein DEFECTIVE IN MERISTEM SILENCING 3 (Voinnet, 2008). There are no evidence for physical interactions between DCL and RDR proteins. It is therefore likely that their functional coupling is a result of co-localisation (Voinnet, 2008). Despite their associations with specific DCL/AGO proteins and separate modes of operation, there may be partial overlaps and redundancies between RDR functions (Voinnet, 2008). Apart from RNA silencing pathways RDRs are likely to be implicated in additional cellular and developmental contexts that await further experimentation. In this light, recent studies showed that RDR6 expression is controlled by abcisic acid, a major stress hormone (Yang et al., 2008), RDR1 plays a role in defence against herbivores (Pandey and Baldwin, 2007), and RDR2 is implicated in UV protection (Pandey and Baldwin, 2008).

Plant heterochromatin is not completely transcriptionally silent, since maintenance and *de novo* methylation of repetitive elements and transposon loci through the actions of DCL3 and AGO4 require active transcription from those loci to produce precursors for

the 24 nt siRNAs that guide TGS. TGS-related transcription of heterochromatic regions is accomplished by plant-specific RNA polymerases with overlapping but distinct functions (Herr et al., 2005; Onodera et al., 2005). NRPD1a and NRPD1b, which are nowadays referred to as Pol IV and Pol V, respectively (Wierzbicki et al., 2008), show significant asymmetries in their activities (Pikaard et al., 2008). Of the roughly 4600 *Arabidopsis* loci that give rise to 24 nt siRNAs >90 % depend on transcription by Pol IV, and about 30 % require the activities of both Pol IV and Pol V, whereas none of these loci appear to be transcribed by Pol V alone (Pikaard et al., 2008). The SNF2 domain-containing putative chromatin-remodelling protein CLASSY1 (CLSY1) co-localises with RDR2 and is important for its localisation. CLSY1 appears to function at the interface between Pol IV and RDR2 and presumably facilitates the generation of dsRNA from Pol IV-dependent transcripts following cleavage by AGO4 (Smith et al., 2007; Pikaard et al., 2008).

Future research is likely to yield additional DCL, AGO, and RDR co-factors that fulfill important tasks in small RNA production, silencing amplification, and the actions of the different effector complexes. A deeper understanding of these co-factors and their interrelations are essential for a comprehensive evaluation of the complex RNA silencing networks that operate in plants

1.5.4. Local and systemic RNA silencing movement are important features in antiviral defence

In contrast to most organisms, with the exception of nematodes, plants have developed unique systems of RNA silencing movement that are crucial components of antiviral defence. RNA silencing movement in plants constitutes the spread of diverse mobile silencing signals from cells in which RNA silencing was initiated to recipient cells not exposed to the respective silencing triggers. In this way, large populations of cells, and subsequently the whole plant, are able to initiate global silencing responses directed against exogenous threats perceived at local points of infections.

Plant RNA silencing movement can be differentiated into three distinct systems (Figure 1.6). Short-range local silencing spread (SLSS) is based on passive transport of

small RNAs through plasmodesmata and has a limited radius of 10-15 cells from the source of the silencing signal (Kalantidis et al., 2008). Extensive local silencing spread (ELSS) is a result of RDR6-dependent amplified RNA silencing and is able to engulf the whole leaf blade (Kalantidis et al., 2008). Systemic silencing is the least well understood silencing movement pathway and is characterised by the transport of mobile silencing signals from metabolic source to metabolic sink through the phloem (Kalantidis et al., 2007). Although RNA silencing movement is frequently observed during co-suppression in transgenic plants and can be artificially induced by *Agrobacterium*-mediated overexpression of sense, antisense, and hairpin transcripts viruses, transposons, and T-DNA-containing genes are the known naturally occurring triggers of RNA silencing spread (Dunoyer et al., 2007), reflecting its role as a defence mechanism against exogenous threats.

Short-range local silencing spread can be seen as the first step of a plant immune response when faced with an invading pathogen (Bagasra and Prilliman, 2004). Depending on quality and quantity of a perceived threat, a systemic silencing response may be initiated, if silencing-inducing features overcome a certain threshold (Kalantidis et al., 2006), even though the precise nature of this systemic silencing threshold and its regulation remain to be uncovered. If the criteria for the induction of systemic silencing spread are not met, local RNA silencing and SLSS may be sufficient to contain a minor infection (Kalantidis et al., 2006). Interestingly, mature guard cells of stomata are refractory to mobile short-range silencing signals (Voinnet et al., 1998; Himber et al., 2003; Kalantidis et al., 2006). During differentiation guard cells become symplastically isolated by blockage of the plasmodesmata, which are cytoplasmic channels connecting all neighbouring plant cells. Hence, the mobile short-range silencing signal is believed to pass from cell to cell through plasmodesmata (Voinnet et al., 1998; Himber et al., 2003; Kalantidis et al., 2006). This movement is dependent on the aperture of the plasmodesmata, and the mobile short-range silencing signal was shown to have a general plasmodesmata-passing mobility similar to proteins of 27-54 kDa (Kobayashi and Zambryski, 2007). The restriction of SLSS to 10-15 cells might hence be the result of plasmodesmata closure surrounding sites of perceived infections as a measure to inhibit cell-to-cell spread of infectious particles.

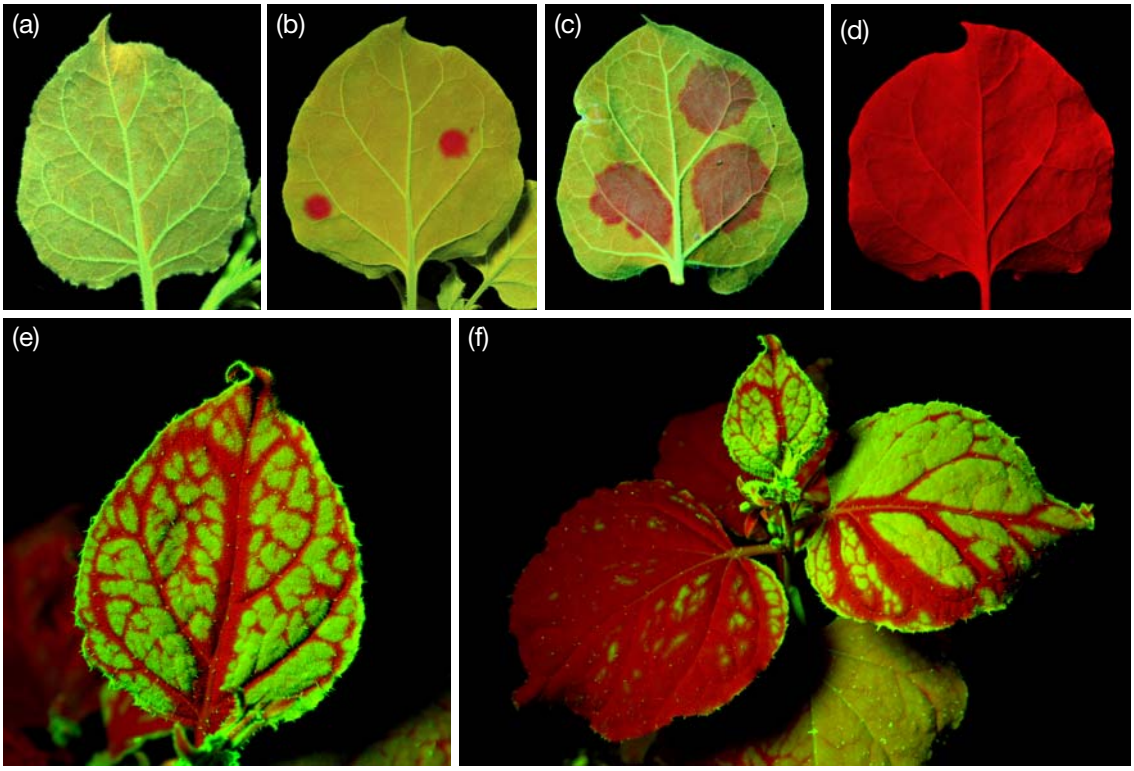

Figure 1.6 Manifestations of RNA silencing of a *GFP* transgene in *N. benthamiana.* **(a)** Not silenced. **(b)** Spontaneous short-range local silencing. **(c)** Agro-infiltration-induced local silencing. **(d)** Fully silenced. **(e)** Systemic silencing. **(f)** Systemic (centre and right leaves) and extensive local silencing (left leaf).
Modified from Kalantidis et al., 2008.

The genetic requirements of SLSS have been studied in detail, showing its dependence on most components of the siRNA-mediated PTGS pathway. The ability for SLSS is specifically lost in *dcl4* mutants, which is strong evidence for 21 nt siRNAs constituting the mobile short-range silencing signals (Dunoyer et al., 2005). In addition, HEN1, DRB4, and AGO1 have been shown to influence SLSS (Hiraguri et al., 2005; Adenot et al., 2006; Jones et al., 2006; Yang et al., 2006c; Dunoyer et al., 2007; Nakazawa et al., 2007), which is not surprising, since they are all crucial components in siRNA-mediated RNA silencing. More unanticipated was the dependence of SLSS on Pol IV, RDR2, and CLSY1, which are components of the 24 nt siRNA-mediated TGS pathway (Dunoyer et al., 2007; Smith et al., 2007). The exact mechanisms how these TGS-related proteins influence RNA silencing spread are still unclear, but it can be expected that SLSS depends on regulated and accurate cross-talk of the overlapping and interconnected RNA silencing pathways operating in plants.

Extensive local silencing spread bears many similarities with SLSS, but it is not subject to the limited range of 10-15 cells. ELSS is characteristic of sink tissues that have perceived mobile systemic silencing signals and depends on the activities of RDR6 and, to a lesser extent, the putative RNA helicase SILENCING-DEFICIENT 3 (Kalantidis et al., 2008). It remains to be investigated why ELSS is observed exclusively in sink tissues that are recipients of the mobile systemic silencing signals, but never in leaves, where the potential threats (*i.e.* viruses or hairpin transcripts in agro-infiltration experiments) are originally perceived.

Systemic RNA silencing spread may be regarded as the plant's most important system to counteract viral infections. Replicating plant viruses are typically mobile and spread from cell to cell as well as through the entire plant from singular points of infections. Plants therefore depend on a defensive system that communicates the identity of an invading pathogen to the entire organism in order to prime an immune response. Although the nature of the systemic silencing signal is still unknown, it is widely accepted that it consists of RNA or at least comprises an RNA component conferring sequence specificity (Jorgensen et al., 1998). Unlike in local silencing spread, siRNAs have been shown to not constitute the mobile signal of systemic silencing (Mallory et al., 2003). It is possible that there are multiple systemic silencing signals working in concert (Fagard and Vaucheret, 2000; Voinnet, 2005b), which will make their identification difficult to achieve in forward genetics screens, since the loss of one type of mobile signal may be compensated by others. RDR6 has been shown to be essential for the reception of the mobile silencing signal, but not for its production (Xie and Guo, 2006). This could indicate that the RNA component of the mobile silencing signal is, at least partially, single-stranded and would hence depend on RDR6 activity to be converted to dsRNA before entering the defensive silencing pathways in recipient tissues. The systemic silencing signal was early-on proposed to move through the phloem system that transports metabolites from source to sink tissues (Voinnet and Baulcombe, 1997; Fagard and Vaucheret, 2000; Mlotshwa et al., 2002). This notion was confirmed by works of Tournier et al. (2006), who also showed that the mobile silencing signal can actually travel from top to bottom of a plant, as long as sink-source relationships are altered accordingly (Tournier et al., 2006). Several species of small RNAs have been identified in phloem sap of curcurbits, including miRNAs and endogenous siRNAs,

along with the protein PHLOEM SMALL RNA-BINDING PROTEIN 1 that was shown to bind small RNAs in the phloem and to facilitate the movement of small single-stranded RNA molecules from cell to cell (Yoo et al., 2004). It is not clear, however, if these findings stand in direct relation to the mobile systemic silencing signal. Identification of this mobile signal is one of the major tasks remaining to understand the full scope of antiviral RNA silencing movement in plants.

1.6. Viruses encode suppressors of RNA silencing to overcome the hosts's immune responses

Since RNA silencing constitutes the plant's primary antiviral defence system, it is not surprising that viruses have developed strategies to counteract the hosts's silencing responses in order to facilitate viral replication, cell-to-cell movement, and systemic long-distance spread. Viral suppressors of silencing (VSRs) have been known for a long time as viral pathogenicity determinants and movement proteins, which only in recent years were realised to act as antagonists of the hosts's RNA silencing systems (Díaz-Pendón and Ding, 2008). All plant viruses are believed to encode for at least one suppressor of silencing of different types.

VSRs can be loosely divided into three categories depending on the functions they facilitate during the viruses's life cycles (Díaz-Pendón and Ding, 2008). Class I VSRs suppress the hosts's abilities for local antiviral silencing, thus leading to enhanced viral replication and increased virus titres. Class I VSRs comprise the potyviral helper component-proteinase (HC-Pro) and the tobamoviral p126 (Díaz-Pendón and Ding, 2008). HC-Pro has been extensively studied and may suppress local RNA silencing by preventing RISC assembly (Ebhardt et al., 2005). Additionally, HC-Pro was shown to bind siRNAs *in vitro* (Mérai et al., 2006; Yu et al., 2006; Shiboleth et al., 2007), similar to p126. Thus, HC-Pro and p126 and their homologues are indicated to inhibit the HEN1-mediated methylation of siRNAs and miRNAs, thereby negatively influencing small RNA stability (Blevins et al., 2006; Csorba et al., 2007; Vogler et al., 2007). Poleoviral P0 employs a distinct strategy of silencing suppression by inducing proteolytic degradation of AGO1 upon interaction (Pfeffer et al., 2002; Pazhouhandeh et al., 2006; Baumberger

et al., 2007; Bortolamiol et al., 2007). Class II VSRs do not facilitate viral replication but are instead implicated in suppressing local RNA silencing spread. Potexviral p25 for example interferes with either assembly or function of RISC (Bayne et al., 2005), in addition to its role as a viral movement protein that facilitates plasmodesmatal translocation and thus cell-to-cell movement of the virus (Díaz-Pendón and Ding, 2008). Most known VSRs belong to Class III and are characterised by the ability to suppress systemic RNA silencing spread. Conversely, they do not appear to be implicated in viral replication or local silencing movement (Díaz-Pendón and Ding, 2008). Prominent examples of Class III VSRs are the well-studied cucumoviral protein 2b, the tombusviral P19, and the carmoviral p38 (Díaz-Pendón and Ding, 2008). Small RNA binding is a common strategy employed by these VSRs. P19 is known to sequester siRNAs, thus preventing their use in RISC-mediated antiviral silencing (Silhavy et al., 2002; Ye et al., 2003; Lakatos et al., 2004; Lakatos et al., 2006). 2b and p38 block the production of siRNAs with similar effects (Ji and Ding, 2001; Guo and Ding, 2002; Soards et al., 2002; Qu et al., 2003; Thomas et al., 2003; Diaz-Pendon et al., 2007). In addition, 2b is also known to suppress the use of already produced siRNAs by interfering with AGO1 function (Zhang et al., 2006). Since siRNAs do not constitute the systemic mobile silencing signal, it still has to be determined how the activities of Class III VSRs prevent systemic silencing spread. Presumably, these VSRs intervene at an early stage of the antiviral response and thus prevent the mobile signal from being produced.

Traditionally most research on viral suppressors of RNA silencing has been conducted in plants, but the phenomenon is not restricted to plant viruses (Li et al., 2002; Bucher et al., 2004; Delgadillo et al., 2004; Chen et al., 2008). The extensive utilisation of repressive small RNA pathways in many cellular functions has naturally raised questions regarding the endogenous regulation of these mechanisms, leading to the identification of a variety of endogenous suppressors of silencing.

1.7. Endogenous suppressors of RNA silencing

In addition to the numerous viral suppressors of silencing, intensive research has been undertaken to identify endogenous proteins that may be regarded as suppressors of the

RNA silencing system. Nevertheless, only a handful of potential endogenous silencing suppressors have been identified to date.

The plant calmodulin-like Ca^{2+} sensor protein REGULATOR OF GENE SILENCING – CALMODULIN-LIKE (rgs-CaM) was the first endogenous factor to be implicated as a silencing suppressor (Anandalakshmi et al., 2000). rgs-CaM was found to be upregulated in response to HC-Pro expression upon viral infection, and ectopic overexpression of rgs-CaM in transgenic plants resulted in the establishment of symptoms partially similar those caused by HC-Pro-containing viruses, even in the absence of a respective virus (Anandalakshmi et al., 2000). Another endogenous plant protein implicated in RNA silencing suppression is RNASE L INHIBITOR 2 (ATRLI2) that is transcriptionally upregulated in plants undergoing RNA silencing (Braz et al., 2004; Sarmiento et al., 2006). *Arabidopsis xrn4* mutants exhibit an increased efficiency of RNA silencing, which may result from an increased accessibility of uncapped mRNAs and miRNA cleavage products for RDR-mediated dsRNA production (Gazzani et al., 2004). Similar results have been presented for XRN2 and XRN3 (Gy et al., 2007). In the same pathway FRY1 (3'(2'), 5'-BISPHOSPHATE NUCLEOTIDASE/INOSITOL POLY-PHOSPHATE 1-PHOSPHATASE) was implicated to confer silencing suppression functionality (Gy et al., 2007). In *C. elegans* loss of the RdRP homologue RRF-3 (RNA-dependent RNA Polymerase Family 3) leads to hypersensitivity towards RNAi (Simmer et al., 2002). It should be noted, however, that the observed characterstics that lead to the annotation of the aforementioned proteins as silencing suppressors are almost exclusively the results of secondary effects or severely disturbed regulatory pathways, making the definition of the respective genes as *bona fide* silencing suppressors difficult to corroborate. Solid evidence have been presented for a repressive effect on RNA silencing when rgs-CaM is overexpressed, mimicking the effect induced by viral HC-Pro expression (Anandalakshmi et al., 2000). Yet, no further studies have been undertaken to elucidate the exact mechanism involved. It must therefore be presumed that the observed silencing suppressor characteristics are secondary effects resulting from disturbances in the plant's complex Ca^{2+} signaling networks (Luan et al., 2002) rather than a primary function of rgs-CaM. In the case of ATRLI2, the observed silencing suppressor activities can only be described as very mild, and no working model has been proposed (Sarmiento et al., 2006) that would justify annotation of ATRLI2 as a *bona fide*

endogenous silencing suppressor. As for XRN2-4 and FRY1, RNA silencing enhancement as a result of loss of function of the respective proteins can be attributed to suppressed default mRNA turnover and quality control mechanisms, thereby allowing 'aberrant' RNA to accumulate and be more readily available for RDR-mediated dsRNA production. Hence, these are secondary effects, and the primary roles of XRN2-4 and FRY1 do not constitute silencing suppression. For *C. elegans* RRF-3 Simmer et al. (2002) proposed that the RdRP homologues RRF-1 and EGO-1 (Enhancer of Glp-One 1) compete with RRF-3 for core components of the RNAi pathway, indicating that the observed RNAi hypersensitity in rrf-3 loss-of-function mutants is the result of a shift in the availability of RNAi components towards RRF-1- and EGO-1-dependent pathways (Simmer et al., 2002). Taken together, all the described endogenous suppressors of RNA silencing have been annotated as such on the basis of secondary effects that do not reflect their primary biological roles.

The first report of a putative *bona fide* endogenous suppressor of silencing came from work in *C. elegans*, where the 3'-5' exonuclease ERI-1 (Enhanced RNAi 1) had been found to negatively affect RNAi through an siRNA-degrading functionality (Kennedy et al., 2004). This function was established by the observations that RNAi is significantly enhanced in *eri-1* mutants and that recombinant ERI-1 protein is able to bind and degrade siRNAs *in vitro* (Kennedy et al., 2004). Numerous studies followed that consolidated ERI-1's role as a factor with a primary role in negative RNA silencing regulation, not only in *C. elegans*, but also across kingdoms. *C. elegans* ERI-1 has been shown to interact physically with DCR-1, but interestingly this is only the case for the longer of two *C. elegans* ERI-1 isoforms (ERI-1b) (Duchaine et al., 2006). Unfortunately, differential functional analyses of ERI-1a and ERI-1b have not been reported to date, but both ERI-1 isoforms are predicted to fulfill different, yet related, tasks in *C. elegans* RNAi regulation (Duchaine et al., 2006). In agreement with these results, *eri-1* mutants are hypersensitive towards viral infection (Schott et al., 2005; Wilkins et al., 2005). ERI-1 is phylogenetically conserved and its homologues have been intensely studied in diverse model organisms. Mouse Eri1 has been reported to be induced by high doses of transfected siRNAs and thus being responsible for the so-called 'rebound effect' (Hong et al., 2005). It was observed that initial RNAi-mediated suppression of target genes subsequent to transfection of respective siRNAs reverts after several days, and this

reversal of RNAi-targeted mRNA levels is dependent on Eri1 (Hong et al., 2005). It was suggested that the siRNA dosage-dependent transcriptional activation of Eri1 is controlled by a putative small RNA levels-sensing transcription factor, but this hypothesis still awaits experimental validation (Zhang, 2005). siRNA passenger strand degradation after strand selection and passenger strand cleavage upon loading into the *Neurospora crassa* Ago protein QDE-2 has been appointed to the *N. crassa* ERI-1 homologue QIP, based on a *qip* loss-of-function phenotype (Maiti et al., 2007). In *S. pombe* Eri1 plays a well-defined role in repressing heterochromatin-derived siRNAs (Bühler et al., 2006; Iida et al., 2006). In *S. pombe eri1* mutants, heterochromatic siRNAs are able to function in *trans* to induce TGS of secondary homologous loci that are not the origin of the respective heterochromatic siRNAs. Such a spread of heterochromatin formation is suppressed by Eri1 in the wildtype, and thus *S. pombe* Eri1 acts as a suppressor of RNA silencing by restricting heterochromatin-derived siRNAs to act in *cis* (Bühler et al., 2006; Iida et al., 2006). Also the human ERI-1 homologue Thex1/3'hExo is implicated in RNA silencing regulation, exemplified by its ability to degrade siRNAs *in vitro* (Kennedy et al., 2004). *In vivo* evidence for its involvement in RNA silencing comes from work in HeLa cells, where overexpression of Thex1/3'hExo results in the efficient suppression of nonsense-mediated transcriptional gene silencing; a unique TGS pathway in which heterochromatinisation of immunoglobulin minigenes is triggered by premature termination codons (Bühler et al., 2005). X-Ray crystallography and structure-function studies furthermore indicate that the nuclease domain of Thex1/3'hExo adopts an RNase H-related fold topology and includes a binding pocket suitable for the accommodation of dinucleotides (Cheng and Patel, 2004). This structural feature may be an important hint for the function of ERI-1 homologues, which appear to have an affinity for dsRNA with short 3' overhangs.

Apart from the ever-growing data on RNA silencing regulation across kingdoms, additional conserved functions have been appointed to ERI-1 homologues, revealing an interesting versatility of this 3'-5' exonuclease protein. In fact, Thex1/3'hExo was the first described ERI-1 homologue, albeit not in the context of RNA silencing regulation (Dominski et al., 2003). Dominski et al., (2003) presented evidence that Thex1/3'hExo binds the conserved 3' stem-loop of histone mRNA *in vivo* in a sequence- and structure-dependent manner (Dominski et al., 2003). The histone mRNA 3' end undergoes

exonucleolytic processing upon maturation, and Thex1/3'hExo is able to fulfill this function *in vitro*, not only for human but also for *Drosophila* histone mRNA (Dominski et al., 2003; Dominski et al., 2005; Yang et al., 2006b). In *thex1/3'hexo* loss-of-function mutants, histone mRNA processing has not been found to be affected (Mullen and Marzluff, 2008), which may be due to redundancies in the respective processing pathway. While the *Drosophila* ERI-1 homologue Snipper showed high efficiency in the degradation of dsRNA and dsDNA with 3'-protruding ends *in vitro*, a function for Snipper in RNA silencing regulation could not be identified *in vivo* (Kupsco et al., 2006). It was proposed that Snipper belongs to a group of ERI-1 homologues not implicated in RNA silencing regulation, based on its phylogenetic grouping with ERI-1 homologues characterised by the lack of a SAP domain (Tomoyasu et al., 2008), which was shown to be essential for RNA binding in SAP domain-containing ERI-1 homologues (Cheng and Patel, 2004; Iida et al., 2006; Yang et al., 2006b).

Recently, a novel function was reported for ERI-1 homologues in mouse, *C. elegans*, and *S. pombe*. Two studies concurrently reported on conserved functions of the respective ERI-1 homologues in catalysing the final trimming step in 3' end maturation of the short 5.8S ribosomal RNA upon interaction with the ribosome (Ansel et al., 2008; Gabel and Ruvkun, 2008). In the particular loss-of-function mutants 2 nt elongated 5.8S rRNA molecules accumulate, and the respective recombinant proteins are able to process those 5.8S rRNA intermediates to the mature forms *in vitro* (Ansel et al., 2008; Gabel and Ruvkun, 2008).

Hence, ERI-1 homologues show an interesting functional versatility across the tree of life. Combining siRNA degradation/RNA silencing suppression and ribosomal RNA processing as functions of the same protein constitutes an interesting bridge between evolutionary distant pathways. While ribosomal RNA processing represents one of the most archaic RNA pathways in eukaryotes, siRNA-mediated gene silencing belongs to the evolutionary youngest RNA-dependent regulatory mechanisms. ERI-1 and its homologues connect these highly divergent systems in a surprising way, and future research will likely yield fascinating novel insights into the relationships between these and also other descendents of the ancient RNA World.

2

Materials and Methods

2.1. Materials

In this section the materials used during this work are listed along with their respective suppliers or manufacturers for reference purposes.

2.1.1. Instruments

Agarose gel electrophoresis equipment	Owl B2 EasyCast
Blotting device	Cleaver Scientific SD20 Semi Dry Midi
Centrifuge	Eppendorf 5810R
	Heraeus Biofuge Stratos
Digital camera	Canon EOS 350D
	Nikon Coolpix 990
Electron microscope	JEOL JEM-100C
Fluorophotometer	Hansatech Handy-PEA
Gel documentation system	Herolab U T-28 MP
Hybridisation bottles	Hybaid
Hybridisation oven	Shel Lab Model 1004
Incubator	Heraeus Instruments

Incubator/shaker	Forma Scientific Orbital Shaker
Laminar flow hood	E.S.I. Flufrance Ariane 18 UV.PI
	E.S.I. Flufrance Biocyt 180 NF X44201
Magnet stirrer/heater	IKA Labortechnik IKAMAG® RET
Mechanical rocker	Scientific Industries Vortex-Genie® 2
Microcentrifuge	Eppendorf 5415D
	Heraeus Biofuge 15R
Microlitre pipettes	Gilson Pipetman®
Microscope (confocal)	Leica SP
Microscope (optical/fluorescent)	Nikon Eclipse E800
PAA gel electrophoresis equipment	Biorad Mini-Protean® 3
	IMBB Workshops
Power supply	Biorad PowerPac Basic
	Pharmacia ECPS 3000/150
	Renner Microcomputer Electrophoresis
Spectrophotometer	NanoDrop® ND-1000
	Perkin Elmer Lambda 2
Thermocycler	MJ Research Mini Cycler
	MJ Research DNA Machine Gradient
UV crosslinking chamber	Stratagene Stratalinker®
UV lamp, handheld	UVP Blak-Ray® B-100AP/R

2.1.2. Consumables

Blotting paper	Whatman 3MM
Disposable Pasteur glass pipettes	Volac
Laboratory film	Pechiney Parafilm™ 'M'
Nitrocellulose transfer membrane, 0.22 µm	Schleicher & Schuell Protran
Nylon transfer membrane, 0.45 µm	Whatman Nytran® N
Petri dishes, 10 cm ø	Sarstedt
Pipette tips	Sarstedt

Polypropylene tubes, 15/50 mL	Sarstedt
Reaction tubes, 0.2/0.5/1.5/2.0 mL	Sarstedt
Safety gloves	Lohmann & Rauscher
Scalpel blades	Paragon
Sterile filters, 0.22 µm	Pall Corporation
X-Ray films	Fuji Super RX

2.1.3. Chemicals

[α-^{32}P]ATP EasyTide®	Perkin-Elmer
[α-^{32}P]CTP EasyTide®	Perkin-Elmer
[γ-^{32}P]ATP EasyTide®	Perkin-Elmer
Acetic acid, glacial	Merck
Acrylamide	Sigma-Aldrich
Agar-agar	Sigma-Aldrich
Agarose	Lonza
Ammonium acetate	Merck
Ammonium persulfate	Fluka
Boric acid	Merck
Bromophenol blue	Sigma-Aldrich
BSA	Merck
Calcium chloride	Sigma-Aldrich
Chloroform	Merck
Coomassie Brilliant Blue	Sigma-Aldrich
Dimethylformamide	Sigma-Aldrich
DMSO	Sigma-Aldrich
DTT	Merck
dNTP set	MBI Fermentas
EDTA	Merck
Ethanol, absolute	Merck
Ethidium bromide	Sigma-Aldrich

Formaldehyde	Merck
Formamide	Merck
Glucose, D(+)	Merck
Glycerol	Merck
HEPES	Merck
Hydrochloric acid, fuming	Merck
IPTG	Sigma-Aldrich
Isopropanol	Merck
Lithium chloride	Merck
Macro-salt mixture Murashige & Skoog	Duchefa
Magnesium chloride	Merck
Magnesium sulfate	Merck
Manganese chloride	Fluka
β-mercaptoethanol	Fluka
MES	Sigma-Aldrich
Methanol	Merck
Micro-salt mixture Murashige & Skoog	Duchefa
MOPS	Merck
Murashige & Skoog growth medium	Duchefa
Nonidet® P40	Fluka
NTP set	MBI Fermentas
Phenol, crystals	Fluka
Phosphoric acid	Merck
PIPES	Merck
Potassium chloride	Merck
Potassium hydroxide	Merck
Potassium phosphate, dibasic	Merck
Potassium phosphate, monobasic	Merck
Sarkosyl	Sigma-Aldrich
SDS	Merck
Sodium acetate	Merck
Sodium chloride	Merck

Sodium citrate trihydrate	Merck
Sodium hydrogen phosphate, dibasic	Sigma-Aldrich
Sodium hydrogen phosphate, monobasic	Sigma-Aldrich
Sodium hydroxide	Merck
Sodium hypochlorite	Sigma-Aldrich
Sorbitol	Sigma-Aldrich
Sucrose	Merck
TEMED	Merck
Tris base	Fluka
Triton® X-100	Merck
Tryptone	Sigma-Aldrich
Tween® 20	Sigma-Aldrich
Urea	Merck
Water, nanopure	Millipore
X-Gal	Sigma-Aldrich
Xylene cyanol FF	Sigma-Aldrich
Yeast extract	Sigma-Aldrich

2.1.4. Antibiotics

Ampicillin	Bristol-Myers Squibb
Chloramphenicol	Sigma-Aldrich
Kanamycin	Sigma-Aldrich
Rifampicin	Duchefa
Spectinomycin	Sigma-Aldrich

2.1.5. Culture media

LB – 1 litre	10 g tryptone
	5 g yeast extract

	10 g NaCl H_2O to 900 mL → Adjust pH to 7.0 with NaOH → Add H_2O to 1 litre → Autoclave
LB-agar – 1 litre	10 g tryptone 5 g yeast extract 10 g NaCl 15 g agar-agar H_2O to 900 mL → Adjust pH to 7.0 with NaOH → Add H_2O to 1 litre → Autoclave

2.1.6. Buffers and solutions

Cactus CTAB solution	50 mM Tris (pH 8.0) 25 mM EDTA 4 M NaCl 1.8 % CTAB
Cactus DNA extraction buffer	50 mM Tris (pH 8) 5 mM EDTA 0.35 M sorbitol → Add 1 % β-mercaptoethanol directly prior to use
Church hybridisation buffer	0.5 M phosphate buffer (pH 7.2) 1 % BSA 1 mM EDTA

	7 % SDS
DNA sample loading dye – 6x	10 mM Tris (pH 7.6)
	60 mM EDTA
	60 % glycerol
	0.03 % bromophenol blue
	→ Use at 1x concentration
MMA	1x macro-salt mixture Murashige & Skoog
	1x micro-salt mixture Murashige & Skoog
	10 mM MES (pH 5.7)
	200 µM acetosyringone
	→ Sterile filtrate
MOPS running buffer – 10x, 1 litre	0.4 M MOPS
	0.1 M sodium acetate
	10 mM EDTA
	→ Adjust pH to 7.0 with NaOH
	→ Use at 1x concentration
Protein purification buffer (Ni-NTA)	10 mM Tris (pH 8.0)
	0.1 M NaCl
	10 % glycerol
	0.1 % Triton® X-100
	→ Add imidazol to desired concentration
	→ Sterile filtrate
Protein running buffer – 10x, 1 litre	30.3 g Tris base
	144.1 g glycin
	10 g SDS
	Add H_2O to 1 litre
	→ Use at 1x concentration

Protein sample loading dye – 4x	4 mL glycerol 2.4 mL 1 M Tris (pH 6.8) 0.8 g SDS (8 % final concentration) 0.5 mL β-mercaptoethanol H_2O to 10 mL → Use at 1x concentration
Protoplast extraction buffer	1x macro-salt mixture Murashige & Skoog 1x micro-salt mixture Murashige & Skoog 0.4 M sucrose 2 mM $CaCl_2$ 25 mM MES (pH 5.7) → Sterile filtrate and add 1 % cellulase and 0.5 % macerozyme directly prior to use
RNA sample loading dye (agarose) – 5x	3.084 mL formamide 720 µL 37 % formaldehyde 80 µL 0.5 M EDTA (pH 8.0) 2 mL glycerol 4 mL 10x MOPS running buffer 0.03 % bromophenol blue H_2O to 10 mL → Use at 1x concentration
RNA sample loading dye (PAGE) – 2x	98 % formamide 10 mM EDTA (pH 8.0) 0.03 % bromophenol blue 0.03 % xylene cyanol FF → Use at 1x concentration
Southern denaturation solution	1.5 M NaCl 0.5 M NaOH

Southern depurination solution	0.2 N HCl
Southern neutralisation solution	1 M Tris (pH 7.5) 1.5 M NaCl
SSC – 20x, 1 litre	175.3 g NaCl 88.2 g sodium citrate trihydrate H_2O to 800 mL → Adjust pH to 7.0 with HCl → Add H_2O to 1 litre → Autoclave → Use at desired final concentration
TAE – 50x, 1 litre	242 g Tris base 100 mL 0.5 M EDTA (pH 8.0) 57.1 mL glacial acetic acid H_2O to 1 litre → Use at 1x concentration
TBE – 10x, 1 litre	108 g Tris base 55 g boric acid 40 mL 0.5 M EDTA (pH 8.0) H_2O to 1 litre → Use at 1x concentration
TE – 1x	10 mM Tris base 1 mM EDTA → Adjust to desired pH with NaOH → Autoclave

2.1.7. Enzymes

Calf intestinal phosphatase	New England Biolabs
Cellulase	Duchefa
DNase I	Roche
Lysozyme	Sigma-Aldrich
Macerozyme	Duchefa
Proteinase K	Invitrogen
Restriction endonucleases	Minotech
	New England Biolabs
RNase A	Qiagen
RNase inhibitor	HT Bioscience
Taq DNA polymerase	Minotech
T4 DNA Ligase	Promega
T4 polynucleotide kinase	New England Biolabs
T4 RNA ligase	New England Biolabs
T7 RNA polymerase	HT Bioscience
Klenow Fragment	Minotech

2.1.8. Kits

Gateway® LR Clonase® II Enzyme Mix	Invitrogen
MicroSpin™ G-25 Spin Columns	Amersham
MicroSpin™ S-200 Spin Columns	Amersham
NucleoBond® Xtra Midi Kit	Macherey-Nagel
NucleoSpin® Extract II	Macherey-Nagel
pGEM®-T Easy Vector System	Promega
Platinum® *Taq* DNA pol. High Fidelity	Invitrogen
PrimeScript™ RT-PCR Kit	TaKaRa
RadPrime DNA Labelling System	Invitrogen
TOPO® TA Cloning® Kit	Invitrogen

TRIzol® Reagent	Invitrogen

2.1.9. Gel electrophoresis size markers

Lambda DNA, *Pst* I-digested	Minotech
100 bp DNA Ladder	New England Biolabs
	Invitrogen
1 kb DNA Ladder	New England Biolabs
	Invitrogen
0.5 – 10 kb RNA Ladder	Invitrogen

2.1.10. Bacterial strains

Agrobacterium tumefaciens C58C1	IMBB, Heraklion, Greece
Escherichia coli DH5α®	Stratagene
Escherichia coli JM109(DE3)-pLysE	Promega
Escherichia coli Library Efficiency DB3.1™	Invitrogen

2.1.11. Plasmid vectors

The full genomic sequence of *Arabidopsis ERL1* was cloned in the binary vector pART27 (Gleave, 1992) for agro-infiltration and plant transformation purposes (construct 35S-At*ERL1*gen). *ERL1* hairpin constructs derived from the *Arabidopsis ERL1* cDNA sequence and from a tobacco *ERL1* EST (EST ID EB681897) were cloned in pART27 (constructs 35S-At*ERL1*hp and 35S-Nt*ERL1*hp) for the RNAi-mediated suppression of the respective transgene or gene. For the construction of a carboxy-terminal fusion of GFP to ERL1, the *Arabidopsis ERL1* cDNA sequence was cloned in pENTR™ 3C (Invitrogen) and subcloned to pB7FWG2 (Karimi et al., 2002) using the Gateway® cloning technology. The *pBIN* 35S-*mGFP4* construct for the overexpression of *GFP*

(Haseloff et al., 1997) was kindly provided by J. Haseloff (Cambridge University, Cambridge, UK). The 35S P19-CymRSV construct (Havelda et al., 2003; Lakatos et al., 2004) was donated by J. Burgyán (ABC, Gödöllö, Hungary). The *GFP* hairpin construct pANe59I had previously been generated in our laboratory (Kościańska et al., 2005).
Please refer to supplementary section 5.1. for detailed maps of 35S-At*ERL1*gen, 35S-At*ERL1*hp, 35S-Nt*ERL1*hp, and 35S-At*ERL-GFP*.

2.1.12. Oligonucleotides

All DNA oligonucleotides (purity: desalted) to be used as PCR primers or probes for northern blot analysis were obtained from Microchemistry Laboratory or Metabion. T_m values were determined using the online primer analysis software provided by Cybergene AB (http://www.cybergene.se/EazyPrimer.htm). RNA oligonucleotides (HPLC-purified) were purchased from VBC Biotech.
A detailed list of all oligonucleotides (DNA and RNA) used during this work can be found in supplementary section 5.1.

2.2. Methods

This section describes the methods used to acquire the results presented in chapter 3. A collection of additional standard methods of molecular biology that came to use during this study can be found as supplementary methods under supplementary section 5.2.

2.2.1. DNA extraction from *Nicotiana benthamiana*

Essentially polysaccharide-free genomic DNA from *N. benthamiana* leaves was extracted using a modified CTAB extraction method (Tel-Zur et al., 1999).
For the extraction of 10-50 µg DNA, *N. benthamiana* leaf material was ground to a fine powder in liquid nitrogen using a mortar and pestle. 1 g of leaf powder was resuspended

in 20 mL cactus DNA extraction buffer, vortexed intensely, and centrifuged at 8.000x g for 15 minutes (4 °C). The supernatant was discarded and the procedure repeated twice. These three initial washing steps remove large amounts of polysaccharides prior to cell lysis. After the third wash, the pellet was resuspended in 5 mL cactus DNA extraction buffer, followed by the addition of 3.5 mL cactus CTAB solution and 600 µL of a 15 % sarkosyl solution. The mixture was vortexed and incubated in a water bath at 55 °C for 60-90 minutes. Subsequently, the lysate was extracted with an equal volume of chloroform and centrifuged at 8.000x g for 15 minutes (4 °C). 0.7 volumes isopropanol and 0.1 volumes of 3 M sodium acetate (pH 5.2) were added to the supernatant to precipitate genomic DNA. After centrifugation at 8.000x g for 30 minutes (4 °C), the DNA pellet was washed once with 70 % ethanol and subsequently resuspended in 500 µL water containing 100 µg/mL RNase A. The DNA/RNase A solution was incubated at 37 °C for 30-60 minutes, followed by standard phenol/chloroform extraction and isopropanol precipitation. The RNase A-treated DNA pellet was finally resuspended in 100 µL water and the DNA concentration was determined using the NanoDrop® spectrophotometer.

2.2.2. Plant RNA extraction

For the extraction of total RNA from plant material, Invitrogen's TRIzol® method was used according to the manufacturer's description. All centrifugation steps were performed at 4 °C, while all other working steps were carried out at room temperature.
100 mg of finely ground plant material were resuspended in 1 mL TRIzol® reagent by vortexing for 30 seconds. After incubation for 5 minutes, cellular debris was pelleted by centrifugation at maximum speed for 10 minutes (4 °C). 200 µL chloroform were added to the cleared supernatant, vortexed, incubated for 15 minutes, and centrifuged at maximum speed for 15 minutes (4 °C). The clear supernatant was mixed with 250 µL isopropanol and 250 µL high salt solution (0.8 M sodium citrate, 1.2 M sodium chloride) and incubated for 10 minutes. After centrifugation at maximum speed for 10 minutes, the RNA pellet was washed once in 70 % ethanol, centrifuged at 7.500x g for 5

minutes, and subsequently resuspended in 100 µL water. On average, 40-100 µg of total RNA were extracted per 100 mg of finely ground plant material.

2.2.3. Northern analysis

The northern blot technique was utilised for comparative gene expression studies. To this end RNA samples were size-fractionated on denaturing agarose or polyacrylamide gels, transferred to nylon membranes, and hybridised with radioactively labelled probes specific for the respective genes of interest.

2.2.3.1. Denaturing agarose gel electrophoresis

For the detection of specific mRNAs or viral RNAs during northern analyses, total RNA was size-fractionated on 1.2 % agarose gels containing 1x MOPS buffer, 1 % formaldehyde, and 7 µg ethidium bromide per 100 mL of agarose solution. Gels were run at 100 V in 1x MOPS running buffer until the bromophenol blue contained in the 5x RNA loading dye had migrated approximately 10 cm. Finished gels were rinsed in water and subsequently blotted using classical capillary transfer.

2.2.3.2. Capillary blotting procedure

Finished agarose northern gels were equilibrated in 10x SSC and the size-fractionated RNA was blotted onto nylon membranes, essentially as described elsewhere (Sambrook and Russel, 2001). After transfer, membranes were briefly rinsed in 2x SSC and subsequently crosslinked using a Stratalinker® device (120 mJ/cm^2). The same capillary blotting procedure was utilised during Southern analysis.

2.2.3.3. Denaturing polyacrylamide gel electrophoresis (PAGE)

For the size-fractionation of smaller RNA molecules, 5-20 % polyacrylamide gels were used. Denaturing PAA gels contained respective amounts of 40 % 38:2 acrylamide:bis-acrylamide, 8 M urea, 0.75 ‰ TEMED, and 0.375 ‰ APS in 1x TBE. After polymerisation gels were pre-run at 22 W in 1x TBE for 1 hour. RNA samples were mixed with 2x RNA sample loading dye (PAGE), boiled for 5 minutes, and quick-chilled on ice before loading. Directly prior to loading, the wells of the gel were carefully rinsed with 1x TBE to flush out precipitated urea. Gels were run at approximately 22 W in 1x TBE, keeping the gel temperature at 50 °C. Suited running-times for each gel had to be determined empirically.
After running, finished polyacrylamide gels were stained with ethidium bromide when necessary to determine RNA integrity and loading equality using a UV gel documentation system.

2.2.3.4. Semi-dry blotting procedure

PAGE-fractionated RNA was blotted onto nylon membranes by semi-dry blotting. For this purpose, gel and membrane were placed between 12 sheets of 1x TBE-soaked blotting paper (6 on either side) and assembled in an SD20 Semi Dry Midi unit. RNA was transferred by applying 3 mA per square centimetre of conductive surface for 30 minutes (4 °C). Afterwards the membrane was briefly rinsed in 2x SSC and subsequently crosslinked using a Stratalinker® device (120 mJ/cm²). The same procedure, with the exception of using nitrocellulose instead of nylon membranes, was employed during western analysis.

2.2.3.5. Radioactive labelling of nucleic acid probes

For the detection of DNA or RNA sequences during Southern and northern analyses, specific probes were labelled radioactively with ^{32}P. Depending on the experiment,

radiolabelled probes were generated either by random-prime labelling of cDNA fragments with Klenow Fragment, or by 5' end labelling of DNA and RNA oligonucleotides with T4 polynucleotide kinase.

2.2.3.5.1. Random-prime labelling of DNA probes

Random-primed DNA probes were used for most mRNA detections in northern analyses as well as Southern hybridisations using Invitrogen's RadPrime DNA Labelling system according to the manufacturer's recommendations. Purified restriction fragments or PCR products between 200 and 500 nt in length served as templates in RadPrime labelling reactions.

50-100 ng of template DNA were denatured at 95 °C for 2 minutes and quick-chilled on ice, followed by the addition of 20 µL 2.5x RadPrime Buffer, 1 µL of 0.5 M dTTP and 0.5 M dGTP each, 1 µL random primers (3 µg/µL), 2 µL [α-^{32}P]ATP and [α-^{32}P]CTP each (3000 Ci/mmol), 40 u Klenow Fragment, and water to a final volume of 50 µL. The reaction mixture was incubated in a water bath at 37 °C for 1 hour and then purified using Amersham's MicroSpin™ S-200 spin columns according to the manufacturer's protocol. Purified random-primed DNA probes were denatured in a wather bath at 95 °C for 5 minutes and quick-chilled on ice before adding them to the hybridisation buffer.

2.2.3.5.2. 5' End labelling of DNA and RNA oligonucleotides

End-labelled oligonucleotide probes (DNA or RNA) were created in 5' end labelling reactions using T4 polynucleotide kinase.

To this end 8 pmol template DNA were mixed with 5 µL 10x PNK reaction buffer, 6 µL [γ-^{32}P]ATP (3000 Ci/mmol), 20 u T4 polynucleotide kinase, and water in a total reaction volume of 50 µL. After 1 hour incubation at 37 °C in a water bath, the thus labelled oligo-nucleotide probes were purified using commercial MicroSpin™ G-25 spin columns (Amersham) according to the manufacturer's specifications. Purified oligonucleotide

probes were briefly denatured at 95 °C and quick-chilled on ice prior to their addition to the hybridisation buffer.

2.2.3.6. Hybridisation, washing, and exposure of northern and Southern membranes

Membranes were pre-hybridised in 10-15 mL pre-warmed Church hybridisation buffer for 1 hour. Pre-hybridisation and hybridisation temperatures were dependent on the size of the RNA to be detected and/or the length of the probe used. Typically, mRNA northerns and Southerns were hybridised at 65 °C using random-primed DNA probes, while small RNA northerns were hybridised at 42-50 °C. Probes were denatured and added to the hybridisation buffer, followed by rotating over-night incubation in a hybridisation oven. The following day, membranes were washed with 10-15 mL of pre-warmed washing solutions in the following order: 1. rinse with 2x SSC/0.1 % SDS; 2. wash 2x 15 minutes with 2x SSC/0.1 % SDS; 3. wash 2x 10 minutes with 1x SSC/0.1 % SDS; 4. wash 2x 5 minutes with 0.5 x SSC/0.1 % SDS. All washing steps were performed at hybridisation temperature. Washed membranes were rinsed in 2x SSC and subsequently sealed in plastic bags while still wet. Such prepared membranes were exposed to X-Ray films in appropriate exposure cassettes. Suited exposure times had to be determined empirically. Exposed X-Ray films were developed automatically using a Curix 60 developer (Agfa). In special cases X-Ray films were developed manually using the Curix 60's solutions for development and fixation, enabling a more precise timing of X-Ray film development.

2.2.4. Southern analysis

With Southern blots the presence and/or copy number of genes and transgenes were determined. To do so, 15-20 µg of genomic *N. benthamiana* DNA were digested with 50-80 u of appropriate restriction enzymes in 150 µL reactions containing the respective reaction buffer at 1x concentration and 100 µM spermidine. The reactions were

incubated at 37 °C for 5 hours. Additional 50-80 u of restriction enzyme(s) were added after 2.5 h to compensate for loss of active enzyme during the incubation time. After incubation samples were isopropanol-precipitated and resuspended in 40 µL of water.
The thus prepared samples were loaded on 0.75 % agarose gels and run at 22 V over night. The following day, gels were continued to run until the bromophenol blue band had migrated at least 10 cm to ensure for proper size separation. Finished gels were depurinated in 0.2 N HCl for 10 minutes, denatured in 1.5 M NaCl/0.5 M NaOH for 45 minutes and neutralised in 1 M Tris (pH 7.5)/1.5 M NaCl for 30+15 minutes (10-minute washes with water between all steps). After equilibrating the gel in 10x SSC, the DNA was transferred to nylon membranes by classical capillary transfer (compare section 2.2.3.2.).

2.2.5. Plant cultivation

N. tabacum and *N. benthamiana* plants were cultivated under greenhouse conditions. Seeds were sown on potting soil and covered with plastic bags to create a high humidity environment for germination. At the two-leaves stage, seedlings were separated to individual pots and again covered with plastic bags. Over the course of 1-2 weeks the bags were slowly opened to facilitate a gradual acclimatisation of the plants to normal humidity levels. Once fully accustomed, individual plants were re-potted to fresh soil (consisting of 3 parts potting soil, 1 part peat moss, 1 part Perloflor Perlite, and 0.1 parts fertiliser) and grown to maturity.
If necessary, seeds were sterilised with 5 % sodium hypochlorite containing a drop of the surfactant Tween® 20 and subsequently plated on MS plates containing appropriate antibiotics.

2.2.6. Plant transformation

Transgenic *N. bentamiana* plants were generated by *Agrobacterium*-mediated lead disc transformation as described before (Horsch et al., 1985; Kościańska et al., 2005). Shoots

that rooted in the presence of 100 µg/mL kanamycin were considered to be transgenic, and molecular analyses (Southern/northern hybridisations) confirmed the presence of the respective transgenes. This work was done by Jutta Maria Helm as part of her PhD thesis.

2.2.7. Virus/viroid infection in *Nicotiana* plants

For infection with *Potato spindle tuber viroid* (PSTVd) strain PH106, young *N. benthamiana* and *N. tabacum* plants were mechanically inoculated as described before (Tabler and Sänger, 1984; Kalantidis et al., 2007). Per millilitre of 1 % K_2HPO_4 100 mg of PSTVd-infected tomato leaf material were ground to sap with a mortar and pestle. 100 µL of the thus created infectious sap were used for the mechanical inoculation of a single carborundum-dusted *Nicotiana* leaf. Two leaves were inoculated per plant. Instead of infectious sap 50 ng of *in vitro* viroid transcript may be used per leaf. Immediately after the abrasive inoculation the leaves were rinsed with water, and thus infected plants were grown to maturity under greenhouse conditions. Full systemic infection of the plants established approximately 3-7 weeks postinfection and persisted until senescence.
In equivalent experiments, infectious sap [in 50 mM phosphate buffer (pH 8.0)] from tobacco plants was used to inoculate young *N. benthamiana* plants with *Plum pox virus* (PPV).

2.2.8. Agro-infiltration

The agro-infiltration technique (Schöb et al., 1997) was used to ectopically express sequences of choice *in planta* in a spatiotemporally controlled manner. For agro-infiltration a to-be-expressed sequence is cloned in a binary expression vector, which is subsequently used to transform competent *A. tumefaciens* cells. A liquid culture of a thus created *A. tumefaciens* strain is injected into the intercellular spaces of the leaf blade, where the desired transcript is subsequently produced for approximately 1-3

weeks. Agro-infiltration-induced expression is confined to the infiltrated space(s) and does not spread. Hence, defined regions of interest can be exposed to expression of the sequence of interest, while neighbouring regions in the same leaf or plant will remain unaffected and may serve as controls.

In practice, liquid *A. tumefaciens* cultures were prepared by inoculating LB medium containing appropriate antibiotics from a glycerol stock of the desired strain and shaking the liquid culture at 28 °C. Once fully grown, typically after over-night incubation, the bacteria were collected by centrifugation at 2.500x g for 15 minutes. The bacterial pellet was resuspended in the same volume of MMA medium as the original liquid culture and incubated shaking at 28 °C for 1-2 h, followed by 2 washes with cold 10 mM $MgCl_2$. Subsequently, the bacteria were resuspended in 10 mM $MgCl_2$ to an OD_{600} of 0.2-0.5, depending on the respective experimental requirements. This working suspension of *A. tumefaciens* was injected into leaves using sterile 1 mL syringes. Small punctuations of the leaf blades served as the entry points for the *A. tumefaciens* suspensions.

2.2.9. Protoplast preparation for microscopy

Protoplasts were prepared for microscopy by cutting fresh leaf material submerged in protoplast extraction buffer into thin slices with a sterile scalpel blade. After cutting, the samples were covered and incubated on an orbital shaker at 50 rpm for at least 8 hours (at room temperature). Subsequently, the leaf slices were removed, and the protoplast extraction buffer containing free protoplasts was transferred to a suitable container (*e.g.* a 15 mL polypropylene tube). In protoplast extraction buffer containing 0.4 M sucrose, intact protoplasts float to the top of the solution forming a distinct upper phase, while cellular debris and fibrous tissue sink to the ground. Samples taken from the upper protoplast phase can directly be used for fluorescence and confocal microscopy, but would not be suitable for protoplast cell culture without further purification and sterilisation.

2.2.10. Preparation of *N. benthamiana* leaf sections for optical and electron microscopy

For light and electron microscopy leaf tissue was fixed with 2 % glutaraldehyde and 2 % paraformaldehyde in 0.1 M cacodylate buffer, washed, and stained with 1 % OsO_4. Fixed tissues were embedded in Durcupan ACM resin (Electron Microscopy Sciences). Transverse leaf sections for optical microscopy were stained with 1 % toluidine blue and viewed with a Nikon Eclipse E800 microscope. Electron microscopical cross sections were analysed with a JEOL JEM-100C Electron Microscope operating at 80 kV.

2.2.11. Circular RT-PCR for the cloning of small rRNA 3' ends

The precise 5' and 3' ends of 5.8S, 5S and 4.5S rRNAs were determined by circular RT-PCR, essentially as described before (Bollenbach et al., 2005). In brief, total RNA was self-ligated with T4 RNA Ligase (NEB) and reverse-transcribed using respective first-strand primers. The obtained cDNAs were amplified by stringent touch-down PCR, and the PCR products were eluted from 8 % acrylamide gels with 300 mM NaCl over night at 4 °C. The purified PCR products were amplified in secondary PCR reactions and subsequently cloned into pCR® II TOPO® (Invitrogen). Individual clones were sequenced using a vector-specific primer.

To verify the location of additional nucleotides at the 3' end of some of these clones, a modified linker was ligated to the 3' ends of total RNA, followed by reverse transcription with a linker-specific primer. The thus created cDNA was PCR-amplified, purified, cloned into pCR® II TOPO®, and sequenced using a vector-specific primer. This work was done by Jutta Maria Helm as part of her PhD thesis.

3

Results

This study investigates characteristics of the 3'-5' exoribonuclease protein ERL1 and its involvements in small RNA pathways in plant model systems. Important milestones in this work comprise the identification and characterisation of a plant ERI-1 homologue, a detailed examination of its abilities to process and/or degrade a variety of RNA substrates in distinct pathways, and the development of a working model for ERL1 in plant ribosomal RNA biogenesis.

3.1. *in silico* characterisation of a plant ERI-1 homologue

As yet the roles of ERI-1 homologues in small RNA pathways have been investigated in a number of model species including *C. elegans*, *S. pombe*, *Drosophila*, mouse and human (Kennedy et al., 2004; Iida et al., 2006; Kupsco et al., 2006; Yang et al., 2006b; Ansel et al., 2008). The ERI-1 family members share a common 3'-5' exonuclease domain (EXOIII: SMART accession number SM00479) (Koonin and Deutscher, 1993) containing a highly conserved DEDD motif (Zuo and Deutscher, 2001). DEDD domain proteins include the bacterial oligoribonuclease and RNase T that degrade small RNA oligonucleotides and are involved in maturation and 3' end processing of small stable RNAs, respectively (Zuo and Deutscher, 2001). In the NCBI Conserved Domain Database (Marchler-Bauer et al., 2007) ERI-1-type EXOIII domains have recently been

3. Results

Figure 3.1 Phylogenetic alignments of ERI-1 homologues. **(a)** Full protein alignment of ERI-1 homologues from animals, fungi, and plants revealing the conserved EXOIII domain. Amino- and carboxy-terminal parts in comparison exhibit a higher degree of variability between species. **(b)** The protein sequences of plant ERI-1 homologues are highly conserved. Important differences are found in the amino-terminal regions, where the *P. trichocarpa* and *S. bicolor* ERL1 homologues harbor large deletions. These areas correspond to chloroplast localisation signals. An approximately 35 aa deletion inside the EXOIII domain of *S. bicolor* ERL1 could not be functionally interpreted yet. **(c)** ERI-1 homologues contain a conserved DEDDh motif that is common to a subfamily of EXOIII proteins, including RNase T and oligoribonuclease (Zuo and Deutscher, 2001). Color code: A, block of similar; A, conservative; A, identical; A, non-similar; A, weakly similar.

annotated as a distinct subfamily termed ERI-1_3'hExo_like (CDD domain cd06133). A DNA/RNA-binding SAP domain (Aravind and Koonin, 2000; Kipp et al., 2000) is present at the amino-terminus of several but not all of the reported ERI-1 homologues. If present, the SAP domain conveys binding specificity to short double-stranded RNA substrates (Cheng and Patel, 2004; Iida et al., 2006; Yang et al., 2006b). The absence of a SAP module, however, is not indicative of a reduced processing efficiency (Kupsco et al., 2006).

BLAST search revealed a single gene in the *Arabidopsis* genome homologous to *C. elegans ERI-1* (locus ID: At3g15140) with a conserved DEDDh EXOIII-type ERI-1_3'hExo_like domain (Figure 3.1 c). Following plant nomenclature conventions, this gene was termed *ERI-1-LIKE 1* (*ERL1*). On the protein level, ERL1 shares 49 % similarity with *C. elegans* ERI-1, making it the closest ERI-1 homologue in *Arabidopsis*. Similarities are most pronounced in the conserved exonuclease domain, while the amino- and carboxy-terminal regions exhibit stronger variability between species (Figure 3.1 a). A subset of ERI-1 homologues (Kupsco et al., 2006; Tomoyasu et al., 2008) does not contain amino-terminal SAP domains. The presence of a SAP domain, however, is not a crucial prerequisite for ERI-1-type nucleases, since the *Drosophila* ERI-1 homologue Snipper lacks this domain without impairment of its catalytic activities (Kupsco et al., 2006).

Highly conserved ERL1 homologues (>80 % similarity on the protein level) were readily identified in all presently sequenced plant genomes (Figure 3.1 b). Despite their strong similarities, ERL1 homologues also exhibit striking differences. *Sorghum bicolor* ERL1 contains a large deletion of approximately 35 amino acids within its EXOIII domain (Figure 3.1 b). It is nevertheless annotated as an ERI-1_3'hExo_like domain *in silico*. The functional significance of this deletion could not be interpreted yet. In addition, the *Populus trichocarpa* and *S. bicolor* ERL1 homologues exhibit large amino-terminal deletions (Figure 3.1 b). The deletion regions correspond to chloroplast localisation signals in *Arabidopsis*, *Vitis vinifera, Oryza sativa* and *N. tabacum* (as discussed below), suggesting a functional diversity of ERL1 proteins in different plant lineages. As indicated by publicly available microarray data (Winter et al., 2007), *Arabidopsis ERL1* is expressed ubiquitously at low levels, but predominantly in imbibed seeds, reproductive organs, and meristems (Figure 3.2). With a mean expression level of 15.69

3. Results

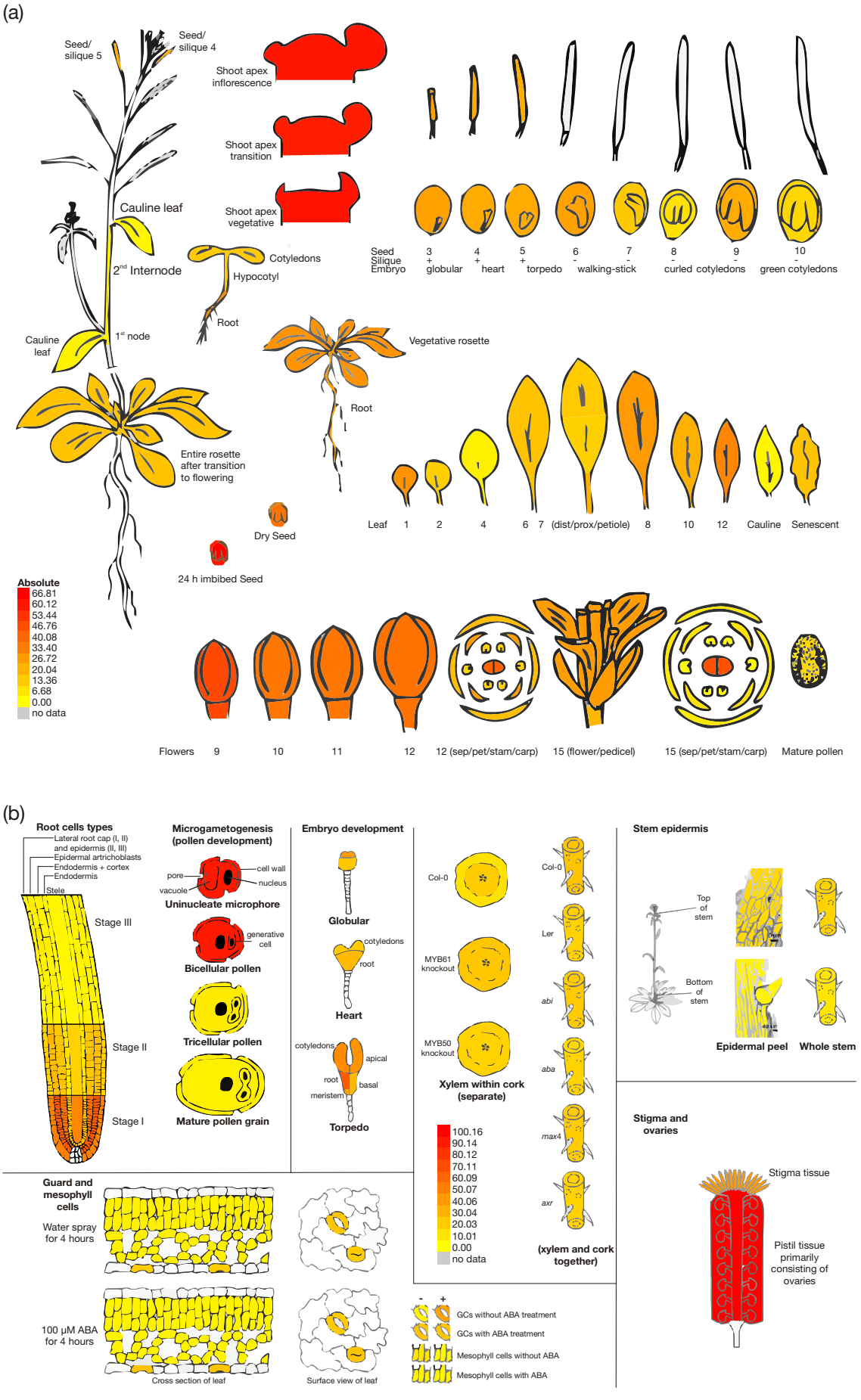
(a)
Seed/ silique 5
Seed/ silique 4
Shoot apex inflorescence
Shoot apex transition
Shoot apex vegetative
Cauline leaf
2nd Internode
Cotyledons
Hypocotyl
Root
Cauline leaf
1st node
Vegetative rosette
Root
Entire rosette after transition to flowering
Dry Seed
24 h imbibed Seed
Absolute
66.81
60.12
53.44
46.76
40.08
33.40
26.72
20.04
13.36
6.68
0.00
no data
Seed Silique Embryo
3 + globular
4 + heart
5 + torpedo
6 - walking-stick
7 -
8 - curled cotyledons
9 -
10 - green cotyledons
Leaf 1 2 4 6 7 (dist/prox/petiole) 8 10 12 Cauline Senescent
Flowers 9 10 11 12 12 (sep/pet/stam/carp) 15 (flower/pedicel) 15 (sep/pet/stam/carp) Mature pollen
(b)
Root cells types
Lateral root cap (I, II) and epidermis (II, III)
Epidermal artrichoblasts
Endodermis + cortex
Endodermis
Stele
Stage III
Stage II
Stage I
Microgametogenesis (pollen development)
pore
vacuole
cell wall
nucleus
Uninucleate microphore
generative cell
Bicellular pollen
Tricellular pollen
Mature pollen grain
Embryo development
Globular
cotyledons
root
Heart
cotyledons
apical
root
basal
meristem
Torpedo
Col-0
MYB61 knockout
MYB50 knockout
Xylem within cork (separate)
100.16
90.14
80.12
70.11
60.09
50.07
40.06
30.04
20.03
10.01
0.00
no data
Col-0
Ler
abi
aba
max4
axr
(xylem and cork together)
Stem epidermis
Top of stem
Bottom of stem
Epidermal peel
Whole stem
Stigma and ovaries
Stigma tissue
Pistil tissue primarily consisting of ovaries
Guard and mesophyll cells
Water spray for 4 hours
100 µM ABA for 4 hours
Cross section of leaf
Surface view of leaf
GCs without ABA treatment
GCs with ABA treatment
Mesophyll cells without ABA
Mesophyll cells with ABA

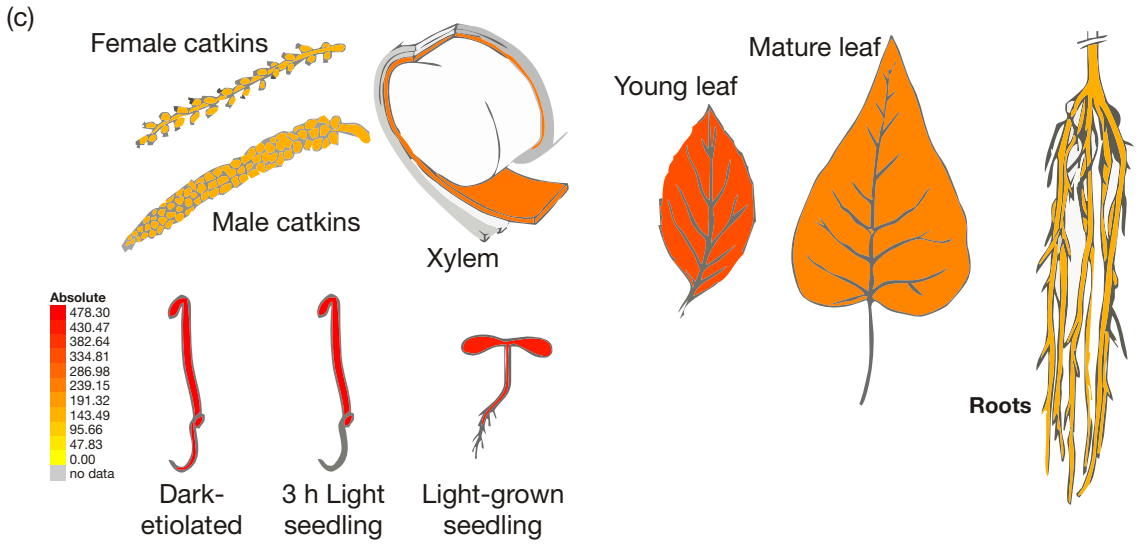

Figure 3.2 Expression patterns of *ERL1* in *Arabidopsis* and *P. trichocarpa* as represented in the eFP Browser at the Bio-Array Resource (Winter et al., 2007). **(a)** Expression map focusing on developmental stages of *Arabidopsis* leaves, flowers, seeds, and meristems. **(b)** Detailed expression analysis of different *Arabidopsis* tissues. **(c)** Expression representation of a putative *P. trichocarpa ERL1* homologue.
Affymetrix expression data normalised by the GCOS method with TGT values of 100 (a+b) or 500 (c). Redrawn and modified from the original representation at http://www.bar.utoronto.ca.

(GCOS-normalised Affymetrix expression data, TGT value of 100) in *Arabidopsis* rosettes (Figure 3.2 a), *ERL1* mRNA is transcribed below detection limit in standard northern hybridisations (compare *ALPHA-TUBULIN* = 582.04). The highest *ERL1* expression can be detected in the shoot apex (Figure 3.2 a) as well as in ovaries and during early pollen development (Figure 3.2 b); whereas expression levels drop in fully differentiated tissues (Figure 3.2 a-b). The putative poplar *ERL1* homologue shows a slightly different expression pattern, with high *ERL1* mRNA levels detectable in seedlings, but not in reproductive organs (Figure 3.2 c). The ratio of *ALPHA-TUBULIN* to *ERL1* expression, however, is comparable between *Arabidopsis* and poplar.

3.2. ERL1 contains an amino-terminal transit peptide and is imported into chloroplasts

The *Arabidopsis* ERL1 amino acid sequence was analysed using a variety of subcellular localisation prediction algorithms, most of which identify an amino-terminal signal peptide conferring chloroplastic localisation (Table 3.1). This chloroplast leader

sequence is predicted to consist of the first 74 amino acids and be cleaved off after import into plastids. The protein sequences of the *P. trichocarpa* and *S. bicolor* ERL1 homologues harbour large amino-terminal deletions and merely consist of the conserved DEDDh domains, thus apparently lacking chloroplast localisation signals (Figure 3.1 b). Consequently, these ERL1 homologues are predicted to exhibit cytoplasmic localisations (data not shown), which strongly indicates different ERL1 functions in poplar and *S. bicolor* compared to *Arabidopsis*, *V. vinifera*, *O. sativa*, and tobacco.

To verify the chloroplastic localisation prediction for *Arabidopsis* ERL1, a carboxy-terminal *ERL1-GFP* fusion construct was generated from the full-length *Arabidopsis ERL1* cDNA (*ERL1-GFP*), driven by the strong constitutive 35S promoter of *Cauliflower mosaiv virus* (Figure 3.3 a). The fusion protein was transiently expressed in wildtype *N. benthamiana* plants by agro-infiltration, and protoplast preparations were analysed with a confocal microscope four days after infiltration (Figure 3.3 a-c). Expression of *ERL1-GFP* results in GFP-free cytoplasm, whereas strong GFP signal can be detected in distinct organelles (Figure 3.3 a). Merging of the signals for GFP and the red autofluorescence of chlorophyll reveals a near-perfect co-localisation, verifying the chloroplastic localisation of ERL1-GFP. In protoplasts derived from cell types containing few chloroplasts (*e.g.* spongy mesophyll cells), GFP signal after *ERL1-GFP* expression was also detected in the cytoplasm (Figure 3.3 b), supposedly due to a shortage of plastids able to import all the ectopically produced ERL1-GFP. It is therefore possible that ERL1 might partially localise to the cytoplasm under physiological

Table 3.1 *in silico* predictions of *Arabidopsis* ERL1 subcellular localisation

Prediction algorithm		
BaCelLo	Chloroplast	Pierleoni et al., 2006
ChloroP	Chloroplast	Emanuelsson et al., 1999
iPSORT	Mitochondrion	Bannai et al., 2002
LOCtree	Chloroplast	Nair and Rost, 2005
MultiLoc	Chloroplast	Höglund et al., 2006
PCLR	Chloroplast	Schein et al., 2001
Predotar	Chloroplast	Small et al., 2004
TargetLoc	Chloroplast	Höglund et al., 2006
TargetP	Chloroplast	Emanuelsson et al., 2007
WoLFPSORT	Chloroplast	Horton et al., 2007

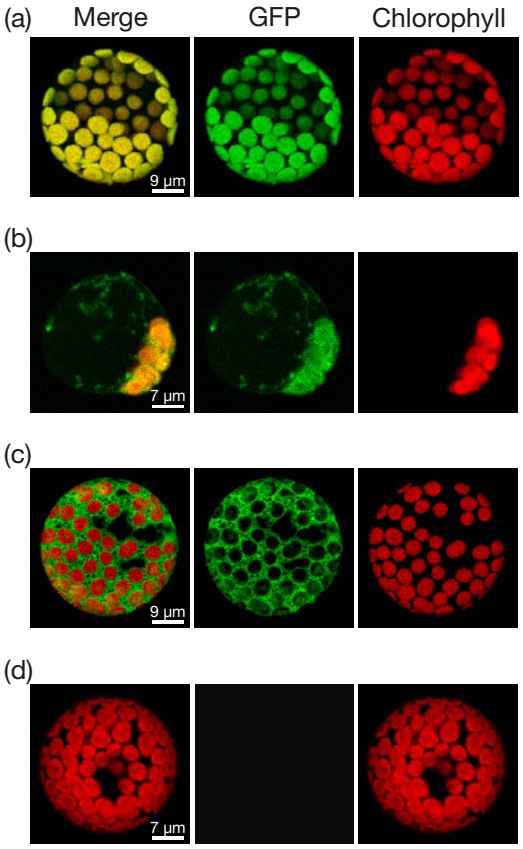

Figure 3.3 Confocal microscopy of agro-infiltrated *N. benthamiana* protoplasts to determine the subcellular localisation of *Arabidopsis* ERL1. **(a)** *ERL1-GFP* expression leads to strong localised GFP signal. Merging of the channels for GFP (green) and chlorophyll (red) results in orange fluorescence of the chloroplasts, indicating a good co-localisation. Hence, ERL1-GFP is imported into the chloroplasts. **(b)** In protoplasts derived from cells with few chloroplasts (*e.g.* cells from the spongy mesophyll) GFP can also be detected as dispersed signal throughout the cytoplasm. Supposedly there are not enough chloroplasts present in these cases to import all the ERL1-GFP produced upon *ERL1-GFP* agro-infiltration. **(c)** Agro-infiltration of plain *GFP* leads to strong GFP signal in the cytoplasm. Without chloroplast leader sequence GFP is excluded from the chloroplasts. This is best visualised in the green GFP channel, where chloroplasts appear as dark islands amidst the GFP-filled cytoplasm. **(d)** In protoplasts derived from untreated wildtype cells chloroplasts fluoresce red due to chlorophyll autofluorescence. No signal can be detected in the GFP channel, ruling out unspecific GFP signals in (a), (b), and (c).

conditions, even though such a cytosolic localisation may be transient. Control expression of plain GFP leads to strong and uniform GFP signal throughout the cytoplasm. Chloroplasts are free of GFP and appear as dark islands amidst the GFP-filled cytoplasm (Figure 3.3 c). Merging of the channels confirms that GFP and chlorophyll signals are exclusive in this case (Figure 3.3 c). In wildtype-derived protoplasts only red chlorophyll autofluorescence can be detected. No GFP signal is present in the green channel, confirming that the GFP signals detected in Figure 3.3 a-c do not originate from unspecific fluorescence.

As yet two chloroplastic 3'-5' exonucleases had been identified: POLYNUCLEOTIDE PHOSPHORYLASE, and an RNase II/R homologue (RNR1), both of them implicated in the 3' end processing of chloroplast mRNAs and ribosomal RNAs (Walter et al., 2002; Bollenbach et al., 2005). Hence, in addition to possible involvements in RNA silencing pathways, implications of ERL1 in the regulation of chloroplast development were investigated during the course of this work. This included an evaluation of ERL1 function in the 3' end processing of plastid-encoded ribosomal RNAs.

3.3. Assessing ERL1 functionality in RNA silencing suppression and siRNA degradation

In order to address, if ERL1 exhibits the same specificity for siRNA degradation and negative RNA silencing regulation as its homologues, a series of agro-infiltration experiments were performed suppressing or overexpressing *ERL1* and assessing the respective effects on RNA silencing and small RNA steady-state levels.

3.3.1. ERL1 fails to affect RNA silencing in *Agrobacterium* co-infiltration assays

In plant viruses, pathogenicity determinents have been shown to act as RNA silencing suppressors (Brigneti et al., 1998). Traditionally, viral genes are tested for silencing suppressor activity by assaying their effects on sense-induced *GFP* silencing in *N. benthamiana* plants. To determine, if ERL1 shows RNA silencing suppressor activity, *Agrobacterium* co-infiltration assays were performed, essentially as described before (Lu et al., 2004). In this assay, *GFP* silencing is induced by overexpression of *GFP* in an already *GFP*-expressing plant. Ectopic *GFP* expression triggers the co-suppression pathway and leads to RNAi-mediated silencing of the transgenically produced *GFP*. *Bona fide* suppressors of silencing are able to inhibit or delay the initiation of RNA silencing when expressed along with the silencing inducer. The assays were performed in *N. benthamiana* line 16c that is characterised by strong and stable *GFP* expression (Ruiz et al., 1998).
To create *ERL1* overexpression (35S-At*ERL1*gen) and suppression (35S-Nt*ERL1*hp) constructs, the genomic sequence of the *Arabidopsis ERL1* gene and a hairpin construct derived from a tobacco *ERL1* EST (EST ID EB681897), respectively, were cloned in the binary vector pART27 (Gleave, 1992) and transformed into *A. tumefaciens* strain C58C1. Equal volumes of an *A. tumefaciens* strain carrying a 35S-*GFP* construct [*pBIN* 35S-*mGFP4* (Haseloff et al., 1997)] serving as the silencing inducer were then mixed with *Agrobacteria* carrying the plasmids for *ERL1* overexpression or *ERL1* suppression. The final concentrations of all strains were adjusted to 0.25 at OD_{600}. 1:1 mixtures with

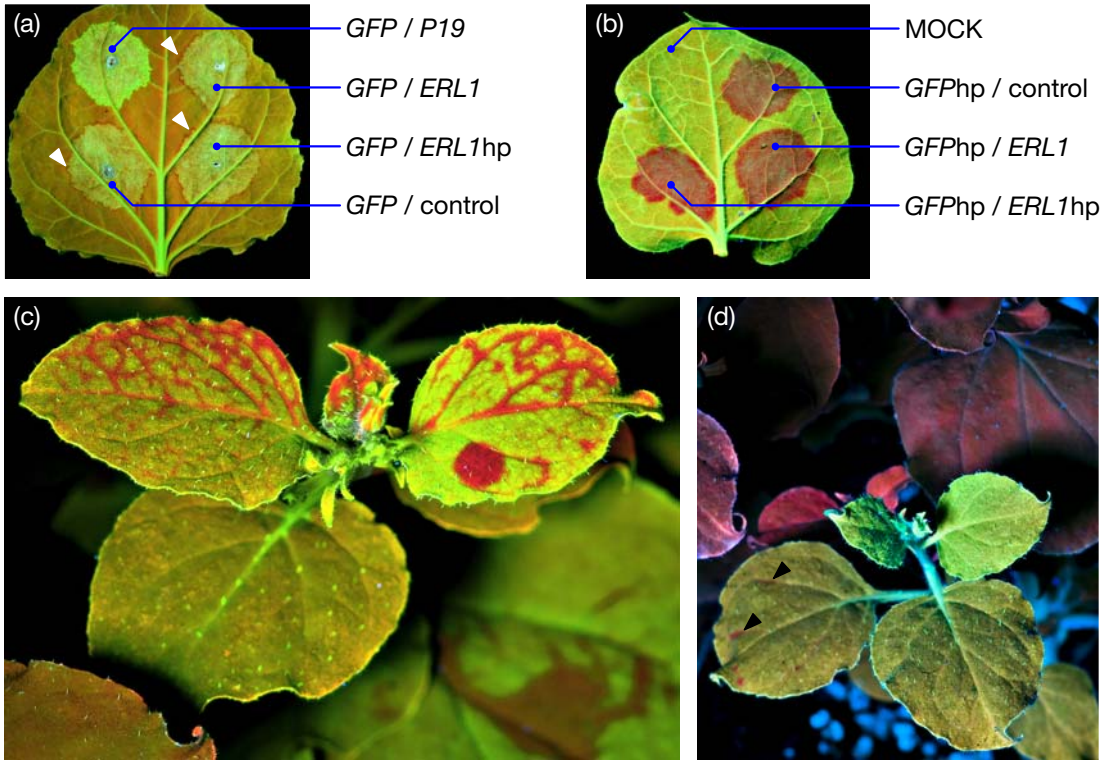

Figure 3.4 *Agrobacterium* co-infiltration assays in *N. benthamiana* line 16c to test *ERL1* for RNA silencing suppressor activity (a-b), and crosses of metastably *GFP*-expressing line *GFP* 6.4 with an *ERL1* overexpressor line (c-d). *GFP* overexpression (a) or a *GFP* hairpin construct (b) were used as inducers of *GFP* silencing, respectively. **(a)** *ERL1* overexpression and suppression have no effect on *GFP* silencing initiation and local silencing spread, comparable to the negative control. *P19* overexpression suppresses the onset of *GFP* silencing. Arrowheads indicate the red ring indicative of both *GFP* silencing and local silencing spread. **(b)** Also when induced with a *GFP* hairpin construct, *GFP* silencing is not affected by *ERL1* overexpression or suppression. The *GFP* silencing pattern and time course are comparable to the negative control. **(c)** Cross of *N. benthamiana* line *GFP* 6.4 with an *ERL1* overexpressor line (6.4x*ERL1*-A). Spontaneous short-range silencing and systemic silencing of *GFP* are not impaired in the *ERL1* overexpression background. **(d)** An independent cross of *GFP* 6.4 with the same *ERL1* overexpressor line (6.4x*ERL1*-B) showing a fully *GFP*-silenced plant (background leaves) with a single *GFP*-expressing branch. Onset of systemic silencing in this branch is indicated by arrowheads. Hence, also in this cross *ERL1* overexpression has no effect on spontaneous *GFP* silencing.
c+d Helm, unpublished results (images by Heiko Tobias Schumacher).

an empty binary plasmid or with a construct expressing the silencing suppressor *P19* of *Cymbidium ringspot virus* [35S P19-CymRSV (Havelda et al., 2003; Lakatos et al., 2004)] served as negative and positive controls, respectively. The *Agrobacterium* mixtures were used to agro-infiltrate distinct patches on 16c leaves, and *GFP* expression and silencing initiation were monitored over time using a handheld Blak-Ray® long-wave UV lamp. Under the conditions tested, *ERL1* was not able to suppress the onset of *GFP* silencing (Figure 3.4). Upon co-expression of *ERL1* and *GFP* (Figure 3.4 a), the red ring of local *GFP* silencing spread (Himber et al., 2003; Kalantidis et al., 2008) appeared at the same

time as in the empty plasmid negative control (Figure 3.4 a). *ERL1* suppression with a hairpin construct similarly had no effect on the RNA silencing time course (Figure 3.4 a). The red ring is not only indicative of RNA silencing initiation but also shows that SLSS was not affected by *ERL1* overexpression or suppression. Co-expression of *P19* on the other hand was able to suppress RNA silencing initiation, exemplified by strong GFP signal in the infiltrated patch and the absence of the red ring of local *GFP* silencing spread over the course of the experiment (Figure 3.4 a). In an equivalent experiment, *ERL1* overexpression and suppression also failed to affect *GFP* silencing when a *GFP* hairpin construct was used to induce silencing (Figure 3.4 b). Taken together, these assays show no ability of *ERL1* to negatively affect RNA silencing. Given its low expression levels and predominantly chloroplastic localisation a possible role of ERL1 in negative RNA silencing regulation may, however, be too weak to be detected in *Agrobacterium* co-infiltration assays that require rather robust silencing suppressors like P19 to counter agro-infiltration-induced RNA silencing.

3.3.2. Constitutive *ERL1* overexpression does not suppress *GFP* silencing in *N. benthamiana*

To overcome limitations of the agro-infiltration technique (*i.e.* its transient nature and an intrinsic variability of infiltration efficiency), *ERL1*-overexpressing *N. benthamiana* plants were generated (refer to section 3.4. for details) and crossed (by JMH) with the metastably *GFP*-expressing line *GFP* 6.4 (Figure 3.4 c-d). Line *GFP* 6.4 has been characterised as frequently exhibiting spontaneous short-range silencing of the *GFP* transgene, manifested as red spots under UV illumination (Kalantidis et al., 2006). The occurrence of spontaneous short-range silencing is typically followed by systemic spread of *GFP* silencing, ultimately leading to fully silenced plants (Kalantidis et al., 2006; Kalantidis et al., 2008). After crossing of line *GFP* 6.4 with *ERL1* overexpressor plants (6.4x*ERL1*), double homozygous individuals were selected from two independent crossings and their progeny analysed for alterations in their RNA silencing phenotypes. Line 6.4x*ERL1*-A (Figure 3.4 c) exhibits red spots of spontaneous short-range *GFP* silencing along with systemic *GFP* silencing spread. Similar observations were made for

the independent line 6.4x*ERL1*-B (Figure 3.4 d). In the depicted example (Figure 3.4 d) a *GFP*-expressing branch is emerging from an otherwise fully silenced plant (background leaves). Arrowheads indicate the onset of systemic *GFP* silencing on this branch. Therewith the *GFP* silencing phenotype of line *GFP* 6.4 is not affected in a genetic background of constitutive *ERL1* overexpression. Hence, a role for ERL1 in the negative regulation of RNA silencing in plants is not supported at this point (Helm, unpublished results).

3.3.3. PSTVd-derived siRNAs are suppressed upon *ERL1* overexpression

Upon infection with *Potato spindle tuber viroid* (PSTVd), *Nicotiana* plants produce large amounts of 21-24 nt siRNA-like RNAs derived from the viroid sequence, but are otherwise symptom-free. These PSTVd siRNAs are easily detectable in northern hybridisations and hence present a suitable reporter system to study possible effects of *ERL1* misexpression on siRNA steady-state levels.

Comparative agro-infiltration time course experiments were conducted by overexpressing *Arabidopsis ERL1* in systemically PSTVd-infected *N. tabacum*. Infiltrations with an empty binary vector served as controls. To study PSTVd siRNA steady-state levels over time, samples were collected every 4th day, and small RNA fractions were subsequently electrophoresed on 20 % PAA gels, northern-blotted, and analysed by hybridisations with PSTVd-specific probes. Non-infiltrated samples of the same plant were used as time points zero. The results of this experiment are summarised in Figure 3.5. 8 days postinfiltration PSTVd siRNA levels are reduced approximately 4-fold in samples that were treated with *ERL1* overexpression (Figure 3.5 a, left panel). The reduction seems to affect the different siRNA size classes (21, 22 and 24 nt) equally (Figure 3.5 a, left panel). In non-treated samples of the same plant PSTVd siRNA levels remain constant over time (Figure 3.5 a, right panel), ruling out an unspecific effect due to aging of the plant or differential progression of the PSTVd infection over the course of the experiment. Agro-infiltration with a control plasmid similarly had no measurable effect on PSTVd siRNA levels (Figure 3.5 a, middle panel). This experiment shows that the steady-state levels of siRNAs produced from PSTVd upon infection of *N. tabacum*

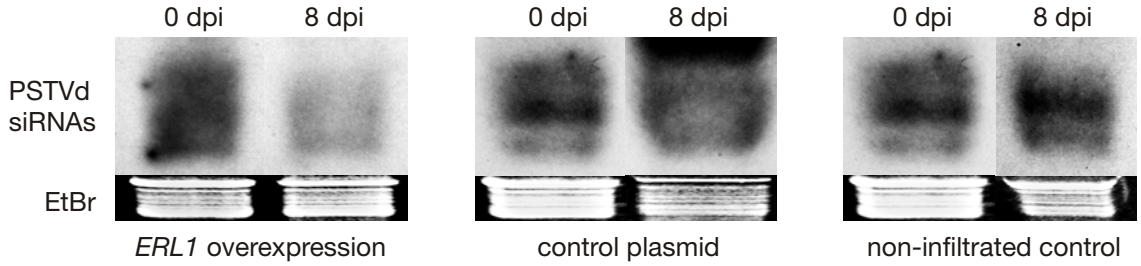

Figure 3.5 Comparative agro-infiltration time course in systemically PSTVd-infected tobacco. 8 days postinfiltration (dpi) overexpression has caused a reduction in PSTVd siRNA levels (left panel). Expression of a control plasmid has no effect on PSTVd siRNA levels (middle panel). In untreated leaves PSTVd siRNA levels remain constant over time (right panel), showing that the reduction in siRNA levels upon *ERL1* overexpression is a specific effect.

are being negatively affected by ectopic agro-infiltration-mediated *Arabidopsis ERL1* overexpression. It cannot be undoubtedly deduced, however, if this reduction in siRNA levels is caused by an siRNA-degrading activity of ERL1, or if this is the result of a secondary effect.

3.3.4. *ERL1*-overexpressing plants are hypersensitive towards viral infection

Since antiviral defence constitutes one of the major functions of RNA silencing in plants, it was investigated how plants with different *ERL1* backgrounds behave upon viral infection. To this end wildtype *N. benthamiana* and *ERL1* overexpressor plants were infected with *Plum pox virus* (PPV).

Under the conditions tested, wildtype *N. benthamiana* plants showed a typical progression of PPV infection, with mild mosaic symptoms developing after 1-2 weeks that persisted until senescence (Figure 3.6 a). *ERL1* overexpressor plants in contrast developed much stronger symptoms with severely crippled leaves (Figure 3.6 b). Only approximately 33 % of the PPV-infected *ERL1*-overexpressing plants survived the infection, while the remaining 67 % had died until six weeks postinfection. Given that PPV infections are typically non-lethal in *Nicotiana* plants, such a high lethality rate implies a hypersensitivity of *ERL1* overexpressor plants towards PPV infection. The surviving *ERL1* overexpressor plants remained dwarves with crippled leaves until senescence and produced only few underdeveloped flowers that failed to produce any

seeds. The slow growth and reduced fertility may to some extent be explained by *ERL1* overexpression itself (compare section 3.4.2. and Figure 3.7). A growth/fertility defect as pronounced as in the PPV-infected individuals, however, has never been observed in the specific bleach-type *ERL1* overexpressor line used in the infection experiments.

12 weeks postinfection total RNA was extracted from wildtype *N. benthamiana* and a surviving *ERL1* overexpressor plant and tested for the respective viral loads in northern hybridisations (Figure 3.6 c). In comparison to wildtype *N. benthamiana*, *ERL1* overexpressor plants accumulate approximately 3-5x higher virus titres. The increase in viral load may explain the observed aggravated symptoms. Whether this hypersensitivity is accountable to an siRNA-degrading activity of ERL1 could, however, not be determined in this experiment. Northern analyses of variegated *ERL1* overexpressor tissues (compare section 3.4.2. and Figures 3.6 and 3.10) showed a significant decrease in the steady-state mRNA levels of two of the four DICER-LIKE proteins, namely *DCL1* and *DCL4* (Figure 3.6 d). Since the DICER-LIKE proteins are crucial core components of RNAi-mediated antiviral defence in plants, the described hypersensitivity towards PPV infection may be caused by a reduction in DCL1-4 production and hence not constitute a primary effect of *ERL1* overexpression. The fact that at least *DCL1* and

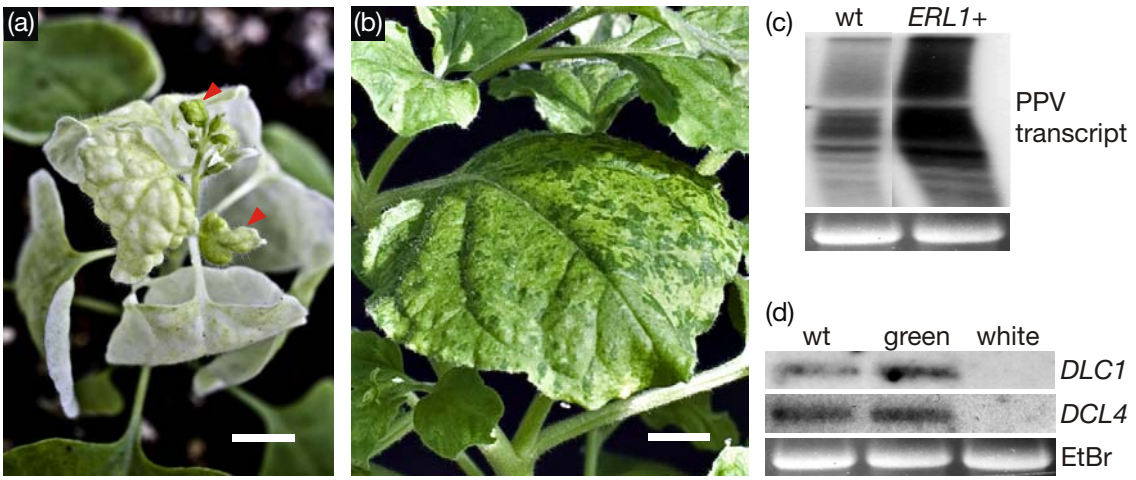

Figure 3.6 *ERL1* overexpressor plants are hypersensitive towards PPV infection and accumulate a higher viral load than wildtype *N. benthamiana*. **(a)** *ERL1*-overexpressing plant (bleach type) two weeks after PPV infection, exhibiting severe symptoms. Systemic leaves are crippled (arrowheads), and the plant stays tiny. **(b)** In the wildtype PPV induces a mild mosaic phenotype. **(c)** PPV-infected *ERL1* overexpressor plants accumulate a higher viral load than the wildtype. Samples were analysed approximately 12 weeks postinfection. **(d)** *DICER-LIKE 1* and *4* are both downregulated in white sectors of *ERL1*-overexpressing plants, while green sectors of the same plant show normal *DCL1* and *DCL4* transcript levels.

DCL4 are downregulated in *ERL1*-overexpressing tissue, however, gives leeway to a possible connection between ERL1 function and RNA silencing pathways. In this context it ought to be remembered that ERI-1 was shown to physically interact with DCR-1 in *C. elegans* (Duchaine et al., 2006).

3.4. Constitutive *ERL1* misexpression leads to multiple abnormalities in transgenic *N. benthamiana* plants

Agro-infiltration is a rapid, straightforward, and practical technique to perform basic functional analyses for genes of interest. Yet, the transient nature of agro-infiltration-mediated ectopic gene expression comprises important limitations, with agro-infiltrated leaves necrotising 7-20 days postinfiltration, depending on the plant species and the developmental stages of the infiltrated leaves. In addition, the efficiencies of agro-infiltrations vary to some extent, depending on numerous endogenous and exogenous factors, making a precise quantitation of results an intricate task. Therefore, a more sophisticated approach had to be taken in order to investigate the biological role of *ERL1* in detail. By *Agrobacterium*-mediated leaf disc transformation and using the same constructs as in the *Agrobacterium* co-infiltration assays (35S-At*ERL1*gen and 35S-Nt*ERL1*hp) a large collection of transgenic *N. benthamiana* lines were created. A total of 13 independent *N. benthamiana* lines were generated that overexpress the genomic version of *Arabidopsis ERL1*. Additional 6 transgenic *N. benthamiana* lines were created that express a tobacco *ERL1*-derived hairpin construct and hence represent *ERL1* suppressor plants. The majority of these transgenic lines are characterised by a multitude of structural and morphological abnormalities that are correlated with *ERL1* misexpression levels. This work was done by Jutta Maria Helm as part of her PhD thesis.

3.4.1. *ERL1* suppression can cause loss of chlorophyll in young plants

Transgenic *N. benthamiana* plants expressing the *N. tabacum ERL1*-derived hairpin construct on occasion show a loss of chlorophyll during early developmental stages

(Figure 3.7 d). The phenotype manifests as gradual bleaching of the first true leaves of *ERL1* suppressor plants (Figure 3.7 d). This abnormality presents infrequently in young plants, and mature *ERL1* suppressor plants are indistinguishable from wildtype *N. benthamiana*.

3.4.2. *ERL1* overexpression results in strong variegation phenotypes

ERL1 overexpressor plants exhibit various abnormalities including slow growth/ dwarfism, reduced seed production, and most commonly loss of chlorophyll leading to a variegated appearance. The observed variegation phenotypes manifest as three distinct varieties in individual *ERL1* overexpressor lines: mosaic, bleach, and self-silencer plants. Exemplary leaves of the different variegation types are depicted in Figure 3.7 a-c. In mosaic plants (Figure 3.7 a) leaves exhibit random distributions of white and green areas that differ in size, shape, and rate of occurrence. The phenotype is already present in seedlings and is maintained until senescence. The mosaic phenotype has no apparent negative effects on plant growth and development. Apart from the variegated appearance mosaic plants are morphologically similar to wildtype and produce normal amounts of seeds. Another variegation phenotype manifestation is depicted in Figure 3.7 b. These bleach-type plants exhibit an overall loss of chlorophyll, leading to pale green, yellow, or even white leaves. Northern analysis revealed that the bleach phenotype is stronger (*i.e.* more chlorophyll is lost) the higher the *Arabidopsis ERL1* transgene is expressed (data not shown). Bleach-type plants weakly overexpressing the *ERL1* transgene resemble the wildtype and are only marked by slightly brighter-than-usual leaves. Highly *ERL1*-overexpressing plants of the bleach type, however, are severely compromised in many aspects of growth, morphology and development. In Figure 3.7 g an approximately 8 weeks old wildtype *N. benthamiana* plant (left) is shown in comparison to a typical *ERL1*-overexpressing plant (right) of the same age that shows stunted internodes and only few and small leaves. Bleach plants of this type stay small for their entire lives, but they reach maturity after several months and produce few seeds. The strongest bleach-type *ERL1*-overexpressing plants exhibit purely white leaves and rarely survive the seedling stage. The few surviving plants in most cases fail to reach

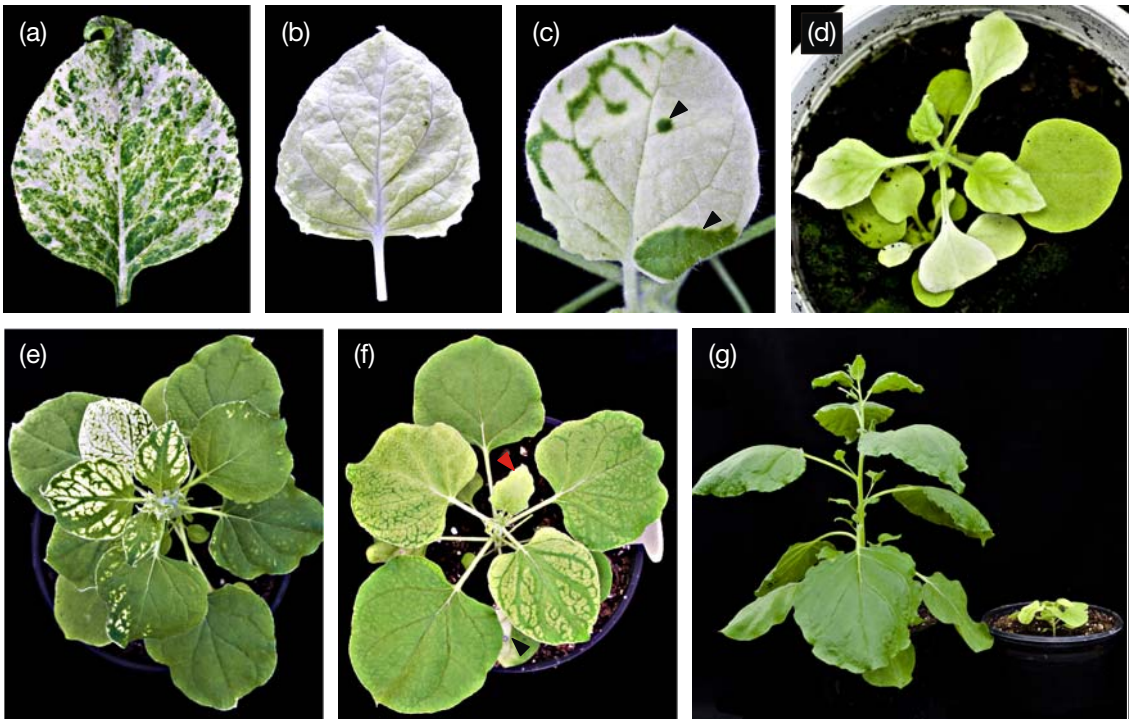

Figure 3.7 *ERL1*-dependent variegation phenotypes in transgenic *N. benthamiana* plants. **(a)** Mosaic *ERL1* overexpressor plants show random patterns of green and white sectors, but are otherwise not impaired in growth and development. **(b)** The bleach phenotype is characterised by an overall loss of chlorophyll. The extent of bleaching is more pronounced the higher the *ERL1* transgene is overexpressed. Shown here is a completely white leaf from a very highly *ERL1*-overexpressing bleach plant. **(c)** Self-silencer *ERL1* overexpressor plants exhibit white leaves with RNA silencing-type spreading of green wildtype-like tissue. Arrowheads indicate spontaneous short-range silencing-type green spots of wildtype-like tissue. **(d)** Young *ERL1* suppressor plant showing loss of chlorophyll. **(e)** Self-silencing *ERL1* overexpressor plant showing different stages of *ERL1* silencing spread. **(f)** Systemic *ERL1* silencing in a bleach-type plant, induced by agro-infiltration with an *ERL1* hairpin construct (black arrowhead indicates the point of agro-infiltration). The red arrowhead shows a newly emerging leaf void of systemic silencing-type spread of wildtype-like tissue. **(g)** Size comparison of a wildtype *N. benthamiana* (left) with a bleach-type *ERL1* overexpressor plant (right) 8 weeks after germination.

maturity and only occasionally produce sparse amounts of seeds. Self-silencer plants (Figure 3.7 c+e) are on average characterised by severe loss chlorophyll that in extreme cases leads to completely white leaves (Figure 3.7 c). The phenotype of chlorophyll-loss, however, is unstable, and self-silencer plants frequently revert to almost wildtype appearance. The time course of this reversion is reminiscent of the phenotype of systemic *GFP* silencing spread (Vaucheret et al., 1998; Voinnet et al., 1998), with vein-centric spreading of green wildtype-like tissue subsequently encompassing the whole leaf blade (Figure 3.7 e). Often this systemic silencing-type reversion to wildtype appearance is preceded by distinct spots of green tissue on otherwise white leaves (Figure 3.7 c, spots indicated by arrowheads). These spots are reminiscent of

spontaneous short-range RNA silencing that is frequently observed in transgenic *GFP*-expressing plants (Kalantidis et al., 2006; Kalantidis et al., 2008). Therefore, the re-appearance of green tissue may be interpreted as a reversion to wildtype in self-silencer *ERL1* overexpressor plants, caused by RNA silencing of the transgene. To confirm that white sector formation is a direct result of *ERL1* overexpression, young *ERL1*-overexpressing plants with a mild bleach phenotype (*i.e.* pale green leaves) were agro-infiltrated with an *Arabidopsis ERL1* hairpin construct (35S-At*ERL1*hp) to induce RNA silencing of the transgene (Figure 3.7 f, point of infiltration indicated by black arrowhead). Several days postinfiltration wildtype-like green tissue started spreading from the veins of systemic leaves, strongly resembling the phenotype of systemic *GFP* silencing spread (Figure 3.7 f). It was observed that in about 50 % of the cases, systemic spread of induced *ERL1* silencing did not propagate more than a few leaves (Figure 3.7 f, red arrowhead indicating a newly emerging leaf void of RNA silencing-type spreading of green tissue), which suggests that systemic RNA silencing may to some extent be suppressed in *ERL1* overexpressor plants. The remaining 50 % of plants continued to systemically silence the *ERL1*-dependent bleaching phenotype and regained wildtype appearance until senescence.

To prove that all the observed variegation phenotypes are dependent on *ERL1* overexpression, leaf material was collected separately from green and white sectors of the same self-silencer plant and tested for *ERL1* expression in northern hybridisations (Figure 3.10 a). The results show clearly that *ERL1* mRNA can only be detected in white tissues but not in green sectors (Figure 3.10 a). Therefore, white sector formation is directly dependent on *ERL1* overexpression, and green sector formation can be interpreted as a recovery phenotype after silencing of the *ERL1* transgene. Despite their high conservation on the protein level the *Arabidopsis* and *Nicotiana ERL1* cDNAs are too divergent, however, to yield fully complementary *Arabidopsis ERL1* 21-mers that could act as siRNAs to silence the endogenous *N. benthamiana ERL1* mRNA. It can therefore be assumed that green sectors in self-silencing *ERL1* overexpressor plants represent a reversion to a wildtype situation rather than a scenario in which also the endogenous *N. benthamiana ERL1* homologue would be suppressed.

It was observed that the manifestations of *ERL1*-dependent variegation phenotypes follow a certain periodicity. In many cases, seedlings with severe phenotypes (bleach,

self-silencing, and mosaic) regain chlorophyll and appear wildtype-like as young plants. Mature plants again develop more severe phenotypes that usually persist until the plants become senescent. The changes between the different phases occur gradually over many weeks. Even though this periodicity is not restricted to certain seasons, it appears that high light regimes (April to September) facilitate stronger bleaching/mosaic phenotypes in *ERL1* overexpressor plants.

3.4.3. Physiological alterations of the photosynthetic apparatus

ERL1 misexpression in *N. benthamiana* leads to various abnormalities, comprising loss of chlorophyll as a unifying characteristic. It can therefore be assumed that these phenotypic variations are accompanied by altered photosynthetic activity and efficiency. To determine basic bio-energetic parameters that characterise the photosynthetic process *in vivo*, analyses of the direct fluorescence of chlorophyll *a* in photosystem II were performed, which reflect initial events of photosynthetic activity (Strasser et al., 2000).

To this end leaf discs of variegated *ERL1* overexpressor plants and wildtype *N. benthamiana* were dark-adapted for 15 minutes, and chlorophyll *a* fluorescence

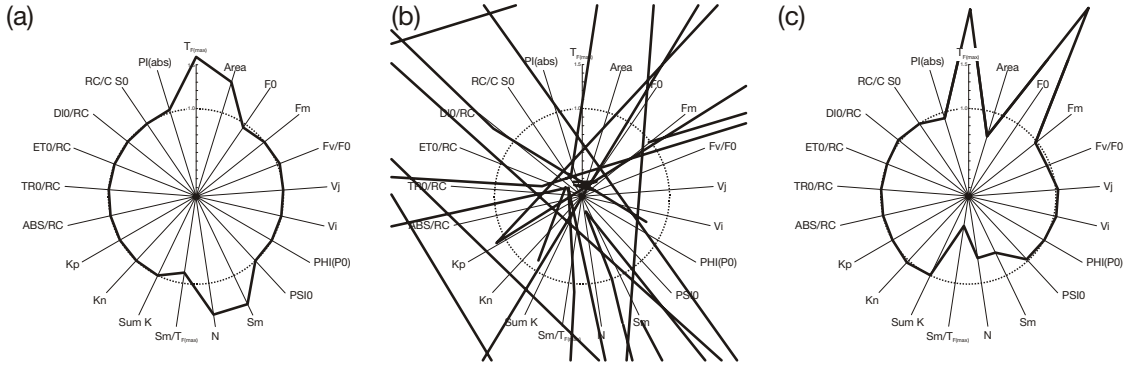

Figure 3.8 Radar plot representations of basic bio-energetic parameters of *ERL1* overexpressor plants as determined by chlorophyll *a* fluorescence measurements. All values in relation to wildtype (dashed circle). **(a)** Green sector of a self-silencer *ERL1* overexpressor plant. While most parameters are in good congruence with the wildtype, the values $T_{F(max)}$, Area, Sm, and N are significantly increased. **(b)** Measurements in white sectors of the same self-silencer plant as in (a) yield chaotic results. **(c)** Similar to (a) mosaic leaves yield mostly wildtype-like measurements, while few values show significant increase or decrease compared to the wildtype. Specifically, $T_{F(max)}$ and F0 are highly increased, while N and Sm are decreased.

measurements (at least triplicates) were performed using a Handy-PEA fluorophotometer (measurements by JMH). The results of these measurements are summarised in Figure 3.8 [for details about the displayed parameters, please refer to (Strasser et al., 2000; Bussotti et al., 2007) and references therein]. Measured wildtype values were defined as 1.0, and all data from the different *ERL1* overexpressor samples were analysed in relation to the wildtype. Green and white sectors of the same *ERL1* self-silencer plants were analysed separately, in order to determine differences in photosynthetic performance between the chlorophyll-less and the recovered green tissues (Figure 3.8 a+b). Chlorophyll *a* fluorescence measurements in green sector samples show a wildtype-like behaviour of the majority of parameters (Figure 3.8 a), with few exceptions. $T_{F(max)}$, the time needed to reach maximum fluorescence, is considerably increased in green sectors, indicating a higher density of photoactive reaction centres (Figure 3.8 a). Accordingly, the number of turnovers of the primary electron acceptor Q_a of photosystem II between F0 and $T_{F(max)}$ (parameter N) is also increased significantly (Figure 3.8 a). The quantities of fluorescence-competent chlorophyll *a* molecules in the antennae structures of photosystem II (parameter F0), however, are comparable to the wildtype (Figure 3.8 a). These measurements point towards enhanced photosynthetic activity in green sectors of self-silencer *ERL1* overexpressor plants as a result of increased turnover of photo-synthetic components; a notion supported by the transcriptional upregulation of *PFTF* and *CLP* in green sectors (compare section 3.5. and Figure 3.10 a). In stark contrast, chlorophyll *a* fluorescence measurements in white sectors of the same *ERL1* overexpressor plant yield only chaotic results (Figure 3.8 b). In light of the total loss of chlorophyll (compare section 3.4.2. and Figure 3.7 a-c) and the lack of properly developed plastids (compare section 3.4.4. Figure 3.9 a), this result can only be interpreted as a complete inability to form a functional photosynthetic apparatus in white sectors. Mosaic leaves show a distinct pattern of chlorophyll *a* fluorescence (Figure 3.8 c). Similar to green sectors, mosaic leaves exhibit a greatly extended $T_{F(max)}$ (Figure 3.8 c). F0, in contrast, is elevated more than 2-fold compared to wildtype, indicating increased amounts of chlorophyll *a* molecules (Figure 3.8 c). This measure-ment is in agreement with the observation of overdeveloped chloroplasts in the green sectors of mosaic-type *ERL1* overexpressor plants (compare section 3.4.4. and Figure 3.9 c). Contrarily to green sectors from self-silencer plants (Figure 3.8 a) the

prolonged $T_{F(max)}$ in mosaic leaves is not associated with an increase in parameter N (Figure 3.8 a). The results from mosaic leaves are, however, difficult to interpret since they represent mixed tissues of physiologically highly divergent green and white sectors. Taken together the chlorophyll *a* fluorescence data for mosaic leaves may be interpreted as overaccumulation of chlorophyll *a* molecules and photosystem II antennae structures. Supposedly, these alterations in the organisation of the photosynthetic apparatus are part of a compensatory measure to overcome the loss of photosynthetically active tissue in bleaching *ERL1* overexpressor tissues (compare section 3.4.4. and Figure 3.9 c).

3.4.4. Histological and ultrastructural alterations of variegated tissues

In order to gain a better understanding for the underlying cause of the *ERL1*-dependent variegation phenotype, leaf sections of different *ERL1* overexpressor lines were analysed by transmission electron microscopy (TEM) and light microscopy. TEM observations revealed significant structural differences between wildtype chloroplasts and those from *ERL1*-overexpressing lines (Figure 3.9). More intriguingly, very similar differences can be seen between white and green sectors of the same *ERL1* overexpressor plants (Figure 3.9). Light microscopical analysis showed disturbed development of leaf tissues in variegated plants, consistent with the observed abnormal plastids in white *ERL1*-overexpressing sectors (Figure 3.9).

White leaf sectors contain only few plastids that are irregular in shape and size and lack the conventional internal structure of chloroplasts (Figure 3.9 a). Instead of stacked grana, white sector plastids contain only rudimentary thylakoids that are dispersed unregularly throughout the stroma (Figure 3.9 a). They resemble undifferentiated proplastids of meristematic tissues and appear to be arrested at an early stage of development. Chloroplasts from *ERL1* suppressor plants in contrast appear relatively similar to wildtype (Figure 3.9 b). *ERL1* suppressor chloroplasts contain canonical grana, but they are enlarged and contain large starch granules (Figure 3.9 b). The

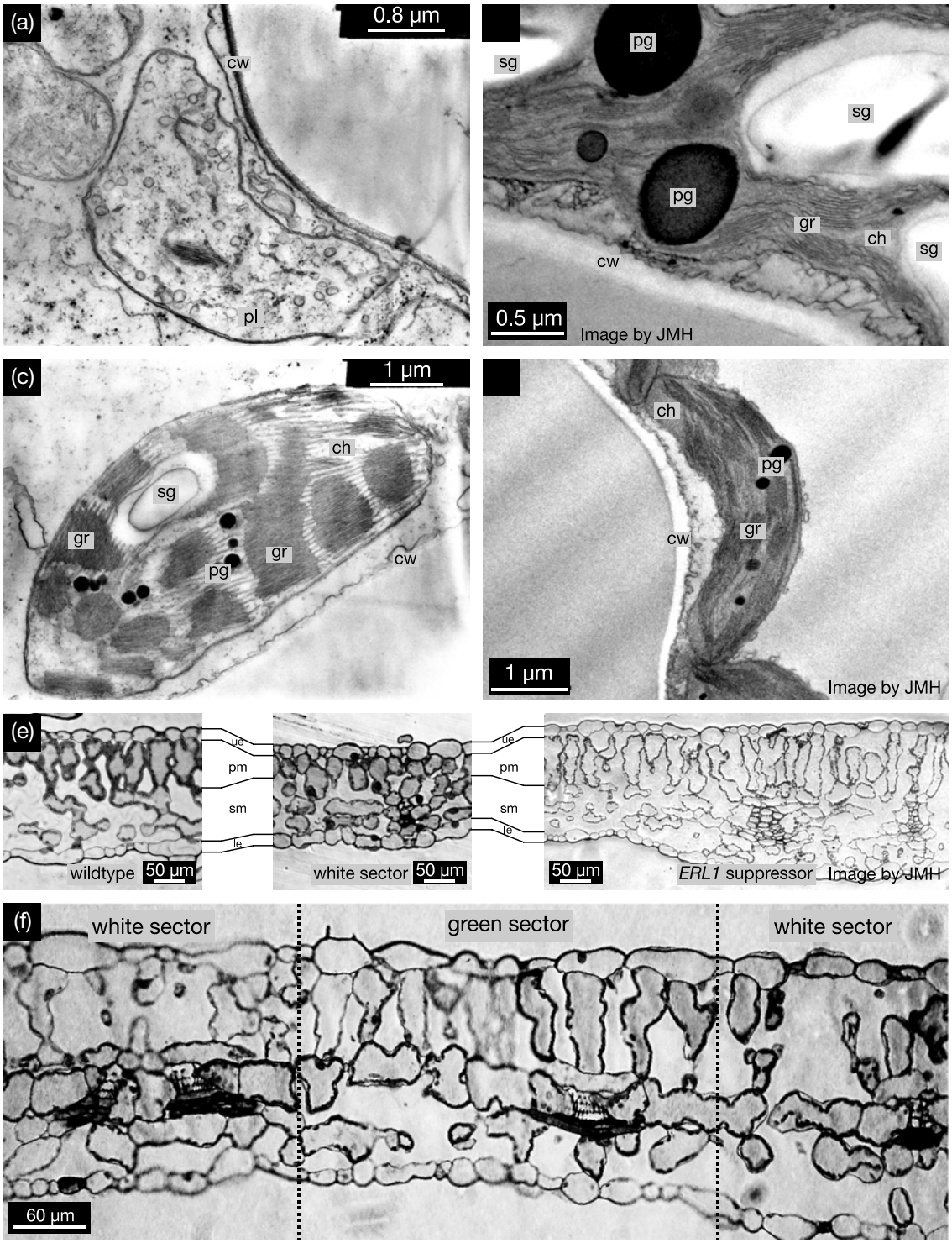

Figure 3.9 Analyses of *ERL1* supressor and overexpressor plants with optical (e+f) and electron microscopes (a-d). **(a)** Unstructured white sector plastid of a bleach-type *ERL1* overexpressor plant. **(b)** Wildtype-like plastid of an *ERL1* suppressor plant. **(c)** Detailed view of a green sector chloroplast from a mosaic leaf with significantly enlarged grana. **(d)** Wildtype chloroplast. **(e)** Transverse sections comparing a wildtype leaf (left) with a white sector of a bleach-type *ERL1* overexpressor plant (middle) and an *ERL1* suppressor plant (right). The white sector lacks a canonical palisade layer and is thinner than wildtype and *ERL1* suppressor leaves. **(f)** Transverse section of a mosaic leaf showing transitions between white (left and right) and green (middle) sectors. ch = chloroplast; cw = cell wall; gr = granum; le = lower epidermis; pg = plastoglobulus; pl = plastid; pm = palisade mesophyll; sg = starch granule; sm = spongy mesophyll; ue = upper epidermis.

presence of starch granules is a hallmark of functional photosysnthesis. When analysed in detail, chloroplasts from green sectors of mosaic-type *ERL1*-overexpressing plants frequently exhibit significantly enlarged grana (Figure 3.9 c). While grana in wildtype chloroplasts typically consist of 3-10 stacked thylakoids (Figure 3.9 d), green sector chloroplasts contain grana that may on occasion comprise more than 30 thylakoids (Figure 3.9 c). This increased density of photosynthetic tissue may, in agreement with results from chlorophyll *a* fluorescence measurements (compare section 3.4.3. and Figure 3.8), constitute a compensatory measure to counterbalance the loss of photosynthetically competent chloroplasts in white sectors. The fact that the *ERL1*-dependent bleaching phenotype can revert to a wildtype-like situation (compare section 3.4.2. and Figure 3.7) implies that the observed proplastid-like plastids in white sectors retain the ability to differentiate into *bona fide* chloroplasts. Therefore, *ERL1* overexpression appears to result in a reversible block in early plastid development.

White sectors of *ERL1* overexpressor plants not only accumulate defective chloroplasts, but also exhibit non-canonical development of the palisade mesophyll, as shown in light microscopical examinations of transverse leaf sections (Figure 3.9 e-f). Wildtype leaves are composed of upper epidermis, palisade mesophyll, spongy mesophyll and lower epidermis (Figure 3.9 e, left panel). While white sector leaves in principle show a similar architecture, they are thinner than wildtype leaves and lack a fully developed palisade mesophyll (Figure 3.9 e, middle panel). Instead, all cells between the epidermides have a roughly globular shape reminiscent of cells belonging to the spongy mesophyll. *ERL1* suppressor leaves have wildtype appearance and contain properly developed palisades, possibly with slightly increased spaces between individual palisades (Figure 3.9 e, right panel). In a mosaic leaf section (Figure 3.9 f) the transitions between white (left and right) and green sectors (middle) are apparent. The green middle sector displays *bona fide* palisade mesophyll, while the two white sectors exhibit large spongy mesophyll-like intercellular spaces throughout the whole section of the leaf (Figure 3.9 f).

The histological and ultrastructural alterations of *ERL1* overexpressor plants described here (underveloped chloroplasts, lack of a canonical palisade mesophyll) are similar to those observed in different variegated mutants and to the phenotypes caused by specific viroids upon infection [*e.g.* (Wang et al., 2000; Bollenbach et al., 2005; Rodio et al., 2007)]. A more detailed comparison with similar reported phenotypes from the

literature may provide a means to identify the *ERL1*-dependent pathway that is disturbed in *ERL1* misexpressor plants.

3.5. Northern analysis reveals a complex pattern of transcriptional misregulation in *ERL1*-overexpressing plants

Transcript levels of genes implicated in chloroplast development and photosynthesis were analysed by RNA gel blot hybridisations to characterise, which pathways are disturbed in transgenic *ERL1* suppressor and overexpressor plants. For this purpose total RNA was separately extracted from green and white tissues of variegated self-silencer *ERL1* overexpressor plants and compared to total RNA from wildtype *N. benthamiana* (Figure 3.10).

After hybridisation with an *ERL1*-specific probe strong *ERL1* signal can be detected in white but not in green sectors (Figure 3.10 a), showing that white sector formation is dependent on high *ERL1* expression. In the wildtype *ERL1* mRNA cannot be detected due to its low expression levels (compare section 3.1. and Figure 3.1). In addition northern hybridisations were performed for a variety of nucleus- and plastid-encoded *Nicotiana* genes to gain a deeper understanding of the physiological traits of *ERL1*-overexpressing plants.

Arabidopsis FTSH2 encodes a metalloprotease involved in the proteolytic turnover of photosystem II proteins, which is a crucial prerequisite for the replacement of photo-damaged components of the photosynthetic apparatus. Its *Nicotiana* homologue *PFTF* is transcribed at similar levels in white sectors and the wildtype, whereas it is upregulated in green sectors (Figure 3.10 a). The same expression pattern was detected for *CLP*, a PFTF antagonist (Figure 3.10 a). Increased *PFTF* and *CLP* levels in green sectors may indicate increased turnover of the photosysnthetic apparatus. This is consistent with the observation of overdeveloped chloroplasts in green sectors of variegated *ERL1* overexpressor plants (compare section 3.4.4. and Figure 3.9 c). The results of the chlorophyll *a* fluorescence measurements that indicate a higher density of photoactive reaction centres in green sectors (compare section 3.4.3. and Figure 3.8 a) point to the same conclusion.

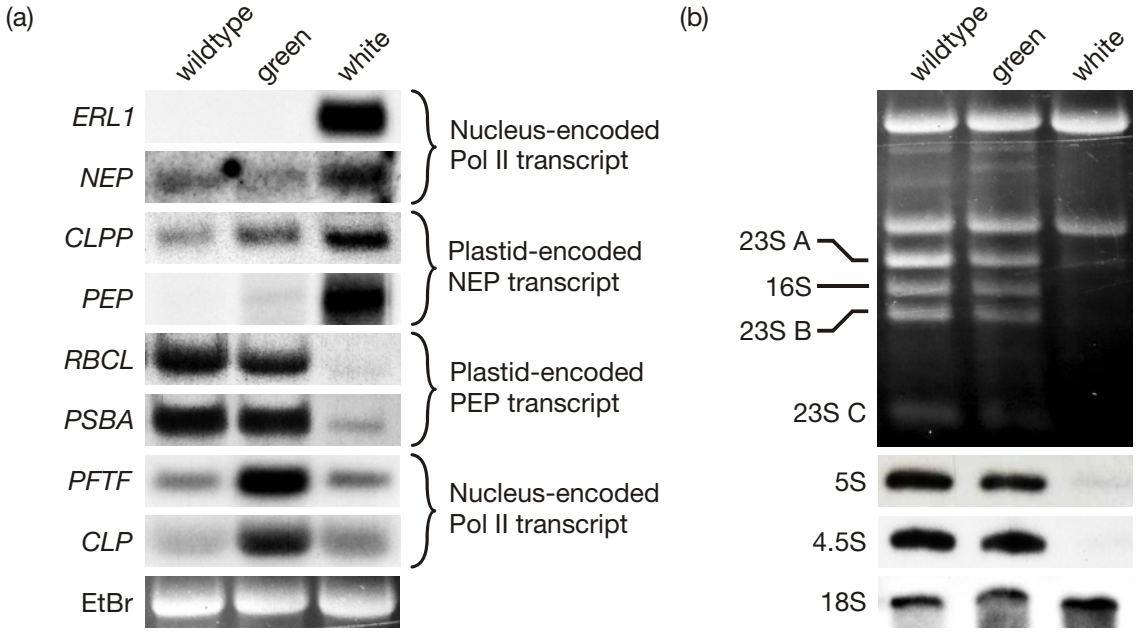

Figure 3.10 Molecular characterisation of important chloroplast-related transcripts in overexpressor plants. **(a)** Genes involved in photosynthesis and chloroplastic transcription show a complex pattern of misregulation in -overexpressing plants. **(b)** Chloroplastic rRNAs are downregulated in white sectors of overexpressor plants. 23S rRNA is present as three distinct isoforms of 1.7 kb (23S A), 1.2/1.0 kb (23S B) and 0.5 kb(23S C).

Two chloroplastic RNA polymerases are responsible for the production of distinct groups of plastid transcripts. The nucleus-encoded polymerase (*NEP*) is found to be upregulated in white sectors (Figure 3.10 a). NEP-dependent transcripts comprise mRNAs for ribosomal proteins and the plastid-encoded polymerase (PEP) encoded by the *RPOB* gene (Hajdukiewicz et al., 1997). A drastic upregulation is observed for the NEP-dependent *RPOB* gene (Figure 3.10 a), and the expression levels of two additional NEP-transcribed genes, *RPL23* and *CLPP*, were tested and both found to be upregulated in white sectors (Figure 3.10 a; data for *RPL23* not shown). Hence, NEP is functional in white sector plastids. PEP mainly transcribes plastid-encoded photosynthesis-related genes and the 4 chloroplastic ribosomal RNAs (Hajdukiewicz et al., 1997). Probes specific for *RBCL* encoding the large subunit of Ribulose-1,5-bisphosphate carboxylase/ oxygenase (RuBisCO) and for *PSBA* encoding the D1 protein of photosystem II detect *RBCL* and *PSBA* at similar levels in wildtype and green sector samples, whereas transcript levels are significantly reduced in white sectors (Figure 3.10 a). The transcriptional downregulation is accompanied by a decrease in protein production, which is exemplified by the loss of a visible RuBisCo band in Coomassie-stained gels of white sector protein extracts (data not shown). The same pattern of transcriptional

downregulation in white sectors was also found to be true for two other key enzymes of the photosynthetic apparatus (*PSAA* and *PSAB*; data not shown). In white sectors, all the chloroplastic rRNAs (23S, 16S, 5S and 4.5S) are significantly downregulated, albeit not completely lost, whereas there is practically no difference in green sectors when compared to the wildtype (Figure 3.10 b, northern blots for 5S and 4.5S rRNA by JMH). The cytosolic 25S and 18s rRNAs as well as the mitochondrial 18S rRNA are comparable in all samples (Figure 3.10 b), showing that specifically plastid ribosomal RNAs are negatively affected in white sectors of *ERL1* overexpressor plants.

In summary, green sector transcription is functional in the nucleus as well as in plastids with transcription patterns similar to the wildtype in most cases. In contrast, transcription by the plastid-encoded RNA polymerase is severely impaired in white sectors, resulting in drastic transcriptional downregulation of PEP-dependent transcripts, including all chloroplastic rRNAs.

3.6. ERL1 plays a role in the maturation of the chloroplastic 5S ribosomal RNA

Macroscopically as well as on the molecular level, the observed variegation phenotypes in *ERL1*-overexpressing *N. benthamiana* plants are most similar to the variegation phenotype peach calico caused by infection of *Prunus persica* with specific strains of *Peach latent mosaic viroid* (PLMVd) (Rodio et al., 2007). Peach calico is the result of dysfunctional maturation of the small chloroplastic ribosomal RNAs, leading to a general breakdown of chloroplast development. Taking into account the properties of *ERL1* homologues in 5.8S rRNA 3' end maturation (Ansel et al., 2008; Gabel and Ruvkun, 2008), it was analysed whether *ERL1* misexpression has a direct influence on chloroplast rRNA maturation, which may cause dysfunctional ribosomes and ultimately result in the observed *ERL1*-dependent variegation phenotypes.

The question was addressed with a comparative agro-infiltration time course assay (Figure 3.11). Large tobacco leaves were infiltrated with *A. tumefaciens* strains carrying constructs for *ERL1* overexpression, *ERL1* suppression, and *GFP* overexpression as a negative control. Samples were collected for six consecutive days and were analysed by

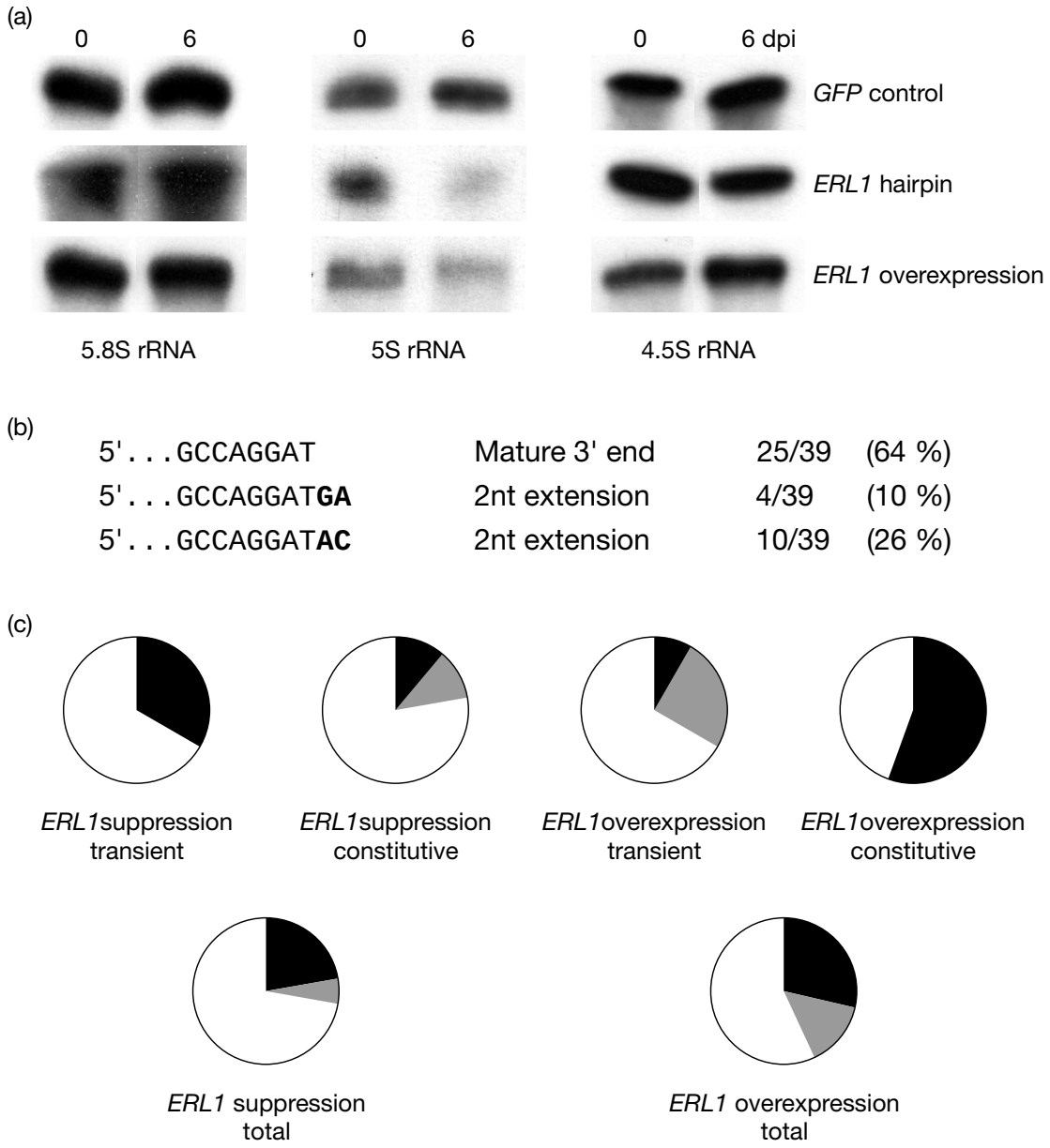

Figure 3.11 Impact of *ERL1* misexpression on small ribosomal RNA steady-state levels and 3' ends. **(a)** 5.8S and 4.5S rRNA steady-state levels are not influenced by *ERL1* suppression, *ERL1* overexpression, and control *GFP* expression. 5S rRNA is downregulated upon *ERL1* suppression and, albeit to a lesser extent, by *ERL1* overexpression. Control *GFP* expression does not affect 5S rRNA steady-state levels. **(b)** Predominant 3' extensions cloned from *ERL1*-misexpressing tissues and their relative rates of occurrence. **(c)** Graphical representations of the relative frequencies of the predominant 3' extensions cloned from *ERL1*-misexpressing tissues.
dpi, days postinfiltration. Color code: ■, +AC; ■, +GA; □, mature.
b+c Helm, unpublished results.

northern hybridisations, probing for 5.8S (cytoplasmic), 5S, and 4.5S (both chloroplastic) ribosomal RNAs. As expected, *GFP* expression had no effect on any of the tested rRNAs (Figure 3.11 a). *ERL1* overexpression and suppression did not affect 5.8S and 4.5S rRNAs (Figure 3.11 a). In the case of 5S rRNA, however, a significant reduction in

transcript levels could be observed over time, when overexpressing or suppressing *ERL1* in this agro-infiltration time course (Figure 3.11 a). It therefore appears that the chloroplastic 5S rRNA may constitute an *in vivo* target of ERL1 activity.

3.6.1. Correct 3' end processing of 5S rRNA is disturbed upon *ERL1* misexpression

To verify an involvement of ERL1 in the biogenesis of short ribosomal RNA species, the precise 3' ends of the respective rRNAs were separately cloned by circular RT-PCR from plant material transiently and constitutively overexpressing and suppressing *ERL1*, and wildtype samples served as controls. This work was done by Jutta Maria Helm as part of her PhD thesis.

As expected wildtype samples yielded the annotated mature 3' ends for all rRNAs tested (data not shown). As for 4.5S and 5.8S rRNAs, only mature 3' ends were cloned in all samples (data not shown). In the case of 5S rRNA, however, 3' extensions of 2 nucleotides were found to accumulate in constitutively as well as transiently *ERL1*-misexpressing samples (Figure 3.11 b). 36 % of all cloned 5S rRNA 3' ends were found to be extended in *ERL1*-misexpressing tissue (Figure 3.11 b-c). These 2 nt extensions of the 5S rRNA 3' end emerge as two predominant populations. Less frequently (29 % of all cloned extensions) a +GA addition was detected (Figure 3.11 b-c), which corresponds to an elongation derived from the genomic precursor sequence of the chloroplastic 5S rRNA. The remaining 71 % of the predominant 5S rRNA 3' extensions comprised +AC (Figure 3.11 b-c) representing untemplated extensions. In addition, single cases of untemplated +CC, +ACC, and +A extensions were found. Relative frequencies of the predominant 3' extensions detected in *ERL1*-suppressing and -overexpression samples (transiently as well as constitutively) are shown in Figure 3.11 c.

These results indicate an involvement of ERL1 in the processing of plant ribosomal RNA. In contrast to animal and fungi, where its homologues were shown to process the cytosolic 5.8S rRNA, the physiological substrate of plant ERL1 is the chloroplastic 5S rRNA (Helm, unpublished results).

4

Discussion

4.1. Two phylogenetic clades of ERI-1 homologues are implicated in distinct functional contexts

The extensive utilisation of repressive small RNA pathways in many cellular functions has raised questions regarding the endogenous regulation of these mechanisms. Over the years a number of factors have been annotated as endogenous negative regulators or suppressors of RNA silencing, implying that the roles of these factors are to prevent RNA silencing responses from overreacting or targeting non-canonical targets (compare section 1.7.). In most cases, however, these annotations were based on secondary effects observed upon loss of function of the respective proteins in question. Therefore, genuine activities for rgs-CaM, ATRLI2, XRN2-4, FRY1, and RRF-3 in RNA silencing suppression are not supported when a strict definition is applied. *Bona fide* suppressors of silencing are those virus-encoded proteins that developed diverse abilities to counteract their hosts's RNA silencing-mediated immune responses as a result of selective pressures in an evolutionary arms race between viruses and their respective hosts. VSRs employ sundry strategies of RNA silencing suppression, but most commonly repressive binding of siRNAs, the mediators of antiviral RNA silencing, constitutes a cornerstone of VSR actions (Lakatos et al., 2006). The as yet only known endogenous factors to employ related strategies of siRNA repression are *C. elegans* ERI-1 and its homologues across the tree of life. Therefore ERI-1 homologues represent the

only endogenous proteins meeting the criteria for annotation as *bona fide* suppressors of silencing (compare section 1.7.). A variety of studies in different model organisms functionally characterised the respective ERI-1 homologues and thus circumstantiated their capacities to negatively modulate RNA silencing pathways through degradative affinities for siRNAs (Kennedy et al., 2004; Bühler et al., 2005; Hong et al., 2005; Bühler et al., 2006; Iida et al., 2006; Hong et al., 2007; Maiti et al., 2007). Unequivocal involvements in RNA silencing regulation could, however, not be appointed to all investigated ERI-1 homologues. Recombinant *Drosophila* Snipper for instance exhibits a noteworthy efficiency in the degradation of structured dsRNA and dsDNA substrates with 3'-protruding ends *in vitro* (Kupsco et al., 2006). Yet, snipper loss-of-function revealed no measurable increase in RNAi efficiency as would be expected in mutants lacking an endogenous RNA silencing suppressor (Kupsco et al., 2006). An alternative Snipper activity has not been proposed thus far, but a recent report regarding the RNA silencing system in the omnivorous beetle *Tribolium castaneum* highlighted a plausible explanation for the lack of a discernable RNA silencing-regulating capacity of the *Drosophila* ERI-1 homologue (Tomoyasu et al., 2008). Phylogenetic analysis of multiple characterised and non-characterised ERI-1 homologues from diverse eukaryotic lineages revealed two phylogenetically distinct ERI-1 subclasses [(Tomoyasu et al., 2008) and Figure 4.1]. The chief differences between Group I and Group II ERI-1 homologues lie in the domain compositions of the respective proteins. Group I ERI-1 homologues contain two functional domains: a conserved ERI-1_3'hExo_like EXOIII domain responsible for 3' to 5' exonucleolytic cleavage and an amino-terminal SAP domain conferring nucleic acid binding capability in a sequence-independent manner. These SAP/EXOIII proteins include the well characterised *C. elegans* ERI-1, human Thex1/3'hExo, mouse and *S. pombe* Eri1, as well as *N. crassa* QIP. They stand in contrast to Group II ERI-1 homologues that are exemplified by *Drosophila* Snipper, *Tribolium* Tnc-Snp, and *Dictyostelium* eriA that all lack the aforementioned SAP domain and solely consist of an ERI-1_3'hExo_like EXOIII domain. Tnc-Snp and eriA have not been functionally characterised yet, but based on results from *Drosophila* Snipper (Kupsco et al., 2006) they are expected to be involved in pathways distinct from RNA silencing regulation (Tomoyasu et al., 2008). Phylogenetically, *Arabidopsis* ERL1 affiliates with Group II ERI-1 homologues, reflecting its lack of a discernable SAP

4. Discussion

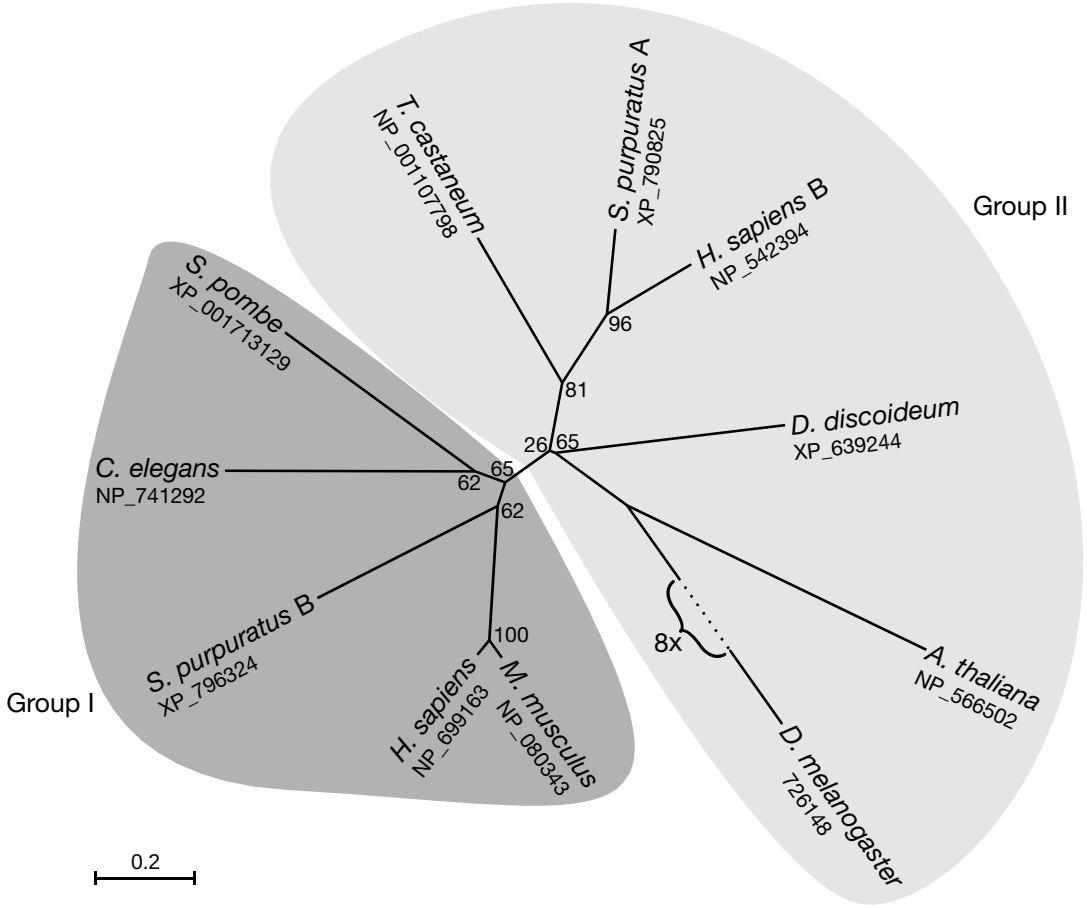

Figure 4.1 Phylogenetic analysis of ERI-1 homologues across kingdoms. ERI-1 homologues lacking a *bona fide* SAP domain constitute a group of proteins (Group II) distinct from SAP domain-containing ERI-1 homologues (Group I). The phylogenetic tree was constructed from full protein sequences of ERI-1 homologues (accession numbers are stated below the respective species names).
The evolutionary history was inferred using the Neighbour-Joining method (Saitou and Nei, 1987). The optimal tree with the sum of branch length = 6.10525861 is shown. The tree is drawn to scale, with branch lengths in the same units as those of the evolutionary distances used to infer the phylogenetic tree. The evolutionary distances were computed using the Poisson correction method (Zuckerhandl and Pauling, 1965) and are in the units of the number of amino acid substitutions per site. Phylogenetic analyses were conducted in MEGA4 (Tamura et al., 2007).

domain (Figure 4.1). This aspect constitutes an important facet for the interpretation of the results presented in this work, since it allows for the inference that ERL1 should be found to be implicated in mechanisms distinct from RNA silencing regulation.

On the protein level *Arabidopsis* ERL1 shares significant homology with animal and fungal ERI-1 homologues (Figure 3.1), which lead to the working hypothesis that ERL1 may be a functional ERI-1 orthologue similarly involved in the negative modulation of plant RNA silencing pathways. The hypothesis was initially tested in *Agrobacterium* co-infiltration assays, which represent the classical method to determine RNA silencing

suppressor activities of viral proteins (Brigneti et al., 1998). In these assays *GFP* silencing is induced either by ectopic overexpression of *GFP* leading to co-suppression of the *GFP* transgene in the 16c plants used for the experiment, or by expression of a *GFP* haipin construct. Silencing induction by hairpin constructs circumvents the necessity for RDR-dependent dsRNA formation upon sensing of a not further specified aberrancy of ectopically overexpressed sense *GFP*. Therefore, the use of either sense *GFP* or a *GFP* hairpin to induce *GFP* silencing theoretically allows for a differential evaluation regarding the specific steps that may be affected by *bona fide* silencing suppressors. Neither *ERL1* suppression nor *ERL1* overexpression, however, showed any measurable effects on *GFP* silencing inititation and spreading in the conducted experiments, regardless whether sense *GFP* or a *GFP* hairpin were used to induce *GFP* silencing (Figure 3.4 a). These results by themselves are strong indications for a non-involvement of ERL1 in RNA silencing regulation. It should be noted, however, that agro-infiltration is a comparatively non-sensitive technique influenced by a variety of endogenous and exogenous factors. The maximal temporal resolution in *Agrobacterium* co-infiltration assays is 1-2 days, and many factors regarding timing as well as qualitative and quantitative requirements of silencing initiation remain uncharacterised. Suppressor of RNA silencing candidates therefore have to exhibit rather pronounced efficiencies in order to be recognised as such in *Agrobacterium* co-infiltration assays. These requirements are typically met by viral suppressors of silencing, since they were under selective pressures to develop potent RNA silencing suppression during host-virus co-evolution in order to facilitate successful infections. The roles of endogenous regulators of silencing in contrast may be envisaged as fine-tuning mechanisms to confine the controlled pathways to function according to specific sets of parameters, rather than to prevent them from fulfilling their purposes in antiviral defence or gene regulation. Consequently, *Agrobacterium* co-infiltration assays may not be sufficiently sensitive to detect the influences of such endogenous regulators of RNA silencing, especially one that is expressed as lowly as *ERL1*. Therefore an alternative strategy had to be employed to validate the results obtained from the *Agrobacterium* co-infiltration assays.

Even the most efficient hairpin constructs are unable to provide complete knockouts of targeted genes, and the respective target mRNAs are always detectable, albeit at significantly reduced levels, in hairpin-treated samples (Wesley et al., 2001). *Arabidopsis*

4. Discussion

ERL1 is transcribed at exceedingly low levels (Figure 3.2), which by itself suggests a comparatively minor regulatory impact. It could hence be expected that partial loss of ERL1, even upon constitutive RNAi-mediated suppression, would not cause discernable alterations in RNA silencing phenotypes. In contrast, severalfold overexpression could intensify ERL1 activity to a point where it may be detectable in a *GFP* silencing-related reporter system. Based on these suppositions transgenic *N. benthamiana* plants were generated that ectopically overexpress the full genomic version of *Arabidopsis ERL1*. Thus created *ERL1* overexpressor plants were crossed with the *GFP*-expressing *N. benthamiana* line *GFP* 6.4 (Kalantidis et al., 2006). Line *GFP* 6.4 exhibits distinct patterns of spontaneous *GFP* silencing initiation that manifest as local foci of *GFP* silencing approximately 30 cells in diameter along with subsequently occurring systemic vein-centric *GFP* silencing spread (Kalantidis et al., 2006). This phenomenon is frequently observed in transgenic plants (Vaucheret et al., 1998; Kalantidis et al., 2006) and may reflect a transgene product dose effect, since the frequency of its occurence appears to be positively correlated with transgene expression levels (Vaucheret et al., 1998; Schubert et al., 2004). Hypothetically, aberrant RNAs occur more frequently the higher a transgene is expressed, thus overcoming a threshold for the initiation of co-suppression-type RNA silencing. Abberancy in this respect may entail the actions of RDR6 producing dsRNA from problematic transgene-derived mRNAs that escape the XRN2-4-mediated cellular RNA quality control systems. Agro-infiltration-mediated silencing initiation saturates the involved RNA silencing pathways, thereby masking possible repressive effects that a weak suppressor of silencing may cause. In contrast, stochastic silencing initiation like in the case of line *GFP* 6.4 should provide a suitably sensitive reporter system for the detection of possible ERL1 involvements in silencing repression. Two independent crosses of *ERL1*-overexpressing *N. benthamiana* plants with line *GFP* 6.4 have been generated during this work (6.4x*ERL1*-A/B). Double homozygous individuals from each line were subsequently analysed for alterations in their *GFP* silencing patterns that could indicate repressive effects resulting from the ectopic *ERL1* overexpression. Lines 6.4x*ERL1*-A and 6.4x*ERL1*-B both showed no differences in comparison to the parent line *GFP* 6.4 in terms of frequency and intensity of spontaneous silencing initiation and its systemic spread (Figure 3.4 b). These results allow for several deductions. First, early steps in RNA silencing and silencing initiation

are not affected by ERL1. These include primary siRNA production from RDR6-dependent *GFP* dsRNA as well as AGO4-mediated target cleavage. Second, SLSS and ELSS are both unaffected in *ERL1* overexpression backgrounds, which includes passive cell-to-cell transport of 21 nt siRNAs through plasmodesmata in spots of SLSS initiation as well as RDR6-amplified silencing spread. Third, neither production nor transport or reception of the systemic mobile silencing signal are suppressed by ERL1. Overall, these aspects allow for no other conclusion than *Arabidopsis* ERL1 not being involved in the regulation of RNA silen-cing pathways. This appears to confirm the proposition of Tomoyasu et al. (2008) that ERI-1 homologues lacking a SAP domain fulfill functions distinct from RNA silencing regulation (Tomoyasu et al., 2008).

Nevertheless, three results obtained during this work appear to suggest a connection between *ERL1* misexpression and altered efficiencies of RNA silencing pathways: PSTVd-derived siRNA steady-state levels reduce upon agro-infiltration-mediated *ERL1* overexpression (Figure 3.5); *ERL1* overexpressor plants are hypersensitive towards viral infection (Figure 3.6); hairpin-induced systemic *ERL1* silencing is partially suppressed in transgenic *ERL1*-overexpressing plants (Figure 3.7). *Prima facie* these results stand in contradiction to the abovementioned conclusion that *Arabidopsis* ERL1 does not have RNA silencing suppression capabilities. A solution for this inconsistency arises from the observation that *DICER-LIKE* steady-state levels are significantly reduced in constitutively *ERL1*-overexpressing tissue (Figure 3.6 d). *DICER-LIKE* repression could account for the aggrevated symptoms and increased viral load in PPV-infected *ERL1* overexpressor plants, for reduced production of PSTVd siRNAs over time upon transient *ERL1* overexpression, and for disturbed systemic spread of *ERL1* silencing in *ERL1*-overexpressing plants after agro-infiltration of an *ERL1* hairpin construct. The exact nature of the cross-talk between *ERL1* and *DICER-LIKE* expression levels remains unresolved at this point. Considering the deleterious effects of *ERL1* overexpression on chloroplasts and the photosynthetic apparatus (discussed below), the dependence of *DCL* expression levels on light and photosynthesis (Kotakis et al., manuscript under revision) may be connected to these phenomena.

4. Discussion

4.2. An assortment of ribonucleases in chloroplast RNA stability and maturation

Bioinformatical analysis of the *Arabidopsis* ERL1 amino acid sequence revealed a predicted chloroplastic localisation (Table 3.1), and subcellular ERL1 localisation in chloroplasts was subsequently verified by carboxy-terminal GFP fusion and confocal microscopy (Figure 3.3). Even though it cannot be excluded that trace amounts of ERL1 remain in the cytoplasm or fulfill a transient cytosolic function (compare Figure 3.3 b), the vast majority of produced ERL1 protein is expected to localise in the chloroplasts under physiological conditions. Chloroplastic localisation is an important factor for the elucidation of ERL1's function *in vivo*, since chloroplasts are regarded an RNA silencing-free compartment (Hegeman et al., 2005), supporting the phylogenetic findings discussed above [(Tomoyasu et al., 2008) and Figure 4.1]. In addition, chloroplastic gene regulation and development are relatively well understood, including the roles of plastid-located ribonucleases, providing rich grounds for determining the biological role of ERL1.

Chloroplasts are of prokaryotic origin and result from the internalisation of a photosynthetically active cyanobacteria-like prokaryote by an archaic plant host approximately 1.5 billion years ago. Since then plastids underwent significant adaptions in order to meet the specific requirements of endosymbiosis in plant cells (Bollenbach et al., 2004). These changes include widespread shuffling of genes from the plastid to the nuclear genome as well as the incorporation of novel regulatory pathways based on host proteins that are imported to plastids posttranslationally. In fact, only a minority of the chloroplast proteome comprise proteins of cyanobacterial origin. The majority of proteins found in chloroplasts are eukaryotic and developed before the endosymbiotic incorporation of plastids (Martin et al., 2002), including ERL1. Nevertheless, plastids retained their own gene expression machinery, and the plastid genome encodes for several dozen mostly photosynthesis-, transcription-, and translation-related proteins and RNAs. Plastid gene regulation is primarily based on posttranscriptional control of mRNA stability in an RNAi-independent manner (Bollenbach et al., 2004). A variety of endo- and exonucleases is involved in mRNA turnover and posttranscriptional control of mRNA steady-state levels mediated by targeted mRNA destabilisation, resembling

the bacterial endonuclease-exonuclease RNA degradation system (Bollenbach et al., 2004). In addition, multiple endonucleolytic cleavages and exonucleolytic resections in the context of 3' end maturation occur for the majority of plastid mRNAs (Stern and Kindle, 1993; Hayes et al., 1996). Therefore, the 3'-5' exonuclease ERL1 can be expected to fill a functional niche in the broader context of plastid RNA 3' end maturation or stability.

In this perspective it is interesting to note the lack of identifyable chloroplast localisation signals in ERL1 homologues of several plant species (Figure 3.1 b). Poplar and *S. bicolor* ERL1 harbour amino-terminal deletions in comparison to ERL1 homologues in *Arabidopsis*, wine, rice, and tobacco. These deletions coincide precisely with the predicted chloroplast leader peptides in the latter species, and poplar and *S. bicolor* ERL1 are consequently predicted to exhibit cytosolic localisations. Due to the fact that only very few plant genomes have been sequenced so far, at present it cannot be determined, if one or the other scenario constitutes an exception or a general trend. The ERL1 chloroplast localisation signals in *Arabidopsis*, wine, rice, and tobacco do not share any degree of homology (Figure 3.1 b), indicating that they represent secondary additions, which the individual ERL1 homologues acquired independently during evolution in response to as yet undefined selective pressures. Based on the near-perfect divergency between the ERL1 chloroplast leader peptides in different plant species, the additions of these localisation signals may represent evolutionary recent events that only occurred once the respective plant species had already diversified from common ancestors. The selective pressures responsible for the transfer of ERL1 activities to chloroplasts can only be speculated about, but they appear to be independent of different ecologies connected with specific plant lineages. This is exemplified by the fact that ERL1 is predicted to be chloroplastically located in both monocotyledons (*i.e.* rice) and dicotyledons (*i.e. Arabidopsis*, wine, and tobacco). On the other hand different ERL1 homologues from both monocotyledons (*i.e. S. bicolor*) and dicotyledons (*i.e.* poplar) do not contain amino-terminal chloroplast leader sequences. Hypothetically, addition of amino-terminal chloroplast localisation signals to the respective ERL1 homologues may not have occurred yet in the evolution of these species. The lack of predictable chloroplast leader peptides, however, does not necessarily exclude the chloroplast import of respective proteins, since a number of alternative plastid

trafficking pathways operate in plants (Inaba and Schnell, 2008). Unfortunately, poplar and *S. bicolor* are not widely used as model organisms for studying gene regulation and chloroplast development, and hence all predictions about possible localisations or roles of ERL1 homologues in these organisms have to be regarded as speculations at this point.

4.3. *ERL1*-dependent variegation phenotypes in transgenic *N. benthamiana* plants suggest a role for ERL1 in early chloroplast development

The majority of all transgenic *ERL1* overexpressor plants generated for this work exhibit diverse morphological and developmental defects, most prominently variegated appearences caused by loss of chlorophyll in white sectors (Figure 3.7). Leaf variegation has long been known as a genetic trait in higher plants that can occur naturally, be the result of mutagenesis, or be caused by infections with specific pathogens (Sakamoto, 2003; Rodio et al., 2007). More specifically, leaf variegation in this context refers to non-lethal formation of neighbouring green and white sectors, where white sector formation is a result of unstable chloroplast development. Typically, white sectors contain undifferentiated proplastid-like plastids, whereas canonical chloroplasts can be observed in green sectors of the same leaves (Sakamoto, 2003). Mixed cells with both canonical as well as undeveloped chloroplasts have rarely been reported. Plastids propagate by division and are not exchanged between plant cells, and consequently the plastid complement of a given population of cells is dictated by the plastid content of the respective parent cells. *Arabidopsis* variegation mutants have been studied in detail, and in most cases mutations of proteins involved in photosynthesis or plastid genome maintenance have been found to be responsible for white sector formation [reviewed in (Sakamoto, 2003)]. It is still unknown, however, how the separation between green and white sectors is regulated, since all cells should be similarly affected by the respective genome mutations (Sakamoto, 2003). Striping mutants in monocotyledons show similar chloroplast defects as *Arabidopsis* variegation mutants (Jenkins, 1924; Newton and Coe, 1986; Han et al., 1992; Martínez-Zapater, 1993), but no evidence have been presented

that striping phenotypes are based on the same mechanisms as their *Arabidopsis* counterparts (Sakamoto, 2003).

Comparisons of the *ERL1*-dependent histological and ultrastructural alterations in white sectors with similar phenotypes in other variegation mutants may provide clues for identifying the pathway affected upon *ERL1* misexpression. Problematic chloroplast differentiation is a joint feature of all plant variegation phenotypes described in the literature and hence by itself is not a precise enough indicator to answer this question. Finding a plant mutant with a similar specific combination of macroscopic, microscopic, and molecular symptoms as observed in *ERL1* overexpressor plants (undeveloped plastids, lack of a *bona fide* palisade mesophyll, suppression of PEP-dependent transcripts, upregulation of NEP-dependent mRNAs; compare Figures 3.7, 3.9, and 3.10) was therefore the aim of this literature research. Several mutants have been described that exhibit undeveloped chloroplasts in white leaf sectors in combination with disturbed formation of the palisade mesophyll, leading to thinner leaves consisting mostly of spongy mesophyll (Reiter et al., 1994; Chatterjee et al., 1996; Babiychuk et al., 1997; Wang et al., 2000). These studies, however, did not contain detailed analyses of transcriptional patterns of chloroplast-related nucleus- and plastid-encoded genes to serve as comparisons with the *ERL1*-dependent alterations. Contrarily, a variety of studies on variegated mutants described transcriptional patterns strongly reminiscent of the results presented in Figure 3.10 (Hess et al., 1993; Allison et al., 1996; De Santis-MacIossek et al., 1999; Zubko and Day, 2002), but they did not present detailed microscopical data for comparison. The best match found in the literature is the albino-variegated phenotype peach calico; a combination of morphological and molecular symptoms induced by infection of peach with a specific variant of the chloroplastically locating viroid PLMVd (Rodio et al., 2007). Viroids are infectious small single-stranded circular RNA molecules 246-401 nt in length that do not contain genetic information but are able to exploit host factors for replication and movement based on their specific secondary and tertiary structures [reviewed in (Diener, 2003; Tabler and Tsagris, 2004; Flores et al., 2005; Ding and Itaya, 2007; Tsagris et al., 2008)]. Viroid infection interferes with host gene regulation and gene expression, which can result in diverse macro- and microscopic as well as molecular symptoms (Itaya et al., 2002). PLMVd variant PC-C40 is 348 nt long and employs a specific secondary structure that is

important for its pathogenicity (Rodio et al., 2007). More specifically, the PC-C40 strain contains a 3'-terminal 12-13 nt insertion that folds into a stable short stem-loop. PLMVd variants lacking this specific stem-loop are infectious but do not cause the peach calico symptoms associated with strain PC-C40. Therefore, the specific secondary structure of this PLMVd variant is able to interfere with chloroplast development, ultimately leading to severe bleaching, non-canonical formation of the palisade mesophyll, and transcriptional misregulation of genes important for chloroplast function (Rodio et al., 2007). On the molecular level, the primary cause for the development of peach calico in PLMVd PC-C40 infections has been appointed to a disturbance in the generation of chloroplastic ribosomal RNAs (Rodio et al., 2007). The mechanism by which PLMVd causes malfunctional rRNA maturation and ribosome function has not been elucidated so far, but the extensive similarities between peach calico and the *ERL1*-dependent variegation phenotypes from macroscopic to molecular levels allowed for a more focused analysis of the molecular defects caused by *ERL1* misexpression.

Functional plastid transcription is based on the actions of two evolutionary divergent RNA polymerases. The plastid-encoded RNA polymerase (PEP) is a multi-subunit bacteria-type RNA polymerase of cyanobacterial origin that is transcribed at relatively low levels (Liere and Börner, 2007). Promoter specificity of PEP is achieved through diverse nucleus-encoded sigma factors. Transcription of the genes for the different PEP subunits is accomplished by the second, nucleus-encoded, plastid RNA polymerase (NEP). The NEP is a single-subunit bacteriophage-type RNA polymerase that is also responsible for mitochondrial transcription (Liere and Börner, 2007). Both polymerases recognise distinct types of promoters and are responsible for the transcription of specific sets of genes (Hajdukiewicz et al., 1997). In brief, PEP transcribes the majority of genes involved in photosynthesis, translation, and general plastid metabolism, whereas NEP-dependent transcripts comprise mRNAs encoding PEP subunits and proteins involved in chlorophyll binding and lipid biosynthesis (Hajdukiewicz et al., 1997). There is, however, ample flexibility and redundancy, since many plastid genes contain dual promoters for both RNA polymerases (Liere and Börner, 2007). Spatiotemporally precise expression of plastid genes is essential for the differentiation of diverse kinds of

mature plastids (*i.e.* chloroplasts, chromoplasts, amyloplasts, etioplasts, or leucoplasts) from proplastids (Baumgartner et al., 1993).

Due to the independence of NEP production on the plastid translation machinery NEP-mediated transcription is not impaired in defective plastids in most of the afore-mentioned variegation phenotypes. This is exemplified by strong accumulation of *PEP* mRNA in white sectors of PLMVd-infected peach (Rodio et al., 2007) and *ERL1*-overexpressing *N. benthamiana* (Figure 3.10). The observed breakdown in PEP-dependent transcript levels can therefore be attributed to dysfunctional PEP protein or a shortage thereof. Productive translation of PEP mRNA evidently requires functional plastid ribosomes, and ribosome biogenesis on its part is dependent on precise maturation of ribosomal RNAs. Even though it is challenging to identify the primary malfunctional step in pathways constituting a cycle of dependence, impairment of plastid translation due to altered plastid rRNA biogenesis is considered to be the original cause for a variety of reported variegation phenotypes (Barkan, 1993; Bellaoui et al., 2003; Bisanz et al., 2003; Bellaoui and Gruissem, 2004; Bollenbach et al., 2005; Rodio et al., 2007). Plastids consequently lacking functional ribosomes cannot synthesise PEP (Hess et al., 1993; Zubko and Day, 2002), leading to a loss of PEP-dependent transcription and a subsequent general breakdown of plastid metabolism.

Taken together the extensive similarities between the *ERL1*-dependent variegation phenotypes and variegated mutants with altered chloroplast rRNA biogenesis along with reported roles of ERI-1 homologues in mouse, *S. pombe*, and *C. elegans* 5.8S rRNA 3' end maturation suggest a possible role for ERL1 in plastid rRNA 3' end processing.

4.4. ERL1 facilitates the final processing step in 5S rRNA 3' end maturation

Typically, once lost plastid ribosomes cannot be re-synthesised in PEP-deficient mutants exhibiting variegation phenotypes due to arrested plastid development (Zubko and Day, 2002). PEP-dependent transcription in *ERL1*-overexpressing tissue is severely impaired, albeit not completely abolished (Figure 3.10). Therefore, *ERL1* overexpression-dependent defective plastids may recover and become photosynthetically active

again once the deleterious factor of *ERL1* overexpression ceases as a result of RNAi-mediated *ERL1* silencing (Figure 3.7 and section 3.4.2.). Identifying the exact biochemical alterations caused by *ERL1* misexpression is an important prerequisite for understanding the dynamics of these processes.

Apart from their involvements in RNA silencing regulation ERI-1 homologues in mouse, *S. pombe*, and *C. elegans* have recently been shown to catalyse the final processing step in 5.8S rRNA maturation (Ansel et al., 2008; Gabel and Ruvkun, 2008). Mouse Eri1 has been shown to interact with ribosomal proteins and specifically 5.8S rRNA in immunoprecipitation experiments (Ansel et al., 2008). This interaction is facilitated by the amino-terminal SAP domain, but the SAP domain is dispensable under conditions of *Eri1* overexpression (Ansel et al., 2008). *eri1*-deficient mice accumulate 3'-elongated 5.8S rRNA molecules, and detailed analyses revealed that these extensions are 2 nt long (Ansel et al., 2008). Recombinant and ectopically produced Eri1 were able to process elongated 5.8S rRNA intermediates to the mature forms *in vitro* and in cultured cells, respectively (Ansel et al., 2008). Analogous reactions are catalysed by the *S. pombe* and *C. elegans* ERI-1 homologues, showing that 5.8S rRNA processing constitutes a conserved activity (Gabel and Ruvkun, 2008). Therefore, plant ERL1 could conceivably be involved in analogous functions in plastid rRNA processing.

The observed dual functions of specific ERI-1 homologues in siRNA degradation and 5.8S rRNA 3' end processing represent a challenging combination in terms of defining ERI-1 substrates. siRNAs are not only significantly shorter than 5.8S rRNA, they are also younger in evolutionary terms, raising questions whether ERI-1 homologues acquired binding specifities towards these divergent substrates at different times during evolution. In addition, the specificity of human Thex1/3'hExo for binding and *in vitro*-processing of the histone mRNA 3' end ought to be remembered in this context, despite lack of data on its function *in vivo* (Dominski et al., 2003; Dominski et al., 2005; Yang et al., 2006b). Leads to basic requirements for ERI-1 substrates may be inferred from secondary structure predictions of as yet identified *bona fide* ERI-1 substrates (Figure 4.2). Precise analyses of the binding affinities of Thex1/3'hExo revealed its specificity for the short 3'-terminal stem-loop of histone mRNA (Dominski et al., 2003; Dominski et al., 2005). Coincidentally, the 3' terminus of *C. elegans* 5.8S rRNA is predicted to fold into a similar, albeit slightly longer, stable stem-loop structure with a

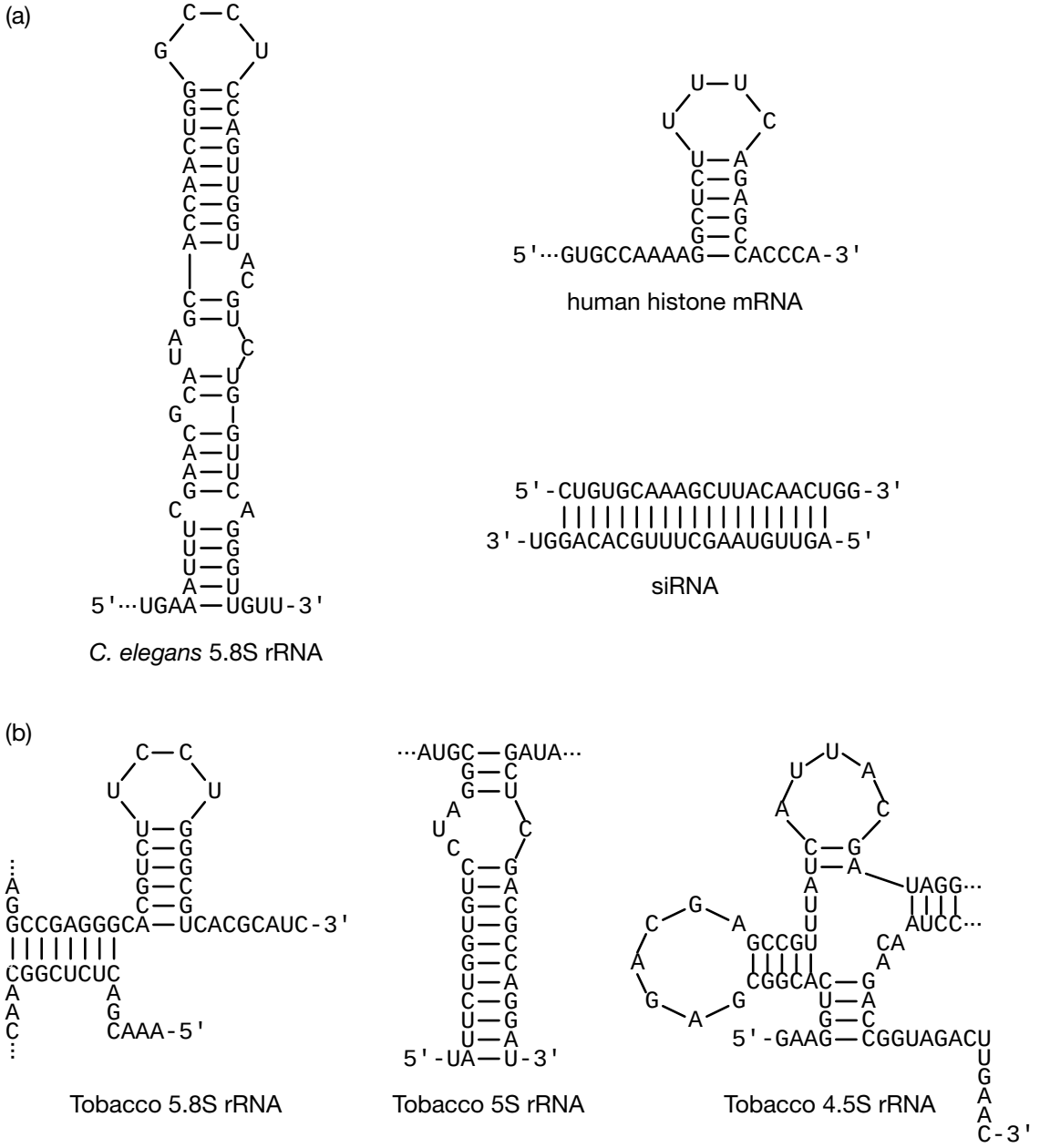

Figure 4.2 Secondary structure predictions of known ERI-1 substrates and small tobacco ribosomal RNAs. **(a)** 5.8S rRNA, human histone mRNA, and canonical siRNAs share structural similarities, *i.e.* short stem(-loop)s with 3' overhangs. **(b)** Tobacco small ribosomal RNAs exhibit complex secondary structures. Tobacco 5S rRNA is structurally most similar to known substrates of animal and fungal ERI-1 homologues.

3'-protruded end (Figure 4.2 a). From a structural point of view, siRNAs may indeed also be interpreted as RNA stems with 3' overhangs, lacking the connecting loop structures (Figure 4.2 a). It can therefore be posited that ERI-1 homologues share a general affinity for relatively short RNA stem(-loop)s with 3' overhangs (Figure 4.2). Secondary structure predictions of tobacco 5.8S, 5S, and 4.5S rRNAs inclose germane aspects in this context (Figure 4.2 b). 4.5S rRNA adopts a highly structured fold and

ends in a 4 nt terminal stem with a short 5' and a long 3' overhang (Figure 4.2 b). In comparison to *C. elegans* 5.8S rRNA and the human histone mRNA 3' terminus the secondary structure of tobacco 4.5S appears too divergent to constitute a substrate for ERL1. Tobacco 5.8S rRNA is naturally very similar to its *C. elegans* homologue in terms of sequence, but it exhibits a long 3' overhang as well as a second complex stem-loop structure directly upstream of the 3'-terminal stem-loop (Figure 4.2 b). This, in addition to its cytosolic localisation, argues against a binding specificity of ERL1 to tobacco 5.8S rRNA. The structure of mature tobacco 5S rRNA, however, exhibits a stable ~16 nt 3'-terminal stem-loop without 3' overhang (Figure 4.2 b) that appears to meet the criteria for ERL1 substrates postulated above.

In order to determine its physiological target, agro-infiltration assays were performed suppressing and overexpressing *ERL1* and analysing the respective effects on the steady-state levels of tobacco 5.8S, 5S, and 4.5S rRNAs (Figure 3.11). As predicted from the secondary structure analyses 5.8S and 4.5S rRNAs do not show altered expression levels upon *ERL1* suppression and overexpression (Figure 3.11 a). 5S rRNA steady-state levels, however, are notably reduced as a result of *ERL1* suppression, which strongly indicates an influence of ERL1 on 5S rRNA biogenesis and confirms the prediction of 5S rRNA as constituting an ERL1 substrate.

Based on the observed repressive effects on 5S rRNA steady-state levels in combination with its identity as a 3'-5' exonuclease ERL1 should be expected to play a role in 5S rRNA 3' end maturation. Therefore, the precise 3' ends of 5.8S, 5S, and 4.5S rRNAs were mapped in wildtype and *ERL1*-misexpressing tissues. Indeed 2 nt 3' extensions were found to accumulate in transiently as well as constitutively *ERL1*-overexpressing and -suppressing samples in the case of 5S rRNA (Figure 3.11 b-c). The fact that similar extensions were found in both *ERL1*-overexpressing and -suppressing samples indicates that the same pathway is being affected in both cases. Surprisingly, however, only 29 % of all cloned extensions correspond to the canonical 5S precursor derived from the plastid genome sequence (+GA extensions). 71 % of the cloned extensions constitute non-templated nucleotides (+AC extensions). At this point it cannot be specified, whether the identified +AC extensions are results of secondary nucleotide additions to formerly mature 5S rRNA, or if they are caused by RNA editing mechanisms acting out of their canonical contexts upon disturbance of the 5S maturation pathway. Non-

templated additions of nucleotides to the 3' ends of tobacco chloroplast transcripts have been reported earlier (Zandueta-Criado and Bock, 2004), and resembling activities were also observed in maize (*Zea mays*) mitochondria (Williams et al., 2000). In both cases, the specific enzymes catalysing the untemplated additions have not been identified so far, but are expected to be functionally related to terminal transferase or tRNA nucleotidyl transferase activities. It can therefore be posited that 5S rRNA may enter an atypical posttranscriptional modification pathway once *ERL1* misexpression intereferes with 5S rRNA maturation.

Mature 5S rRNA undergoes a multistep processing pathway and ends in a stable stem-loop without 3' overhang (Figure 4.2 b). The finding of 5S rRNA with 2 nt 3' extensions in *ERL1* misexpression backgrounds allows for the interpretation that in a wildtype situation ERL1 catalyses the removal of those nucleotides as the final processing step during 5S rRNA biogenesis. At the same time, this activity resembles characteristics of metazoan and *S. pombe* ERI-1 homologues, which have been proposed to cleave the 2 nt 3' overhangs of siRNAs (Kennedy et al., 2004; Iida et al., 2006; Kupsco et al., 2006; Yang et al., 2006b). Yet, a majority of 5S rRNA sequences in *ERL1* misexpression backgrounds correspond to correctly processed 5S rRNA, indicating that ERL1 function might be redundant and could be compensated for by other proteins. This conception is supported by results from *Arabidopsis rnr1* loss-of-function mutants (Bollenbach et al., 2005). *Arabidopsis rnr1* mutants exhibit similar morphological defects as *ERL1*-overexpressing *N. benthamiana* plants and accumulate 3'-elongated 5S and 4.5S rRNA transcripts along with *bona fide* 5S and 4.5S rRNAs (Bollenbach et al., 2005). Bollenbach et al. (2005) proposed that a yet unknown 3'-5' exonuclease activity may act redundantly to RNR1 in 4.5S and 5S rRNA 3'-end maturation (Bollenbach et al., 2005).

Based on the results presented in this work, the versatile 3'-5' exonuclease ERL1 may constitute this activity in the case of 5S rRNA.

5

References

Adenot, X., Elmayan, T., Lauressergues, D., Boutet, S., Bouché, N., Gasciolli, V., and Vaucheret, H. (2006). DRB4-dependent TAS3 trans-acting siRNAs control leaf morphology through AGO7. Curr Biol **16,** 927-932.

Agorio, A., and Vera, P. (2007). ARGONAUTE4 is required for resistance to *Pseudomonas syringae* in *Arabidopsis*. Plant Cell **19,** 3778-3790.

Allen, E., Xie, Z., Gustafson, A., and Carrington, J. (2005). microRNA-directed phasing during trans-acting siRNA biogenesis in plants. Cell **121,** 207-221.

Allison, L., Simon, L., and Maliga, P. (1996). Deletion of rpoB reveals a second distinct transcription system in plastids of higher plants. EMBO J **15,** 2802-2809.

Ambros, V. (2001). microRNAs: tiny regulators with great potential. Cell **107,** 823-826.

Ambros, V., Lee, R., Lavanway, A., Williams, P., and Jewell, D. (2003). MicroRNAs and other tiny endogenous RNAs in *C. elegans*. Curr Biol **13,** 807-818.

Anandalakshmi, R., Marathe, R., Ge, X., Herr, J.J., Mau, C., Mallory, A., Pruss, G., Bowman, L., and Vance, V. (2000). A calmodulin-related protein that suppresses posttranscriptional gene silencing in plants. Science **290,** 142-144.

Ansel, K., Pastor, W., Rath, N., Lapan, A., Glasmacher, E., Wolf, C., Smith, L., Papadopoulou, N., Lamperti, E., Tahiliani, M., Ellwart, J., Shi, Y., Kremmer, E., Rao, A., and Heissmeyer, V. (2008). Mouse Eri1 interacts with the ribosome and catalyzes 5.8S rRNA processing. Nat Struct Mol Biol **15,** 523-530.

Aravind, L., and Koonin, E. (2000). SAP - a putative DNA-binding motif involved in chromosomal organization. Trends Biochem Sci **25,** 112-114.

Axtell, M., and Bowman, J. (2008). Evolution of plant microRNAs and their targets. Trends Plant Sci **13,** 343-349.

5. References

Babiychuk, E., Fuangthong, M., Van Montagu, M., Inzé, D., and Kushnir, S. (1997). Efficient gene tagging in *Arabidopsis thaliana* using a gene trap approach. Proc Natl Acad Sci U S A **94,** 12722-12727.

Bagasra, O., and Prilliman, K. (2004). RNA interference: the molecular immune system. J Mol Histol **35,** 545-553.

Ban, N., Nissen, P., Hansen, J., Moore, P., and Steitz, T. (2000). The complete atomic structure of the large ribosomal subunit at 2.4 A resolution. Science **289,** 905-920.

Barkan, A. (1993). Nuclear mutants of maize with defects in chloroplast polysome assembly have altered chloroplast RNA metabolism. Plant Cell **5,** 389-402.

Bartel, D. (2004). MicroRNAs: genomics, biogenesis, mechanism, and function. Cell **116,** 281-297.

Bartel, D. (2009). MicroRNAs: target recognition and regulatory functions. Cell **136,** 215-233.

Batista, P., Ruby, J., Claycomb, J., Chiang, R., Fahlgren, N., Kasschau, K., Chaves, D., Gu, W., Vasale, J., Duan, S., Conte, D.J., Luo, S., Schroth, G., Carrington, J., Bartel, D., and Mello, C. (2008). PRG-1 and 21U-RNAs interact to form the piRNA complex required for fertility in *C. elegans*. Mol Cell **31,** 67-78.

Baumberger, N., Tsai, C., Lie, M., Havecker, E., and Baulcombe, D. (2007). The Polerovirus silencing suppressor P0 targets ARGONAUTE proteins for degradation. Curr Biol **17,** 1609-1614.

Baumgartner, B., Rapp, J., and Mullet, J. (1993). Plastid genes encoding the transcription/translation apparatus are differentially transcribed early in barley (*Hordeum vulgare*) chloroplast development (evidence for selective stabilization of *psbA* mRNA). Plant Physiol **101,** 781-791.

Bayne, E., Rakitina, D., Morozov, S., and Baulcombe, D. (2005). Cell-to-cell movement of *Potato potexvirus X* is dependent on suppression of RNA silencing. Plant J **44,** 471-482.

Bellaoui, M., and Gruissem, W. (2004). Altered expression of the *Arabidopsis* ortholog of *DCL* affects normal plant development. Planta **219,** 819-826.

Bellaoui, M., Keddie, J., and Gruissem, W. (2003). DCL is a plant-specific protein required for plastid ribosomal RNA processing and embryo development. Plant Mol Biol **53,** 531-543.

Benner, S.A., Carrigan, M.A., Ricardo, A., and Frye, F. (2006). Setting the stage: the history, chemistry, and geobiology behind RNA. In The RNA World, R.F. Gesteland, T.R. Cech, and J.F. Atkins, eds (New York: Cold Spring Harbor Laboratory Press), pp. 1-22.

Bernstein, E., Caudy, A., Hammond, S., and Hannon, G. (2001). Role for a bidentate ribonuclease in the initiation step of RNA interference. Nature **409,** 363-366.

Birney, E., Stamatoyannopoulos, J., Dutta, A., Guigó, R., Gingeras, T., Margulies, E., Weng, Z., Snyder, M., Dermitzakis, E., Thurman, R., Kuehn, M., Taylor, C.,

5. References

Neph, S., Koch, C., Asthana, S., Malhotra, A., Adzhubei, I., Greenbaum, J., Andrews, R., Flicek, P., Boyle, P., Cao, H., Carter, N., Clelland, G., Davis, S., Day, N., Dhami, P., Dillon, S., Dorschner, M., Fiegler, H., Giresi, P., Goldy, J., Hawrylycz, M., Haydock, A., Humbert, R., James, K., Johnson, B., Johnson, E., Frum, T., Rosenzweig, E., Karnani, N., Lee, K., Lefebvre, G., Navas, P., Neri, F., Parker, S., Sabo, P., Sandstrom, R., Shafer, A., Vetrie, D., Weaver, M., Wilcox, S., Yu, M., Collins, F., Dekker, J., Lieb, J., Tullius, T., Crawford, G., Sunyaev, S., Noble, W., Dunham, I., Denoeud, F., Reymond, A., Kapranov, P., Rozowsky, J., Zheng, D., Castelo, R., Frankish, A., Harrow, J., Ghosh, S., Sandelin, A., Hofacker, I., Baertsch, R., Keefe, D., Dike, S., Cheng, J., Hirsch, H., Sekinger, E., Lagarde, J., Abril, J., Shahab, A., Flamm, C., Fried, C., Hackermüller, J., Hertel, J., Lindemeyer, M., Missal, K., Tanzer, A., Washietl, S., Korbel, J., Emanuelsson, O., Pedersen, J., Holroyd, N., Taylor, R., Swarbreck, D., Matthews, N., Dickson, M., Thomas, D., Weirauch, M., Gilbert, J., Drenkow, J., Bell, I., Zhao, X., Srinivasan, K., Sung, W., Ooi, H., Chiu, K., Foissac, S., Alioto, T., Brent, M., Pachter, L., Tress, M., Valencia, A., Choo, S., Choo, C., Ucla, C., Manzano, C., Wyss, C., Cheung, E., Clark, T., Brown, J., Ganesh, M., Patel, S., Tammana, H., Chrast, J., Henrichsen, C., Kai, C., Kawai, J., Nagalakshmi, U., Wu, J., Lian, Z., Lian, J., Newburger, P., Zhang, X., Bickel, P., Mattick, J., Carninci, P., Hayashizaki, Y., Weissman, S., Hubbard, T., Myers, R., Rogers, J., Stadler, P., Lowe, T., Wei, C., Ruan, Y., Struhl, K., Gerstein, M., Antonarakis, S., Fu, Y., Green, E., Karaöz, U., Siepel, A., Taylor, J., Liefer, L., Wetterstrand, K., Good, P., Feingold, E., Guyer, M., Cooper, G., Asimenos, G., Dewey, C., Hou, M., Nikolaev, S., Montoya-Burgos, J., Löytynoja, A., Whelan, S., Pardi, F., Massingham, T., Huang, H., Zhang, N., Holmes, I., Mullikin, J., Ureta-Vidal, A., Paten, B., Seringhaus, M., Church, D., Rosenbloom, K., Kent, W., Stone, E., Batzoglou, S., Goldman, N., Hardison, R., Haussler, D., Miller, W., Sidow, A., Trinklein, N., Zhang, Z., Barrera, L., Stuart, R., King, D., Ameur, A., Enroth, S., Bieda, M., Kim, J., Bhinge, A., Jiang, N., Liu, J., Yao, F., Vega, V., Lee, C., Ng, P., Yang, A., Moqtaderi, Z., Zhu, Z., Xu, X., Squazzo, S., Oberley, M., Inman, D., Singer, M., Richmond, T., Munn, K., Rada-Iglesias, A., Wallerman, O., Komorowski, J., Fowler, J., Couttet, P., Bruce, A., Dovey, O., Ellis, P., Langford, C., Nix, D., Euskirchen, G., Hartman, S., Urban, A., Kraus, P., Van Calcar, S., Heintzman, N., Kim, T., Wang, K., Qu, C., Hon, G., Luna, R., Glass, C., Rosenfeld, M., Aldred, S., Cooper, S., Halees, A., Lin, J., Shulha, H., Xu, M., Haidar, J., Yu, Y., Iyer, V., Green, R., Wadelius, C., Farnham, P., Ren, B., Harte, R., Hinrichs, A., Trumbower, H., Clawson, H., Hillman-Jackson, J., Zweig, A., Smith, K., Thakkapallayil, A., Barber, G., Kuhn, R., Karolchik, D., Armengol, L., Bird, C., de Bakker, P., Kern, A., Lopez-Bigas, N., Martin, J., Stranger, B., Woodroffe, A., Davydov, E., Dimas, A., Eyras, E.,

5. References

Hallgrímsdóttir, I., Huppert, J., Zody, M., Abecasis, G., Estivill, X., Bouffard, G., Guan, X., Hansen, N., Idol, J., Maduro, V., Maskeri, B., McDowell, J., Park, M., Thomas, P., Young, A., Blakesley, R., Muzny, D., Sodergren, E., Wheeler, D., Worley, K., Jiang, H., Weinstock, G., Gibbs, R., Graves, T., Fulton, R., Mardis, E., Wilson, R., Clamp, M., Cuff, J., Gnerre, S., Jaffe, D., Chang, J., Lindblad-Toh, K., Lander, E., Koriabine, M., Nefedov, M., Osoegawa, K., Yoshinaga, Y., Zhu, B., and de Jong, P. (2007). Identification and analysis of functional elements in 1% of the human genome by the ENCODE pilot project. Nature **447,** 799-816.

Bisanz, C., Bégot, L., Carol, P., Perez, P., Bligny, M., Pesey, H., Gallois, J., Lerbs-Mache, S., and Mache, R. (2003). The *Arabidopsis* nuclear *DAL* gene encodes a chloroplast protein which is required for the maturation of the plastid ribosomal RNAs and is essential for chloroplast differentiation. Plant Mol Biol **51,** 651-663.

Blevins, T., Rajeswaran, R., Shivaprasad, P., Beknazariants, D., Si-Ammour, A., Park, H., Vazquez, F., Robertson, D., Meins, F.J., Hohn, T., and Pooggin, M. (2006). Four plant Dicers mediate viral small RNA biogenesis and DNA virus induced silencing. Nucleic Acids Res **34,** 6233-6246.

Bohmert, K., Camus, I., Bellini, C., Bouchez, D., Caboche, M., and Benning, C. (1998). AGO1 defines a novel locus of *Arabidopsis* controlling leaf development. EMBO J **17,** 170-180.

Bollenbach, T., Schuster, G., and Stern, D. (2004). Cooperation of endo- and exoribonucleases in chloroplast mRNA turnover. Prog Nucleic Acid Res Mol Biol **78,** 305-337.

Bollenbach, T., Lange, H., Gutierrez, R., Erhardt, M., Stern, D., and Gagliardi, D. (2005). RNR1, a 3'-5' exoribonuclease belonging to the RNR superfamily, catalyzes 3' maturation of chloroplast ribosomal RNAs in *Arabidopsis thaliana*. Nucleic Acids Res **33,** 2751-2763.

Bortolamiol, D., Pazhouhandeh, M., Marrocco, K., Genschik, P., and Ziegler-Graff, V. (2007). The Polerovirus F box protein P0 targets ARGONAUTE1 to suppress RNA silencing. Curr Biol **17,** 1615-1621.

Braz, A., Finnegan, J., Waterhouse, P., and Margis, R. (2004). A plant orthologue of RNase L inhibitor (RLI) is induced in plants showing RNA interference. J Mol Evol **59,** 20-30.

Brennecke, J., Aravin, A., Stark, A., Dus, M., Kellis, M., Sachidanandam, R., and Hannon, G. (2007). Discrete small RNA-generating loci as master regulators of transposon activity in *Drosophila*. Cell **128,** 1089-1103.

Brigneti, G., Voinnet, O., Li, W., Ji, L., Ding, S., and Baulcombe, D. (1998). Viral pathogenicity determinants are suppressors of transgene silencing in *Nicotiana benthamiana*. EMBO J **17,** 6739-6746.

5. References

Brodersen, P., Sakvarelidze-Achard, L., Bruun-Rasmussen, M., Dunoyer, P., Yamamoto, Y., Sieburth, L., and Voinnet, O. (2008). Widespread translational inhibition by plant miRNAs and siRNAs. Science **320,** 1185-1190.

Bucher, E., Hemmes, H., de Haan, P., Goldbach, R., and Prins, M. (2004). The influenza A virus NS1 protein binds small interfering RNAs and suppresses RNA silencing in plants. J Gen Virol **85,** 983-991.

Bühler, M., Verdel, A., and Moazed, D. (2006). Tethering RITS to a nascent transcript initiates RNAi- and heterochromatin-dependent gene silencing. Cell **125,** 873-886.

Bühler, M., Mohn, F., Stalder, L., and Mühlemann, O. (2005). Transcriptional silencing of nonsense codon-containing immunoglobulin minigenes. Mol Cell **18,** 307-317.

Bussotti, F., Strasser, R., and Schaub, M. (2007). Photosynthetic behavior of woody species under high ozone exposure probed with the JIP-test: a review. Environ Pollut **147,** 430-437.

Carthew, R., and Sontheimer, E. (2009). Origins and mechanisms of miRNAs and siRNAs. Cell **136,** 642-655.

Casas-Mollano, J., Rohr, J., Kim, E., Balassa, E., van Dijk, K., and Cerutti, H. (2008). Diversification of the core RNA interference machinery in *Chlamydomonas reinhardtii* and the role of DCL1 in transposon silencing. Genetics **179,** 69-81.

Chalfie, M., Horvitz, H., and Sulston, J. (1981). Mutations that lead to reiterations in the cell lineages of *C. elegans*. Cell **24,** 59-69.

Chan, S. (2008). Inputs and outputs for chromatin-targeted RNAi. Trends Plant Sci **13,** 383-389.

Chatterjee, M., Sparvoli, S., Edmunds, C., Garosi, P., Findlay, K., and Martin, C. (1996). DAG, a gene required for chloroplast differentiation and palisade development in *Antirrhinum majus*. EMBO J **15,** 4194-4207.

Chaudhuri, K., and Chatterjee, R. (2007). MicroRNA detection and target prediction: integration of computational and experimental approaches. DNA Cell Biol **26,** 321-337.

Chellappan, P., and Jin, H. (2009). Discovery of plant microRNAs and short interfering RNAs by deep parallel sequencing. In Plant Hormones - Methods and Protocols, S. Cutler and D. Bonetta, eds (Berlin/Heidelberg: Humana Press.

Chen, I.A., Hanczyk, M.M., Sazani, P.L., and Szostak, J.W. (2006). Protocells: Genetic Polymers Inside Membrane Vesicles. In The RNA World, R.F. Gesteland, T.R. Cech, and J.F. Atkins, eds (New York: Cold Spring Harbor Laboratory Press), pp. 57-88.

Chen, W., Zhang, Z., Chen, J., Zhang, J., Wu, Y., Huang, Y., Cai, X., and Huang, A. (2008). HCV core protein interacts with Dicer to antagonize RNA silencing. Virus Res **133,** 250-258.

5. References

Chen, X., Li, N., and Ellington, A. (2007). Ribozyme catalysis of metabolism in the RNA world. Chem Biodivers **4,** 633-655.

Cheng, Y., and Patel, D. (2004). Crystallographic structure of the nuclease domain of 3'hExo, a DEDDh family member, bound to rAMP. J Mol Biol **343,** 305-312.

Cheng, Y., Sequeira, S., Malinina, L., Tereshko, V., Söllner, T., and Patel, D. (2004). Crystallographic identification of Ca2+ and Sr2+ coordination sites in synaptotagmin I C2B domain. Protein Sci **13,** 2665-2672.

Covey, S.N., Al-Kaff, N.S., Lángara, A., and Turner, D.S. (1997). Plants combat infection by gene silencing. Nature **385**.

Crick, F. (1968). The origin of the genetic code. J Mol Biol **38,** 367-379.

Csorba, T., Bovi, A., Dalmay, T., and Burgyán, J. (2007). The p122 subunit of *Tobacco mosaic virus* replicase is a potent silencing suppressor and compromises both small interfering RNA- and microRNA-mediated pathways. J Virol **81,** 11768-11780.

Curtin, S., Watson, J., Smith, N., Eamens, A., Blanchard, C., and Waterhouse, P. (2008). The roles of plant dsRNA-binding proteins in RNAi-like pathways. FEBS Lett **582,** 2753-2760.

Das, P., Bagijn, M., Goldstein, L., Woolford, J., Lehrbach, N., Sapetschnig, A., Buhecha, H., Gilchrist, M., Howe, K., Stark, R., Matthews, N., Berezikov, E., Ketting, R., Tavaré, S., and Miska, E. (2008). Piwi and piRNAs act upstream of an endogenous siRNA pathway to suppress Tc3 transposon mobility in the *Caenorhabditis elegans* germline. Mol Cell **31,** 79-90.

de Jong, D., Eitel, M., Jakob, W., Osigus, H., Hadrys, H., Desalle, R., and Schierwater, B. (2009). Multiple Dicer genes in the early diverging metazoa. Mol Biol Evol.

De Santis-MacIossek, G., Kofer, W., Bock, A., Schoch, S., Maier, R., Wanner, G., Rüdiger, W., Koop, H., and Herrmann, R. (1999). Targeted disruption of the plastid RNA polymerase genes rpoA, B and C1: molecular biology, biochemistry and ultrastructure. Plant J **18,** 477-489.

Delgadillo, M., Sáenz, P., Salvador, B., García, J., and Simón-Mateo, C. (2004). Human influenza virus NS1 protein enhances viral pathogenicity and acts as an RNA silencing suppressor in plants. J Gen Virol **85,** 993-999.

Diaz-Pendon, J., Li, F., Li, W., and Ding, S. (2007). Suppression of antiviral silencing by *Cucumber mosaic virus* 2b protein in *Arabidopsis* is associated with drastically reduced accumulation of three classes of viral small interfering RNAs. Plant Cell **19,** 2053-2063.

Díaz-Pendón, J., and Ding, S. (2008). Direct and indirect roles of viral suppressors of RNA silencing in pathogenesis. Annu Rev Phytopathol **46,** 303-326.

Diener, T. (2003). Discovering viroids - a personal perspective. Nat Rev Microbiol **1,** 75-80.

5. References

Ding, B., and Itaya, A. (2007). Viroid: a useful model for studying the basic principles of infection and RNA biology. Mol Plant Microbe Interact **20,** 7-20.

Djikeng, A., Shi, H., Tschudi, C., and Ullu, E. (2001). RNA interference in *Trypanosoma brucei*: cloning of small interfering RNAs provides evidence for retroposon-derived 24-26-nucleotide RNAs. RNA **7,** 1522-1530.

Doench, J., Petersen, C., and Sharp, P. (2003). siRNAs can function as miRNAs. Genes Dev **17,** 438-442.

Dominski, Z., Yang, X., Purdy, M., and Marzluff, W. (2005). Differences and similarities between *Drosophila* and mammalian 3' end processing of histone pre-mRNAs. RNA **11,** 1835-1847.

Dominski, Z., Yang, X., Kaygun, H., Dadlez, M., and Marzluff, W. (2003). A 3' exonuclease that specifically interacts with the 3' end of histone mRNA. Mol Cell **12,** 295-305.

Dong, Z., Han, M., and Fedoroff, N. (2008). The RNA-binding proteins HYL1 and SE promote accurate in vitro processing of pri-miRNA by DCL1. Proc Natl Acad Sci U S A **105,** 9970-9975.

Duchaine, T., Wohlschlegel, J., Kennedy, S., Bei, Y., Conte, D.J., Pang, K., Brownell, D., Harding, S., Mitani, S., Ruvkun, G., Yates, J.r., and Mello, C. (2006). Functional proteomics reveals the biochemical niche of *C. elegans* DCR-1 in multiple small-RNA-mediated pathways. Cell **124,** 343-354.

Dunoyer, P., Himber, C., and Voinnet, O. (2005). DICER-LIKE 4 is required for RNA interference and produces the 21-nucleotide small interfering RNA component of the plant cell-to-cell silencing signal. Nat Genet **37,** 1356-1360.

Dunoyer, P., Himber, C., and Voinnet, O. (2006). Induction, suppression and requirement of RNA silencing pathways in virulent *Agrobacterium tumefaciens* infections. Nat Genet **38,** 138-139.

Dunoyer, P., Himber, C., Ruiz-Ferrer, V., Alioua, A., and Voinnet, O. (2007). Intra- and intercellular RNA interference in *Arabidopsis thaliana* requires components of the microRNA and heterochromatic silencing pathways. Nat Genet **39,** 848-856.

Dykxhoorn, D., and Lieberman, J. (2005). The silent revolution: RNA interference as basic biology, research tool, and therapeutic. Annu Rev Med **56,** 401-423.

Ebhardt, H., Thi, E., Wang, M., and Unrau, P. (2005). Extensive 3' modification of plant small RNAs is modulated by helper component-proteinase expression. Proc Natl Acad Sci U S A **102,** 13398-13403.

Ebisuya, M., Yamamoto, T., Nakajima, M., and Nishida, E. (2008). Ripples from neighbouring transcription. Nat Cell Biol **10,** 1106-1113.

Faehnle, C., and Joshua-Tor, L. (2007). Argonautes confront new small RNAs. Curr Opin Chem Biol **11,** 569-577.

Fagard, M., and Vaucheret, H. (2000). Systemic silencing signal(s). Plant Mol Biol **43,** 285-293.

5. References

Fang, Y., and Spector, D. (2007). Identification of nuclear dicing bodies containing proteins for microRNA biogenesis in living *Arabidopsis* plants. Curr Biol **17,** 818-823.

Farazi, T., Juranek, S., and Tuschl, T. (2008). The growing catalog of small RNAs and their association with distinct Argonaute/Piwi family members. Development **135,** 1201-1214.

Felippes, F., and Weigel, D. (2009). Triggering the formation of tasiRNAs in *Arabidopsis thaliana*: the role of microRNA miR173. EMBO Rep **10,** 264-270.

Fire, A., Xu, S., Montgomery, M., Kostas, S., Driver, S., and Mello, C. (1998). Potent and specific genetic interference by double-stranded RNA in *Caenorhabditis elegans*. Nature **391,** 806-811.

Flores, R., Hernández, C., Martínez de Alba, A., Daròs, J., and Di Serio, F. (2005). Viroids and viroid-host interactions. Annu Rev Phytopathol **43,** 117-139.

Friedman, R., Farh, K., Burge, C., and Bartel, D. (2009). Most mammalian mRNAs are conserved targets of microRNAs. Genome Res **19,** 92-105.

Gabel, H., and Ruvkun, G. (2008). The exonuclease ERI-1 has a conserved dual role in 5.8S rRNA processing and RNAi. Nat Struct Mol Biol **15,** 531-533.

Gazzani, S., Lawrenson, T., Woodward, C., Headon, D., and Sablowski, R. (2004). A link between mRNA turnover and RNA interference in *Arabidopsis*. Science **306,** 1046-1048.

Gilbert, W. (1986). The RNA World. Nature **319,** 618.

Gleave, A. (1992). A versatile binary vector system with a T-DNA organisational structure conducive to efficient integration of cloned DNA into the plant genome. Plant Mol Biol **20,** 1203-1207.

Gobeil, L., Plante, P., Rohani, M., Ouellette, M., and Provost, P. (2008). Involvement of Dcr1 in post-transcriptional regulation of gene expression in *Schizosaccharomyces pombe*. Front Biosci **13,** 2203-2215.

Grimson, A., Srivastava, M., Fahey, B., Woodcroft, B., Chiang, H., King, N., Degnan, B., Rokhsar, D., and Bartel, D. (2008). Early origins and evolution of microRNAs and Piwi-interacting RNAs in animals. Nature **455,** 1193-1197.

Guerrier-Takada, C., Gardiner, K., Marsh, T., Pace, N., and Altman, S. (1983). The RNA moiety of ribonuclease P is the catalytic subunit of the enzyme. Cell **35,** 849-857.

Guo, H., and Ding, S. (2002). A viral protein inhibits the long range signaling activity of the gene silencing signal. EMBO J **21,** 398-407.

Gy, I., Gasciolli, V., Lauressergues, D., Morel, J., Gombert, J., Proux, F., Proux, C., Vaucheret, H., and Mallory, A. (2007). *Arabidopsis* FIERY1, XRN2, and XRN3 are endogenous RNA silencing suppressors. Plant Cell **19,** 3451-3461.

Haasnoot, J., and Berkhout, B. (2009). Nucleic acids-based therapeutics in the battle against pathogenic viruses. In Antiviral Strategies, H.-G. Kräusslich and R. Bartenschlager, eds (Berlin/Heidelberg: Springer), pp. 243-263.

5. References

Hafner, M., Landgraf, P., Ludwig, J., Rice, A., Ojo, T., Lin, C., Holoch, D., Lim, C., and Tuschl, T. (2008). Identification of microRNAs and other small regulatory RNAs using cDNA library sequencing. Methods **44,** 3-12.

Hajdukiewicz, P., Allison, L., and Maliga, P. (1997). The two RNA polymerases encoded by the nuclear and the plastid compartments transcribe distinct groups of genes in tobacco plastids. EMBO J **16,** 4041-4048.

Hamilton, A., and Baulcombe, D. (1999). A species of small antisense RNA in posttranscriptional gene silencing in plants. Science **286,** 950-952.

Han, C., Coe, E.J., and Martienssen, R. (1992). Molecular cloning and characterization of iojap (ij), a pattern striping gene of maize. EMBO J **11,** 4037-4046.

Han, M., Goud, S., Song, L., and Fedoroff, N. (2004). The *Arabidopsis* double-stranded RNA-binding protein HYL1 plays a role in microRNA-mediated gene regulation. Proc Natl Acad Sci U S A **101,** 1093-1098.

Haseloff, J., Siemering, K., Prasher, D., and Hodge, S. (1997). Removal of a cryptic intron and subcellular localization of green fluorescent protein are required to mark transgenic *Arabidopsis* plants brightly. Proc Natl Acad Sci U S A **94,** 2122-2127.

Havelda, Z., Hornyik, C., Crescenzi, A., and Burgyán, J. (2003). *In situ* characterization of *Cymbidium ringspot tombusvirus* infection-induced posttranscriptional gene silencing in *Nicotiana benthamiana*. J Virol **77,** 6082-6086.

Hayes, R., Kudla, J., Schuster, G., Gabay, L., Maliga, P., and Gruissem, W. (1996). Chloroplast mRNA 3'-end processing by a high molecular weight protein complex is regulated by nuclear encoded RNA binding proteins. EMBO J **15,** 1132-1141.

Hegeman, C., Halter, C., Owens, T., and Hanson, M. (2005). Expression of complementary RNA from chloroplast transgenes affects editing efficiency of transgene and endogenous chloroplast transcripts. Nucleic Acids Res **33,** 1454-1464.

Herr, A. (2005). Pathways through the small RNA world of plants. FEBS Lett **579,** 5879-5888.

Herr, A., Jensen, M., Dalmay, T., and Baulcombe, D. (2005). RNA polymerase IV directs silencing of endogenous DNA. Science **308,** 118-120.

Hess, W., Prombona, A., Fieder, B., Subramanian, A., and Börner, T. (1993). Chloroplast rps15 and the rpoB/C1/C2 gene cluster are strongly transcribed in ribosome-deficient plastids: evidence for a functioning non-chloroplast-encoded RNA polymerase. EMBO J **12,** 563-571.

Himber, C., Dunoyer, P., Moissiard, G., Ritzenthaler, C., and Voinnet, O. (2003). Transitivity-dependent and -independent cell-to-cell movement of RNA silencing. EMBO J **22,** 4523-4533.

5. References

Hinas, A., Reimegård, J., Wagner, E., Nellen, W., Ambros, V., and Söderbom, F. (2007). The small RNA repertoire of *Dictyostelium discoideum* and its regulation by components of the RNAi pathway. Nucleic Acids Res **35,** 6714-6726.

Hiraguri, A., Itoh, R., Kondo, N., Nomura, Y., Aizawa, D., Murai, Y., Koiwa, H., Seki, M., Shinozaki, K., and Fukuhara, T. (2005). Specific interactions between DICER-LIKE proteins and HYL1/DRB-family dsRNA-binding proteins in *Arabidopsis thaliana*. Plant Mol Biol **57,** 173-188.

Höfgen, R., and Willmitzer, L. (1988). Storage of competent cells for *Agrobacterium transformation*. Nucleic Acids Res **16,** 9877.

Hong, J., Zhao, Y., Li, Z., and Huang, W. (2007). esiRNA to eri-1 and adar-1 genes improving high doses of c-myc-directed esiRNA effect on mouse melanoma growth inhibition. Biochem Biophys Res Commun **361,** 373-378.

Hong, J., Qian, Z., Shen, S., Min, T., Tan, C., Xu, J., Zhao, Y., and Huang, W. (2005). High doses of siRNAs induce eri-1 and adar-1 gene expression and reduce the efficiency of RNA interference in the mouse. Biochem J **390,** 675-679.

Horsch, R.B., Fry, J.E., Hoffmann, N.L., Eichholtz, D., Rogers, S.G., and Fraley, R.T. (1985). A simple and general method for transferring genes into plants. Science **227,** 1229-1231.

Horwich, M., Li, C., Matranga, C., Vagin, V., Farley, G., Wang, P., and Zamore, P. (2007). The *Drosophila* RNA methyltransferase, DmHen1, modifies germline piRNAs and single-stranded siRNAs in RISC. Curr Biol **17,** 1265-1272.

Houwing, S., Berezikov, E., and Ketting, R. (2008). Zili is required for germ cell differentiation and meiosis in zebrafish. EMBO J **27,** 2702-2711.

Hunter, C., Sun, H., and Poethig, R. (2003). The *Arabidopsis* heterochronic gene *ZIPPY* is an ARGONAUTE family member. Curr Biol **13,** 1734-1739.

Hutvagner, G., and Simard, M. (2008). Argonaute proteins: key players in RNA silencing. Nat Rev Mol Cell Biol **9,** 22-32.

Iida, T., Kawaguchi, R., and Nakayama, J. (2006). Conserved ribonuclease, Eri1, negatively regulates heterochromatin assembly in fission yeast. Curr Biol **16,** 1459-1464.

Inaba, T., and Schnell, D. (2008). Protein trafficking to plastids: one theme, many variations. Biochem J **413,** 15-28.

Inoue, H., Nojima, H., and Okayama, H. (1990). High efficiency transformation of *Escherichia coli* with plasmids. Gene **96,** 23-28.

Itaya, A., Matsuda, Y., Gonzales, R., Nelson, R., and Ding, B. (2002). *Potato spindle tuber viroid* strains of different pathogenicity induces and suppresses expression of common and unique genes in infected tomato. Mol Plant Microbe Interact **15,** 990-999.

Jaskiewicz, L., and Filipowicz, W. (2008). Role of Dicer in posttranscriptional RNA silencing. In RNA Interference, P.J. Paddision and P.K. Vogt, eds (Berlin/Heidelberg: Springer), pp. 77-97.

5. References

Jenkins, M.T. (1924). Heritable characters of maize XX—Iojap-striping, a chlorophyll defect. Journal of Heredity **15,** 467-472.

Ji, L., and Ding, S. (2001). The suppressor of transgene RNA silencing encoded by *Cucumber mosaic virus* interferes with salicylic acid-mediated virus resistance. Mol Plant Microbe Interact **14,** 715-724.

Jones, L., Keining, T., Eamens, A., and Vaistij, F. (2006). Virus-induced gene silencing of argonaute genes in *Nicotiana benthamiana* demonstrates that extensive systemic silencing requires Argonaute1-like and Argonaute4-like genes. Plant Physiol **141,** 598-606.

Jorgensen, R., Atkinson, R., Forster, R., and Lucas, W. (1998). An RNA-based information superhighway in plants. Science **279,** 1486-1487.

Joyce, G.F., and Orgel, L.E. (1999). Prospects for understanding the origin of the RNA World. In The RNA World, R.F. Gesteland, T.R. Cech, and J.F. Atkins, eds (New York: Cold Spring Harbor Laboratory Press), pp. 49-77.

Kalantidis, K., Tsagris, M., and Tabler, M. (2006). Spontaneous short-range silencing of a *GFP* transgene in *Nicotiana benthamiana* is possibly mediated by small quantities of siRNA that do not trigger systemic silencing. Plant J **45,** 1006-1016.

Kalantidis, K., Schumacher, H.T., Alexiadis, T., and Helm, J.M. (2008). RNA silencing movement in plants. Biol Cell **100,** 13-26.

Kalantidis, K., Denti, M., Tzortzakaki, S., Marinou, E., Tabler, M., and Tsagris, M. (2007). Virp1 is a host protein with a major role in *Potato spindle tuber viroid* infection in *Nicotiana* plants. J Virol **81,** 12872-12880.

Kapoor, M., Arora, R., Lama, T., Nijhawan, A., Khurana, J., Tyagi, A., and Kapoor, S. (2008). Genome-wide identification, organization and phylogenetic analysis of DICER-LIKE, Argonaute and RNA-dependent RNA Polymerase gene families and their expression analysis during reproductive development and stress in rice. BMC Genomics **9,** 451.

Karimi, M., Inzé, D., and Depicker, A. (2002). GATEWAY vectors for *Agrobacterium*-mediated plant transformation. Trends Plant Sci **7,** 193-195.

Kazazian, H.J. (2004). Mobile elements: drivers of genome evolution. Science **303,** 1626-1632.

Kennedy, S., Wang, D., and Ruvkun, G. (2004). A conserved siRNA-degrading RNase negatively regulates RNA interference in *C. elegans.* Nature **427,** 645-649.

Kim, V., and Nam, J. (2006). Genomics of microRNA. Trends Genet **22,** 165-173.

Kipp, M., Göhring, F., Ostendorp, T., van Drunen, C., van Driel, R., Przybylski, M., and Fackelmayer, F. (2000). SAF-Box, a conserved protein domain that specifically recognizes scaffold attachment region DNA. Mol Cell Biol **20,** 7480-7489.

Kirino, Y., and Mourelatos, Z. (2007). The mouse homolog of HEN1 is a potential methylase for Piwi-interacting RNAs. RNA **13,** 1397-1401.

5. References

Kobayashi, K., and Zambryski, P. (2007). RNA silencing and its cell-to-cell spread during *Arabidopsis* embryogenesis. Plant J **50,** 597-604.

Koonin, E., and Deutscher, M. (1993). RNase T shares conserved sequence motifs with DNA proofreading exonucleases. Nucleic Acids Res **21,** 2521-2522.

Kościańska, E., Kalantidis, K., Wypijewski, K., Sadowski, J., and Tabler, M. (2005). Analysis of RNA silencing in agroinfiltrated leaves of *Nicotiana benthamiana* and *Nicotiana tabacum*. Plant Mol Biol **59,** 647-661.

Kotakis, C., Vrettos, N., Kotsis, D., Tsagris, M., Kotzabasis, K., Kalantidis, K. (under revision). Light intensity affects RNA silencing in transgenic *Nicotiana benthamiana* plants. The Plant Journal.

Kruger, K., Grabowski, P., Zaug, A., Sands, J., Gottschling, D., and Cech, T. (1982). Self-splicing RNA: autoexcision and autocyclization of the ribosomal RNA intervening sequence of *Tetrahymena*. Cell **31,** 147-157.

Kupsco, J., Wu, M., Marzluff, W., Thapar, R., and Duronio, R. (2006). Genetic and biochemical characterization of *Drosophila* Snipper: A promiscuous member of the metazoan 3'hExo/ERI-1 family of 3' to 5' exonucleases. RNA **12,** 2103-2117.

Kurihara, Y., Takashi, Y., and Watanabe, Y. (2006). The interaction between DCL1 and HYL1 is important for efficient and precise processing of pri-miRNA in plant microRNA biogenesis. RNA **12,** 206-212.

Kurth, H., and Mochizuki, K. (2009). 2'-O-methylation stabilizes Piwi-associated small RNAs and ensures DNA elimination in *Tetrahymena*. RNA **15,** 675-685.

Lagos-Quintana, M., Rauhut, R., Lendeckel, W., and Tuschl, T. (2001). Identification of novel genes coding for small expressed RNAs. Science **294,** 853-858.

Lakatos, L., Szittya, G., Silhavy, D., and Burgyán, J. (2004). Molecular mechanism of RNA silencing suppression mediated by p19 protein of tombusviruses. EMBO J **23,** 876-884.

Lakatos, L., Csorba, T., Pantaleo, V., Chapman, E., Carrington, J., Liu, Y., Dolja, V., Calvino, L., López-Moya, J., and Burgyán, J. (2006). Small RNA binding is a common strategy to suppress RNA silencing by several viral suppressors. EMBO J **25,** 2768-2780.

Lau, N., Lim, L., Weinstein, E., and Bartel, D. (2001). An abundant class of tiny RNAs with probable regulatory roles in *Caenorhabditis elegans*. Science **294,** 858-862.

Laubinger, S., Sachsenberg, T., Zeller, G., Busch, W., Lohmann, J., Rätsch, G., and Weigel, D. (2008). Dual roles of the nuclear cap-binding complex and SERRATE in pre-mRNA splicing and microRNA processing in *Arabidopsis thaliana*. Proc Natl Acad Sci U S A **105,** 8795-8800.

Lee, R., and Ambros, V. (2001). An extensive class of small RNAs in *Caenorhabditis elegans*. Science **294,** 862-864.

Lee, R., Feinbaum, R., and Ambros, V. (1993). The *C. elegans* heterochronic gene lin-4 encodes small RNAs with antisense complementarity to lin-14. Cell **75,** 843-854.

5. References

Li, H., Li, W., and Ding, S. (2002). Induction and suppression of RNA silencing by an animal virus. Science **296,** 1319-1321.

Li, J., Yang, Z., Yu, B., Liu, J., and Chen, X. (2005). Methylation protects miRNAs and siRNAs from a 3'-end uridylation activity in *Arabidopsis.* Curr Biol **15,** 1501-1507.

Liere, K., and Börner, T. (2007). Transcription and transcriptional regulation in plastids. In Cell and Molecular Biology of Plastids (Berlin/Heidelberg: Springer), pp. 121-174.

Lindbo, J., Silva-Rosales, L., Proebsting, W., and Dougherty, W. (1993). Induction of a highly specific antiviral state in transgenic plants: implications for regulation of gene expression and virus resistance. Plant Cell **5,** 1749-1759.

Liu, J., Carmell, M., Rivas, F., Marsden, C., Thomson, J., Song, J., Hammond, S., Joshua-Tor, L., and Hannon, G. (2004). Argonaute2 is the catalytic engine of mammalian RNAi. Science **305,** 1437-1441.

Liu, Q., Yao, X., Pi, L., Wang, H., Cui, X., and Huang, H. (2008). The *ARGONAUTE10* gene modulates shoot apical meristem maintenance and leaf polarity establishment by repressing miR165/166 in *Arabidopsis*. Plant J.

Lobbes, D., Rallapalli, G., Schmidt, D., Martin, C., and Clarke, J. (2006). SERRATE: a new player on the plant microRNA scene. EMBO Rep **7,** 1052-1058.

Lu, C., and Fedoroff, N. (2000). A mutation in the *Arabidopsis HYL1* gene encoding a dsRNA binding protein affects responses to abscisic acid, auxin, and cytokinin. Plant Cell **12,** 2351-2366.

Lu, R., Folimonov, A., Shintaku, M., Li, W., Falk, B., Dawson, W., and Ding, S. (2004). Three distinct suppressors of RNA silencing encoded by a 20-kb viral RNA genome. Proc Natl Acad Sci U S A **101,** 15742-15747.

Luan, S., Kudla, J., Rodriguez-Concepcion, M., Yalovsky, S., and Gruissem, W. (2002). Calmodulins and calcineurin B-like proteins: calcium sensors for specific signal response coupling in plants. Plant Cell **14 Suppl,** S389-400.

Maiti, M., Lee, H., and Liu, Y. (2007). QIP, a putative exonuclease, interacts with the *Neurospora* Argonaute protein and facilitates conversion of duplex siRNA into single strands. Genes Dev **21,** 590-600.

Mallory, A., and Bouché, N. (2008). MicroRNA-directed regulation: to cleave or not to cleave. Trends Plant Sci **13,** 359-367.

Mallory, A., Mlotshwa, S., Bowman, L., and Vance, V. (2003). The capacity of transgenic tobacco to send a systemic RNA silencing signal depends on the nature of the inducing transgene locus. Plant J **35,** 82-92.

Malone, C., and Hannon, G. (2009). Small RNAs as guardians of the genome. Cell **136,** 656-668.

Marchler-Bauer, A., Anderson, J., Derbyshire, M., DeWeese-Scott, C., Gonzales, N., Gwadz, M., Hao, L., He, S., Hurwitz, D., Jackson, J., Ke, Z., Krylov, D., Lanczycki, C., Liebert, C., Liu, C., Lu, F., Lu, S., Marchler, G., Mullokandov,

M., Song, J., Thanki, N., Yamashita, R., Yin, J., Zhang, D., and Bryant, S. (2007). CDD: a conserved domain database for interactive domain family analysis. Nucleic Acids Res **35,** D237-240.

Margis, R., Fusaro, A., Smith, N., Curtin, S., Watson, J., Finnegan, E., and Waterhouse, P. (2006). The evolution and diversification of Dicers in plants. FEBS Lett **580,** 2442-2450.

Martin, W., Rujan, T., Richly, E., Hansen, A., Cornelsen, S., Lins, T., Leister, D., Stoebe, B., Hasegawa, M., and Penny, D. (2002). Evolutionary analysis of *Arabidopsis*, cyanobacterial, and chloroplast genomes reveals plastid phylogeny and thousands of cyanobacterial genes in the nucleus. Proc Natl Acad Sci U S A **99,** 12246-12251.

Martínez-Zapater, J.M. (1993). Genetic analysis of variegated mutants in *Arabidopsis*. Journal of Heredity **84,** 138-140.

Mattick, J. (2007). A new paradigm for developmental biology. J Exp Biol **210,** 1526-1547.

Meister, G., Landthaler, M., Patkaniowska, A., Dorsett, Y., Teng, G., and Tuschl, T. (2004). Human Argonaute2 mediates RNA cleavage targeted by miRNAs and siRNAs. Mol Cell **15,** 185-197.

Mérai, Z., Kerényi, Z., Kertész, S., Magna, M., Lakatos, L., and Silhavy, D. (2006). Double-stranded RNA binding may be a general plant RNA viral strategy to suppress RNA silencing. J Virol **80,** 5747-5756.

Mlotshwa, S., Voinnet, O., Mette, M., Matzke, M., Vaucheret, H., Ding, S., Pruss, G., and Vance, V. (2002). RNA silencing and the mobile silencing signal. Plant Cell **14 Suppl,** S289-301.

Molnár, A., Schwach, F., Studholme, D., Thuenemann, E., and Baulcombe, D. (2007). miRNAs control gene expression in the single-cell alga *Chlamydomonas reinhardtii*. Nature **447,** 1126-1129.

Montgomery, T., Howell, M., Cuperus, J., Li, D., Hansen, J., Alexander, A., Chapman, E., Fahlgren, N., Allen, E., and Carrington, J. (2008). Specificity of ARGONAUTE7-miR390 interaction and dual functionality in TAS3 trans-acting siRNA formation. Cell **133,** 128-141.

Mullen, T., and Marzluff, W. (2008). Degradation of histone mRNA requires oligouridylation followed by decapping and simultaneous degradation of the mRNA both 5' to 3' and 3' to 5'. Genes Dev **22,** 50-65.

Nakazawa, Y., Hiraguri, A., Moriyama, H., and Fukuhara, T. (2007). The dsRNA-binding protein DRB4 interacts with the Dicer-like protein DCL4 *in vivo* and functions in the trans-acting siRNA pathway. Plant Mol Biol **63,** 777-785.

Napoli, C., Lemieux, C., and Jorgensen, R. (1990). Introduction of a chimeric *CHALCONE SYNTHASE* gene into petunia results in reversible co-suppression of homologous genes in *trans*. Plant Cell **2,** 279-289.

5. References

Newton, K., and Coe, E. (1986). Mitochondrial DNA changes in abnormal growth (nonchromosomal stripe) mutants of maize. Proc Natl Acad Sci U S A **83,** 7363-7366.

Nissen, P., Hansen, J., Ban, N., Moore, P., and Steitz, T. (2000). The structural basis of ribosome activity in peptide bond synthesis. Science **289,** 920-930.

Onodera, Y., Haag, J., Ream, T., Nunes, P., Pontes, O., and Pikaard, C. (2005). Plant nuclear RNA polymerase IV mediates siRNA and DNA methylation-dependent heterochromatin formation. Cell **120,** 613-622.

Pak, J., and Fire, A. (2007). Distinct populations of primary and secondary effectors during RNAi in *C. elegans*. Science **315,** 241-244.

Pandey, S., and Baldwin, I. (2007). RNA-directed RNA polymerase 1 (RdR1) mediates the resistance of *Nicotiana attenuata* to herbivore attack in nature. Plant J **50,** 40-53.

Pandey, S., and Baldwin, I. (2008). Silencing RNA-directed RNA polymerase 2 increases the susceptibility of *Nicotiana attenuata* to UV in the field and in the glasshouse. Plant J **54,** 845-862.

Park, M., Wu, G., Gonzalez-Sulser, A., Vaucheret, H., and Poethig, R. (2005). Nuclear processing and export of microRNAs in *Arabidopsis*. Proc Natl Acad Sci U S A **102,** 3691-3696.

Pazhouhandeh, M., Dieterle, M., Marrocco, K., Lechner, E., Berry, B., Brault, V., Hemmer, O., Kretsch, T., Richards, K., Genschik, P., and Ziegler-Graff, V. (2006). F-box-like domain in the polerovirus protein P0 is required for silencing suppressor function. Proc Natl Acad Sci U S A **103,** 1994-1999.

Peragine, A., Yoshikawa, M., Wu, G., Albrecht, H., and Poethig, R. (2004). SGS3 and SGS2/SDE1/RDR6 are required for juvenile development and the production of trans-acting siRNAs in *Arabidopsis*. Genes Dev **18,** 2368-2379.

Pfeffer, S., Dunoyer, P., Heim, F., Richards, K., Jonard, G., and Ziegler-Graff, V. (2002). P0 of beet *Western yellows virus* is a suppressor of posttranscriptional gene silencing. J Virol **76,** 6815-6824.

Pikaard, C., Haag, J., Ream, T., and Wierzbicki, A. (2008). Roles of RNA polymerase IV in gene silencing. Trends Plant Sci **13,** 390-397.

Ponjavic, J., Ponting, C., and Lunter, G. (2007). Functionality or transcriptional noise? Evidence for selection within long noncoding RNAs. Genome Res **17,** 556-565.

Ponting, C., Oliver, P., and Reik, W. (2009). Evolution and functions of long noncoding RNAs. Cell **136,** 629-641.

Qi, Y., and Hannon, G. (2005). Uncovering RNAi mechanisms in plants: biochemistry enters the foray. FEBS Lett **579,** 5899-5903.

Qu, F., Ren, T., and Morris, T. (2003). The coat protein of *Turnip crinkle virus* suppresses posttranscriptional gene silencing at an early initiation step. J Virol **77,** 511-522.

5. References

Ramachandran, V., and Chen, X. (2008). Small RNA metabolism in *Arabidopsis*. Trends Plant Sci **13,** 368-374.

Rand, T., Ginalski, K., Grishin, N., and Wang, X. (2004). Biochemical identification of Argonaute 2 as the sole protein required for RNA-induced silencing complex activity. Proc Natl Acad Sci U S A **101,** 14385-14389.

Rand, T., Petersen, S., Du, F., and Wang, X. (2005). Argonaute2 cleaves the anti-guide strand of siRNA during RISC activation. Cell **123,** 621-629.

Ratcliff, F., Harrison, B., and Baulcombe, D. (1997). A similarity between viral defense and gene silencing in plants. Science **276,** 1558-1560.

Reinhart, B., and Bartel, D. (2002). Small RNAs correspond to centromere heterochromatic repeats. Science **297,** 1831.

Reinhart, B., Slack, F., Basson, M., Pasquinelli, A., Bettinger, J., Rougvie, A., Horvitz, H., and Ruvkun, G. (2000). The 21-nucleotide *let-7* RNA regulates developmental timing in *Caenorhabditis elegans.* Nature **403,** 901-906.

Reiter, R., Coomber, S., Bourett, T., Bartley, G., and Scolnik, P. (1994). Control of leaf and chloroplast development by the *Arabidopsis* gene *pale cress.* Plant Cell **6,** 1253-1264.

Rivas, F., Tolia, N., Song, J., Aragon, J., Liu, J., Hannon, G., and Joshua-Tor, L. (2005). Purified Argonaute2 and an siRNA form recombinant human RISC. Nat Struct Mol Biol **12,** 340-349.

Rodio, M., Delgado, S., De Stradis, A., Gómez, M., Flores, R., and Di Serio, F. (2007). A viroid RNA with a specific structural motif inhibits chloroplast development. Plant Cell **19,** 3610-3626.

Ruby, J., Jan, C., Player, C., Axtell, M., Lee, W., Nusbaum, C., Ge, H., and Bartel, D. (2006). Large-scale sequencing reveals 21U-RNAs and additional microRNAs and endogenous siRNAs in *C. elegans.* Cell **127,** 1193-1207.

Ruiz, M., Voinnet, O., and Baulcombe, D. (1998). Initiation and maintenance of virus-induced gene silencing. Plant Cell **10,** 937-946.

Saito, K., Sakaguchi, Y., Suzuki, T., Siomi, H., and Siomi, M. (2007). Pimet, the Drosophila homolog of HEN1, mediates 2'-O-methylation of Piwi- interacting RNAs at their 3' ends. Genes Dev **21,** 1603-1608.

Sakamoto, W. (2003). Leaf-variegated mutations and their responsible genes in *Arabidopsis thaliana.* Genes Genet Syst **78,** 1-9.

Sambrook, J., and Russel, D.W. (2001). Molecular cloning - a laboratory manual. (New York: Cold Spring Harbor Laboratory Press).

Sarmiento, C., Nigul, L., Kazantseva, J., Buschmann, M., and Truve, E. (2006). AtRLI2 is an endogenous suppressor of RNA silencing. Plant Mol Biol **61,** 153-163.

Schöb, H., Kunz, C., and Meins, F.J. (1997). Silencing of transgenes introduced into leaves by agroinfiltration: a simple, rapid method for investigating sequence requirements for gene silencing. Mol Gen Genet **256,** 581-585.

5. References

Schott, D., Cureton, D., Whelan, S., and Hunter, C. (2005). An antiviral role for the RNA interference machinery in *Caenorhabditis elegans*. Proc Natl Acad Sci U S A **102,** 18420-18424.

Schubert, D., Lechtenberg, B., Forsbach, A., Gils, M., Bahadur, S., Schmidt, R. (2004). Silencing in *Arabidopsis* T-DNA transformants: the predominant role of a gene-specific RNA sensing mechanism versus position effects. Plant Cell **16,** 2561-2572.

Shabalina, S., and Koonin, E. (2008). Origins and evolution of eukaryotic RNA interference. Trends Ecol Evol **23,** 578-587.

Shiboleth, Y., Haronsky, E., Leibman, D., Arazi, T., Wassenegger, M., Whitham, S., Gaba, V., and Gal-On, A. (2007). The conserved FRNK box in HC-Pro, a plant viral suppressor of gene silencing, is required for small RNA binding and mediates symptom development. J Virol **81,** 13135-13148.

Sijen, T., Steiner, F., Thijssen, K., and Plasterk, R. (2007). Secondary siRNAs result from unprimed RNA synthesis and form a distinct class. Science **315,** 244-247.

Silhavy, D., Molnár, A., Lucioli, A., Szittya, G., Hornyik, C., Tavazza, M., and Burgyán, J. (2002). A viral protein suppresses RNA silencing and binds silencing-generated, 21- to 25-nucleotide double-stranded RNAs. EMBO J **21,** 3070-3080.

Simmer, F., Tijsterman, M., Parrish, S., Koushika, S., Nonet, M., Fire, A., Ahringer, J., and Plasterk, R. (2002). Loss of the putative RNA-directed RNA polymerase RRF-3 makes *C. elegans* hypersensitive to RNAi. Curr Biol **12,** 1317-1319.

Smith, L., Pontes, O., Searle, I., Yelina, N., Yousafzai, F., Herr, A., Pikaard, C., and Baulcombe, D. (2007). An SNF2 protein associated with nuclear RNA silencing and the spread of a silencing signal between cells in *Arabidopsis*. Plant Cell **19,** 1507-1521.

Soards, A., Murphy, A., Palukaitis, P., and Carr, J. (2002). Virulence and differential local and systemic spread of cucumber mosaic virus in tobacco are affected by the CMV 2b protein. Mol Plant Microbe Interact **15,** 647-653.

Sonenberg, N., and Hinnebusch, A. (2009). Regulation of translation initiation in eukaryotes: mechanisms and biological targets. Cell **136,** 731-745.

Song, L., Han, M., Lesicka, J., and Fedoroff, N. (2007). *Arabidopsis* primary microRNA processing proteins HYL1 and DCL1 define a nuclear body distinct from the Cajal body. Proc Natl Acad Sci U S A **104,** 5437-5442.

Steitz, T., and Moore, P. (2003). RNA, the first macromolecular catalyst: the ribosome is a ribozyme. Trends Biochem Sci **28,** 411-418.

Stern, D., and Kindle, K. (1993). 3'end maturation of the *Chlamydomonas reinhardtii* chloroplast atpB mRNA is a two-step process. Mol Cell Biol **13,** 2277-2285.

Strasser, R.J., Srivastava, A., and Tsimilli-Michael, M. (2000). The fluorescence transient as a tool to characterize and screen photosynthetic samples. In Probing

Photosynthesis: Mechanisms, Regulation and Adaptation, M. Yunus, U. Pathre, and P. Mohanty, eds (London: Taylor and Francis), pp. 445-483.

Strobel, S., and Cochrane, J. (2007). RNA catalysis: ribozymes, ribosomes, and riboswitches. Curr Opin Chem Biol **11,** 636-643.

Tabler, M., and Sänger, H. (1984). Cloned single- and double-stranded DNA copies of *Potato spindle tuber viroid* (PSTV) RNA and co-inoculated subgenomic DNA fragments are infectious. EMBO J **3,** 3055-3062.

Tabler, M., and Tsagris, M. (2004). Viroids: petite RNA pathogens with distinguished talents. Trends Plant Sci **9,** 339-348.

Tel-Zur, N., Abbo, S., Myslabodski, D., and Mizrahi, Y. (1999). Modified CTAB procedure for DNA isolation from epiphytic cacti of the genera *Hylocereus* and *Selenicereus* (Cactaceae). Plant Molecular Biology Reporter **17,** 249-254.

Telfer, A., and Poethig, R. (1998). *HASTY*: a gene that regulates the timing of shoot maturation in *Arabidopsis thaliana.* Development **125,** 1889-1898.

Thomas, C., Leh, V., Lederer, C., and Maule, A. (2003). *Turnip crinkle virus* coat protein mediates suppression of RNA silencing in *Nicotiana benthamiana.* Virology **306,** 33-41.

Tomoyasu, Y., Miller, S., Tomita, S., Schoppmeier, M., Grossmann, D., and Bucher, G. (2008). Exploring systemic RNA interference in insects: a genome-wide survey for RNAi genes in *Tribolium*. Genome Biol **9,** R10.

Tournier, B., Tabler, M., and Kalantidis, K. (2006). Phloem flow strongly influences the systemic spread of silencing in GFP *Nicotiana benthamiana* plants. Plant J **47,** 383-394.

Tsagris, E., Martínez de Alba, A., Gozmanova, M., and Kalantidis, K. (2008). Viroids. Cell Microbiol **10,** 2168-2179.

van der Krol, A., Mur, L., Beld, M., Mol, J., and Stuitje, A. (1990). Flavonoid genes in petunia: addition of a limited number of gene copies may lead to a suppression of gene expression. Plant Cell **2,** 291-299.

Vaucheret, H. (2008). Plant ARGONAUTES. Trends Plant Sci **13,** 350-358.

Vaucheret, H., Vazquez, F., Crété, P., and Bartel, D. (2004). The action of ARGONAUTE1 in the miRNA pathway and its regulation by the miRNA pathway are crucial for plant development. Genes Dev **18,** 1187-1197.

Vaucheret, H., Béclin, C., Elmayan, T., Feuerbach, F., Godon, C., Morel, J., Mourrain, P., Palauqui, J., and Vernhettes, S. (1998). Transgene-induced gene silencing in plants. Plant J **16,** 651-659.

Vazquez, F., Gasciolli, V., Crété, P., and Vaucheret, H. (2004). The nuclear dsRNA binding protein HYL1 is required for microRNA accumulation and plant development, but not posttranscriptional transgene silencing. Curr Biol **14,** 346-351.

Vogler, H., Akbergenov, R., Shivaprasad, P., Dang, V., Fasler, M., Kwon, M., Zhanybekova, S., Hohn, T., and Heinlein, M. (2007). Modification of small

RNAs associated with suppression of RNA silencing by tobamovirus replicase protein. J Virol **81,** 10379-10388.

Voinnet, O. (2005a). Induction and suppression of RNA silencing: insights from viral infections. Nat Rev Genet **6,** 206-220.

Voinnet, O. (2005b). Non-cell autonomous RNA silencing. FEBS Lett **579,** 5858-5871.

Voinnet, O. (2008). Use, tolerance and avoidance of amplified RNA silencing by plants. Trends Plant Sci **13,** 317-328.

Voinnet, O. (2009). Origin, biogenesis, and activity of plant microRNAs. Cell **136,** 669-687.

Voinnet, O., and Baulcombe, D. (1997). Systemic signalling in gene silencing. Nature **389,** 553.

Voinnet, O., Vain, P., Angell, S., and Baulcombe, D. (1998). Systemic spread of sequence-specific transgene RNA degradation in plants is initiated by localized introduction of ectopic promoterless DNA. Cell **95,** 177-187.

Walter, M., Kilian, J., and Kudla, J. (2002). PNPase activity determines the efficiency of mRNA 3'-end processing, the degradation of tRNA and the extent of polyadenylation in chloroplasts. EMBO J **21,** 6905-6914.

Wang, Y., Duby, G., Purnelle, B., and Boutry, M. (2000). Tobacco *VDL* gene encodes a plastid DEAD box RNA helicase and is involved in chloroplast differentiation and plant morphogenesis. Plant Cell **12,** 2129-2142.

Watanabe, Y., Tomita, M., and Kanai, A. (2007). Computational methods for microRNA target prediction. In MicroRNA Methods, J.J. Rossi and G.J. Hannon, eds (Elsevier Inc.), pp. 65-86.

Waters, L., and Storz, G. (2009). Regulatory RNAs in bacteria. Cell **136,** 615-628.

Wesley, S., Helliwell, C., Smith, N., Wang, M., Rouse, D., Liu, Q., Gooding, P., Singh, S., Abbott, D., Stoutjesdijk, P., Robinson, S., Gleave, A., Green, A., and Waterhouse, P. (2001). Construct design for efficient, effective and high-throughput gene silencing in plants. Plant J **27,** 581-590.

Wierzbicki, A., Haag, J., and Pikaard, C. (2008). Noncoding transcription by RNA polymerase Pol IVb/Pol V mediates transcriptional silencing of overlapping and adjacent genes. Cell **135,** 635-648.

Wilkins, C., Dishongh, R., Moore, S., Whitt, M., Chow, M., and Machaca, K. (2005). RNA interference is an antiviral defence mechanism in *Caenorhabditis elegans.* Nature **436,** 1044-1047.

Williams, M., Johzuka, Y., and Mulligan, R. (2000). Addition of non-genomically encoded nucleotides to the 3'-terminus of maize mitochondrial mRNAs: truncated rps12 mRNAs frequently terminate with CCA. Nucleic Acids Res **28,** 4444-4451.

Wimberly, B., Brodersen, D., Clemons, W.J., Morgan-Warren, R., Carter, A., Vonrhein, C., Hartsch, T., and Ramakrishnan, V. (2000). Structure of the 30S ribosomal subunit. Nature **407,** 327-339.

5. References

Wingard, S.A. (1928). Hosts and symptoms of ringspot, a virus disease of plants. Journal of Agricultural Research **37,** 127-153.

Winter, D., Vinegar, B., Nahal, H., Ammar, R., Wilson, G., and Provart, N. (2007). An "electronic fluorescent pictograph" browser for exploring and analyzing large-scale biological data sets. PLoS ONE **2,** e718.

Wolf, Y., and Koonin, E. (2007). On the origin of the translation system and the genetic code in the RNA world by means of natural selection, exaptation, and subfunctionalization. Biol Direct **2,** 14.

Xie, Q., and Guo, H. (2006). Systemic antiviral silencing in plants. Virus Res **118,** 1-6.

Xie, Z., and Qi, X. (2008). Diverse small RNA-directed silencing pathways in plants. Biochim Biophys Acta **1779,** 720-724.

Yang, J., Seo, H., Han, S., Yoon, E., Yang, M., and Lee, W. (2008). Phytohormone abscisic acid control RNA-dependent RNA polymerase 6 gene expression and post-transcriptional gene silencing in rice cells. Nucleic Acids Res **36,** 1220-1226.

Yang, L., Liu, Z., Lu, F., Dong, A., and Huang, H. (2006a). SERRATE is a novel nuclear regulator in primary microRNA processing in *Arabidopsis*. Plant J **47,** 841-850.

Yang, X., Purdy, M., Marzluff, W., and Dominski, Z. (2006b). Characterization of 3'hExo, a 3' exonuclease specifically interacting with the 3' end of histone mRNA. J Biol Chem **281,** 30447-30454.

Yang, Z., Ebright, Y., Yu, B., and Chen, X. (2006c). HEN1 recognizes 21-24 nt small RNA duplexes and deposits a methyl group onto the 2' OH of the 3' terminal nucleotide. Nucleic Acids Res **34,** 667-675.

Ye, K., Malinina, L., and Patel, D. (2003). Recognition of small interfering RNA by a viral suppressor of RNA silencing. Nature **426,** 874-878.

Yigit, E., Batista, P., Bei, Y., Pang, K., Chen, C., Tolia, N., Joshua-Tor, L., Mitani, S., Simard, M., and Mello, C. (2006). Analysis of the *C. elegans* Argonaute family reveals that distinct Argonautes act sequentially during RNAi. Cell **127,** 747-757.

Yoo, B., Kragler, F., Varkonyi-Gasic, E., Haywood, V., Archer-Evans, S., Lee, Y., Lough, T., and Lucas, W. (2004). A systemic small RNA signaling system in plants. Plant Cell **16,** 1979-2000.

Yoshikawa, M., Peragine, A., Park, M., and Poethig, R. (2005). A pathway for the biogenesis of trans-acting siRNAs in *Arabidopsis*. Genes Dev **19,** 2164-2175.

Yu, B., Chapman, E., Yang, Z., Carrington, J., and Chen, X. (2006). Transgenically expressed viral RNA silencing suppressors interfere with microRNA methylation in *Arabidopsis*. FEBS Lett **580,** 3117-3120.

Yu, B., Yang, Z., Li, J., Minakhina, S., Yang, M., Padgett, R., Steward, R., and Chen, X. (2005). Methylation as a crucial step in plant microRNA biogenesis. Science **307,** 932-935.

5. References

Yusupov, M., Yusupova, G., Baucom, A., Lieberman, K., Earnest, T., Cate, J., and Noller, H. (2001). Crystal structure of the ribosome at 5.5 A resolution. Science **292,** 883-896.

Zandueta-Criado, A., and Bock, R. (2004). Surprising features of plastid ndhD transcripts: addition of non-encoded nucleotides and polysome association of mRNAs with an unedited start codon. Nucleic Acids Res **32,** 542-550.

Zhang, J. (2005). Dampening the silencing effect of RNA interference in mammals. Biochem J **390,** e5-6.

Zhang, X., Yuan, Y., Pei, Y., Lin, S., Tuschl, T., Patel, D., and Chua, N. (2006). *Cucumber mosaic virus*-encoded 2b suppressor inhibits *Arabidopsis* Argonaute1 cleavage activity to counter plant defense. Genes Dev **20,** 3255-3268.

Zheng, X., Zhu, J., Kapoor, A., and Zhu, J. (2007). Role of *Arabidopsis* AGO6 in siRNA accumulation, DNA methylation and transcriptional gene silencing. EMBO J **26,** 1691-1701.

Zubko, M., and Day, A. (2002). Differential regulation of genes transcribed by nucleus-encoded plastid RNA polymerase, and DNA amplification, within ribosome-deficient plastids in stable phenocopies of cereal albino mutants. Mol Genet Genomics **267,** 27-37.

Zuo, Y., and Deutscher, M. (2001). Exoribonuclease superfamilies: structural analysis and phylogenetic distribution. Nucleic Acids Res **29,** 1017-1026.

6

Supplements

6.1. Oligonucleotide sequences and plasmid vector maps

Sequences, applications, sizes, and T_m values of all olignonucleotides used during this work are listet in Table S6.1. Detailed maps of important vectors that were used to obtain the presented results are depicted in Figure S6.1.

6.2. Supplementary methods

In this section important standard methods of molecular biology are described for reference purposes. In addition, methods underlying supplementary results can be found here.

6.2.1. Cultivation of bacteria

E. coli and *A. tumefaciens* were grown in/on LB medium with antibiotics added as selective markers when appropriate.

Liquid cultures up to 5 mL were set up in 15 ml glass tubes, while larger cultures were set up in Erlenmeyer flasks of appropriate sizes. Antibiotics were added to final

concentrations of 100 µg/mL when appropriate. Cultures were incubated at suitable temperatures (typically 37 °C for *E. coli* and 28 °C for *A. tumefaciens*) while shaking at 200-250 rpm in an orbital incubator/shaker.

For growth on nutrient plates, bacteria were plated on LB-agar plates containing the appropriate antibiotics using a Drygalski spreader. Plates were incubated at 37 °C over night in the case of *E. coli* and at 28 °C for two days in the dark in the case of *A. tumefaciens*.

6.2.2. Preparation of chemically competent bacteria

Chemically competent *E. coli* cells were prepared as described elsewhere (Inoue et al., 1990). DH5α® cells were streaked on an LB-agar plate in the absence of antibiotics and incubated over night at 37 °C. The next day a 250 mL shaking culture of SOB medium [2 % tryptone, 0.5 % yeast extract, 10 mM NaCl, 2.5 mM KCl, 1 mM $MgCl_2$ (pH 7.0)] was inoculated with bacteria from the LB plate by picking a colony with a sterile pipette tip and transferring the tip to a 2-litre flask containing the SOB medium. Cells were grown to an OD_{600} of 0.6-0.8 at 18 °C with vigorous shaking at 250 rpm. The flask was then put on ice for 10 minutes, and the cells were subsequently harvested at 2.500x g for 10 minutes at 4 °C. The bacterial pellet was gently resuspended in 80 ml of ice-cold TB [10 mM PIPES, 15 mM $CaCl_2$, 250 mM KCl, 55 mM $MnCl_2$ (pH 6.7)], incubated on ice for 10 minutes, and harvested as before. The pellet was then resuspended in 20 ml of TB, and DMSO was added to a final concentration of 7 % while carefully swirling the tube. After incubation on ice for 10 minutes, the cells were dispensed into aliquots of 100 µL in 1.5 mL reaction tubes and quick-frozen in liquid nitrogen. The frozen competent cells were stored at -80 °C.

Competent cells of *A. tumefaciens* were prepared by growing a 5 mL starter culture of *A. tumefaciens* strain C58C1 in LB containing 100 µg/mL rifampicin at 28 °C over night. The next day 2 mL of the starter culture were used to inoculate 50 mL LB/rifampicin. Cells were grown shaking at 250 rpm and 28 °C to an OD_{600} of 0.6-0.8. Afterwards the culture was chilled on ice for 10 minutes and subsequently harvested at 2500x g for 10 minutes (4 °C). The cells were resuspended in 1 mL of ice-cold 20 mM CaCl2 and

Table S6.1 Sequences and applications of oligonucleotides used during this study

Name	Length	Melting temperature	Sequence 5'-3'
PCR primers for vector constructions:			
15140-L-SpeI	29 nt	57.2 °C	CGACTAGTGTACAAAGATGGATGATCCTG
15140-R-HindIII	30 nt	58.2 °C	CGAAGCTTCCATGAGTTTTATTCCACACTG
15140-R-XbaI	30 nt	58.2 °C	CGTCTAGACCATGAGTTTTATTCCACACTG
At-Eri-Bam-F	26 nt	56.4 °C	GGATCCATGGCGTCCGCATTCTCTGC
At-Eri-Bam-R	30 nt	57.8 °C	GCGGCCGCTTACTTGATCCTGTTCTTGAAG
Eri-Mature-Nde-For	30 nt	61.4 °C	CATATGGAAAATGCAAGGTGGAGACCCATG
Eri-Compl-For	25 nt	55.0 °C	CATATGATGGCGTCCGCATTCTCTG
Eri-Compl-Rev	25 nt	53.4 °C	GGATCCTTACTTGATCCTGTTCTTG
Eri-Hind-For	29 nt	60.4 °C	AAGCTTACGAAAATGGCGTCCGCATTCTC
Eri-Bam-Rev	29 nt	59.6 °C	GGATCCCACCACATCACATTTAGGCGTAA
Eri noStop R	32 nt	60.6 °C	GCGGCCGCCTCTTGATCCTGTTCTTGAAGAGA
bp52-Forward	21 nt	56.8 °C	CTTCTTCAGGAAAACTCATAC
bp52-Reverse	22 nt	57.4 °C	CATGCAATTCTTCATATAGAAC
PCR primers for the production of probe templates:			
18S For	23 nt	60.0 °C	TCAACCATAAACGATGCCGACCA
18S Rev	22 nt	59.8 °C	GCGTGCGGCCCAGAACATCTAA
5.8S For	20 nt	56.0 °C	GCAACGGATATCTCGGCTCT
5.8S Rev	20 nt	56.0 °C	TAATGGCTTCGGGCGCAACT
NEP For	23 nt	59.6 °C	TTTGATGCGCACTCATGGATCTA
NEP Rev	23 nt	59.6 °C	GCAAATTCAAGGATTCCTCGACA
Nt-CLP-Bam-F	29 nt	60.4 °C	GGATCCGAAAGGAGGCCGTCGTATAGGTT
Nt-CLP-Not-R	31 nt	60.8 °C	GCGGCCGCATCTGAGGGAGTTCCGCTAGTGC
psbA For	23 nt	60.0 °C	TAACCATGAGCGGCTACGATGTT
psbA Rev	22 nt	59.0 °C	GTAGCTTGTTACATGGGTCGTG

Table S6.1 *continued*

Name	Length	Melting temperature	Sequence 5'-3'
rbcL For	23 nt	59.6 °C	TGCGAATCCCTCCTGCTTATGTT
rbcL Rev	23 nt	60.0 °C	CCAAGCTAGTATTTGCGGTGAAT
rpoB For	23 nt	60.0 °C	CTTCCAGCTACTTTATCGCCTAC
rpoB Rev	23 nt	60.4 °C	CTTATATGCCGTGGGAGGGTTAC
Tob-Pftf Forward	27 nt	58.8 °C	GGATCCCCCGAGAGGTTTACCGCAGTG
Tob-Pftf Reverse	30 nt	58.6 °C	GCGGCCGCGGTGTCCTCATGGCTATAACTT
Sequencing primers:			
Eri-Seq1-For	22 nt	58.2 °C	TACAGCGGAATGCGGAATTAAA
Eri-Seq2-Rev	23 nt	59.2 °C	TGCCATTAAAGATAGGAAGCTGT
Eri-Seq3-Rev	23 nt	59.2 °C	ACGCATGCATTAAGGATTGACTA
Eri-Seq4-Rev	23 nt	59.2 °C	GCGGAAGATTGATGTTTGAAACT
M13 Forward	16 nt	48.2 °C	GTAAAACGACGGCCAG
M13 Reverse	17 nt	49.8 °C	CAGGAAACAGCTATGAC
pART7Pro	18 nt	52.2 °C	CACTATCCTTCGCAAGAC
pART7Ter	19 nt	53.4 °C	CATTAGAATGAACCGAAAC
pENTR For	20 nt	55.6 °C	GACTGATAGTGACCTGTTCG
pENTR Rev	20 nt	55.6 °C	GATAGTGACCTGTTCGTTGC
Sp6 Primer	18 nt	51.0 °C	ATTTAGGTGACACTATAG
T7 Primer	20 nt	54.8 °C	TAATACGACTCACTATAGGG
Oligo probes:			
4.5S Probe	40 nt	75.9 °C	ATCCTGGCGTCGAGCTATTTTTCCGCAGGACCTCCCCTAC
5S Probe	40 nt	75.1 °C	GGATGCCTCAGCTGCATACATCACTGCACTTCCACTTGAC
ClpP Probe	45 nt	78.3 °C	CCTTGTGAGGGTTTCACGCAGTTTCAGCAGTTCTTCCGCTTCCAG
rpl23 Probe	45 nt	78.3 °C	GCCGATTTCCCCTCTTTTGCAATCAGTTTCGCTACAGCACCCGCT

Table S6.1 *continued*

Name	Length	Melting temperature	Sequence 5'-3'
PCR primers to produce templates for *in vitro* transcription:			
T7 4.5S For	44 nt	60.7 °C	TTGTAATACGACTCACTATAGGGAAGGTCACGGCGAGACGAGCC
4.5S Rev	19 nt	54.6 °C	GTTCAAGTCTACCGGTCTG
4.5S Cl.1 Rev	19 nt	54.2 °C	GAACAGTTCAAGTCTACCG
T7 5S For	44 nt	59.0 °C	TTGTAATACGACTCACTATAGGTATTCTGGTGTCCTAGGCGTAG
5S Rev	19 nt	54.6 °C	ATCCTGGCGTCGAGCTATT
5S Cl.1 Rev	19 nt	53.0 °C	TTAAGCTTTTCATCATCCT
5S Cl.2 Rev	17 nt	49.0 °C	AAGCTTTTCATCATCCT
5S+20 Rev	19 nt	53.4 °C	AGGTGTTAAGCTTTTCATC
PCR Primers for circular RT-PCR:			**PCR Primers for circular RT-PCR:**
4.5S-circular F	22 nt	59.4 °C	AGGCATCCTAACAGACCGGTAG
4.5S-circular R	23 nt	59.6 °C	TCCACTTGACACCTATCGTAATG
5.8S-circular F	17 nt	51.0 °C	CGCCCGAAGCCATTAGG
5.8S-circular R	18 nt	52.6 °C	CGATGGTTCACGGGATTC
5S-circular F	19 nt	54.2 °C	TAAACTCTACTGCGGTGAC
5S-circular R	19 nt	54.6 °C	CAAGTTCGGGATGGATTGG
linker mod	22	58.6 °C	ATCGTCACAACAAATGGCATC-ddC
linker REV	21 nt	57.2 °C	GATGCCATTTGTTGTGACGAT
5S linker FOR	19 nt	54.2 °C	ACCAATCCATCCCGAACTT
RNA oligonucleotides for ERL1 *in vitro* assays:			
21/2 for	21 nt		UUCCAUGGCCAACACUUGUCA
21/2 rev	21 nt		ACAAGUGUUGGCCAUGGAACA

6. Supplements

(a)

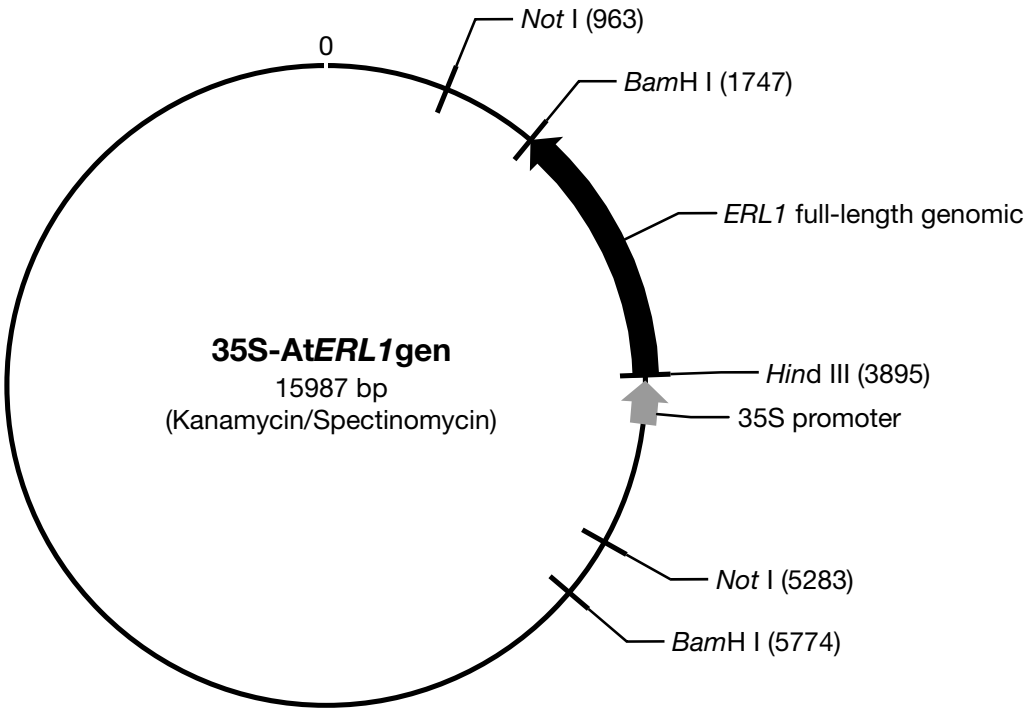

(b)

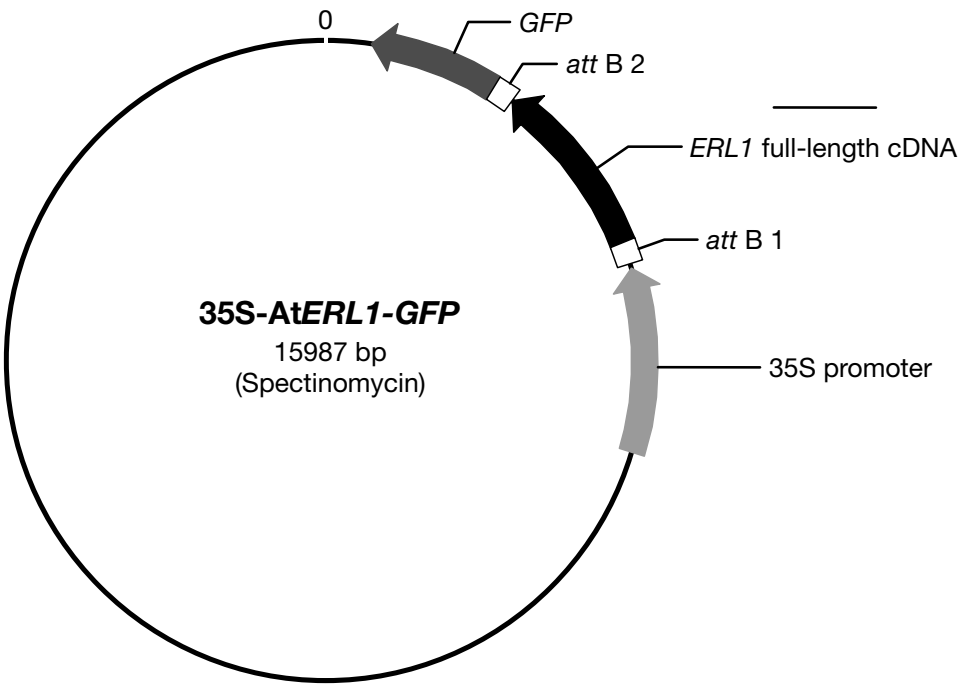

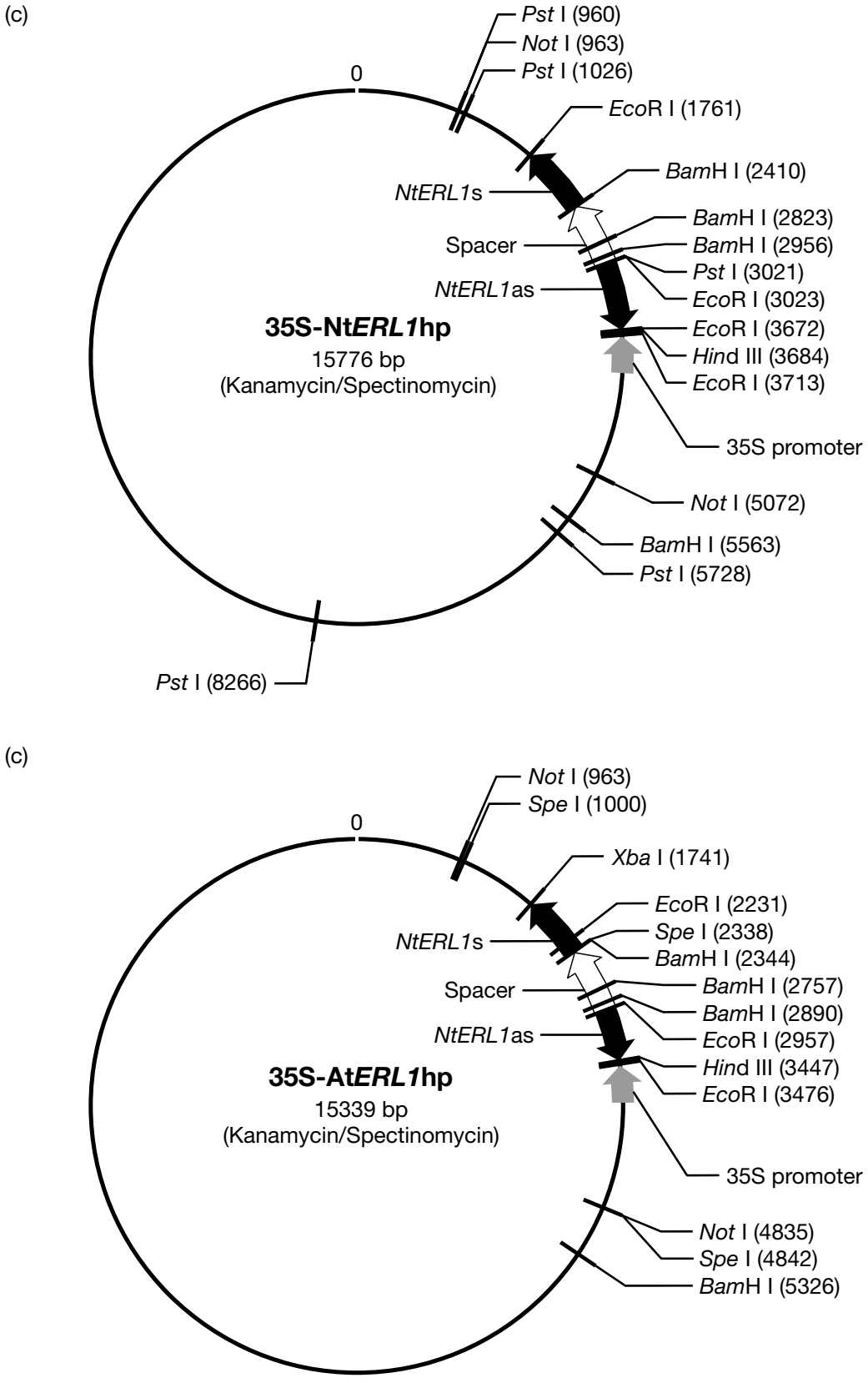

Figure S6.1 Maps of plasmid vectors used during this work. **(a)** 35S-At*ERL1*gen for overexpression of full length *Arabidopsis ERL1* (genomic). **(b)** 35S-At*ERL1-GFP* for the expression of carboxy-terminally *GFP*-tagged *Arabidopsis ERL1*. **(c)** 35S-Nt*ERL1*hp for RNAi-mediated suppression of *Nicotiana ERL1*. **(d)** 35S-At*ERL1*hp for RNAi-mediated suppression of *Arabidopsis ERL1*.

dispensed into 100 µL aliquots. The aliquots of competent *A. tumefaciens* cells were quick-frozen in liquid nitrogen and stored at -80 °C.
Thus prepared cells remained competent for heat-shock (*E. coli*) and freeze-thaw (*A. tumefaciens*) transformation for several months when stored at -80 °C.

6.2.3. Transformation of chemically competent bacteria

For the heat-shock transformation of chemically competent DH5α® cells 50 µL of compentent cells were thawed on ice and mixed with the appropriate amount of DNA to be transformed, the actual amount of DNA being dependent on the specific reaction setup. The bacteria/DNA mixture was incubated on ice for 20 minutes, incubated in a 42 °C waterbath for 30 seconds, and quickly chilled on ice. After 2 minutes incubation on ice, 250 µl of room temperature LB were added, followed by 1 h incubation with vigorous shaking at 250 rpm (37 °C). Subsequently, the transformed bacteria were spread on a selective LB-agar plates and incubated over night at 37 °C.
Competent cells of *A. tumefaciens* were transformed using the freeze-thaw method (Höfgen and Willmitzer, 1988) with few modifications. Competent *A. tumefaciens* cells were thawed on ice and mixed with 1 µg of the plasmid to be transformed. After 10 minutes incubation on ice, the bacteria/DNA mixture was quick-frozen in liquid nitrogen and incubated therein for 1 minute. Afterwards the cells were incubated in a waterbath at 37 °C for 10 minutes, followed by the addition of 250 mL LB medium. The cells were then incubated shaking at 250 rpm and 28 °C for 4 h and subsequently plated on LB/rifampicin plates containing appropriate selective antibiotics. After 2 days incubation at 28 °C in the dark, 10-100 colonies can be expected on average, which constitute transformed *A. tumefaciens* that can be used to inoculate 5 mL starter cultures.

6.2.4. Plasmid preparation

Plasmid preparations (mini scale) were performed using a classical alkalyic lysis protocol (Sambrook and Russel, 2001). For large-scale plasmid preparations the

NucleoBond® Xtra Midi Kit by Machery-Nagel was used according to the manufacturer's specifi-cations.

6.2.5. Determination of nucleic acid concentrations

Nucleic acid concentrations were determined using a NanoDrop® ND-1000 spectrophotometer following the manufacturer's instructions and using the appropriate modules for DNA or RNA measurements in the NanoDrop® software.

6.2.6. Cleavage of dsDNA with restriction endonucleases

Site-specific cleavage of dsDNA was achieved by treatment with restriction endonucleases. All restriction enzymes used in this work were purchased from Minotech or New England Biolabs and used in the reaction setups and buffer conditions recommended by the manufacturers. Typically 1 µg of DNA was cleaved by incubation with 1 u of a respective restriction enzyme at 37 °C for 1 h. If necessary, enzyme concentrations and incubation times were adjusted empirically to facilitate efficient cleavage.

6.2.7. Polymerase chain reaction

A typical PCR reaction for the amplification of a DNA fragment contained specific forward and reverse primers at 0.5 µM each, PCR reaction buffer at 1x concentration, $MgCl_2$ at concentrations of 1.5-2.5 mM, 200 µM of each deoxyribonucleotide in a dNTP mix, 0.5-2 u *Taq* polymerase, and empirically determined amounts of template DNA in 25-50 µL reactions.

Thermocycler programs for each reaction had to be determined empirically. In general, PCR programs comprised initial template denaturation for 5-10 minutes, followed by 25-35x repeated cycles of denaturation (30 seconds at 95 °C), annealing (45-60 °C,

depending on primer T_m values and applications), and extension (30 seconds per kb of DNA to be synthesised at 72 °C). A final 5-minute extension step at 72 °C was added to finalise each PCR program. Special applications or the use of speciality polymerases may require deviations from the standard protocol.
PCR primers were designed using the Oligo® Primer Analysis Software (Version 6.67), and primer T_m values were calculated using the EazyPrimer™ primer design utility found at http://www.cybergene.se/EazyPrimer.htm.

6.2.8. Agarose gel electrophoresis

Gels with an agarose concentration of 0.6-2.5 % (w/v) were prepared in 1x TAE containing 5 µg ethidium bromide per 100 mL of agarose solution. Gels were run in 1x TAE running buffer at 20-100 V depending on gel size and application. The optimal running times for each gel were determined empirically. DNA/RNA bands were visualised using a Herolab U T-28 MP gel documentation system.

6.2.9. Ligation of DNA fragments

Standard ligation reactions were performed by incubating restriction enzyme-cut vector and insert DNA fragments at a ratio of 3:1 with 1 u T4 DNA ligase and ligase buffer at 1x concentration at 16 °C for 1 h (10 µL reaction volume), followed by heat-shock transformation of competent DH5α® cells. Typically 5 µL of a ligation reaction were used for transformation. The remaining 5 µL were incubated over night at 4 °C as a backup.

6.2.10. DNA sequencing

All sequencing reactions were performed by an internal sequencing service at the Institute of Molecular Biology & Biotechnology, Heraklion, Greece.

6.2.11. cDNA synthesis by reverse transcription

cDNA was synthesised using gene-specific primers (compare Table S6.1) and the PrimeScript™ RT-PCR kit (TaKaRa) according to the manufacturer's protocol.

6.2.12. *in vitro* transcription

in vitro transcription was utilised to produce 5.8S, 5S, and 4.5S rRNA and specific processing intermediates thereof for use in *in vitro* ERL1 binding and cleavage assays.
To this end 1 µg of T7 promoter-containing dsDNA served as the transcription template in 50 µL reactions containing 1x T7 RNA polymerase reaction buffer, 10 u RNase inhibitor, 2 mM of each ribonucleotide in an NTP mix, 10 mM DTT, and 250 u T7 RNA polymerase. In practice DNA template, T7 reaction buffer, RNase inhibitor, NTP mix, and DTT were combined in 45 µL water, and this mixture was incubated at 37 °C for 1 h for equilibration. Subsequently, 5 µL T7 RNA polymerase (50 u/µL) were added, and the final reaction mixture was incubated at 37 °C for 2 h, followed by the addition of 1 µL DNase I and incubation at 37 °C for 15 minutes. Thus prepared RNA was purified by classical phenol/chloroform extraction and isopropanol precipitation. Finally the *in vitro*-transcribed RNA was resuspended in 50 µL water, and the RNA concentratrion was determined spectrophotometrically.

6.2.13. Purification of recombinant ERL1 protein

Recombinant ERL1 protein was expressed in *E. coli* strain JM109(DE3) plyse. For this purpose the full and mature (*i.e.* lacking the chloroplast leader sequence) *ERL1* cDNA sequences were cloned in-frame in the vector pET-15b providing an amino-terminal 6xHis-tag. For expression, respective cells were grown in LB containing 100 µg/mL carbenicillin to an OD_{600} of 0.6-0.8 at 37 °C. Protein expression was then induced by addition of IPTG to a concentration of 0.5 mM, and the subsequently ERL1-expressing bacteria were collected after incubation at 37 °C for 3 h (2500x g, 20 minutes, 4 °C).

The cells were resuspended in protein purification buffer and lysed with 1 mg/mL lysozyme on ice for 1 h. After lysis bacterial debris was pelleted at 15000x g for 10 minutes (4 °C), and the cleared recombinant ERL1 protein-containing supernatant was loaded on a Ni-NTA column equilibrated with protein purification buffer. After 2 washes with protein purification buffer containing 20 and 30 mM imidazole, respectively, the recombinant protein was eluted three times with protein purification buffer containing 400 mM imidazole.
This work was performed by Stephanie Eckhardt and Ioannis Vlatakis as part of their Master projects. For additional details please refer to the Master Thesis "Functional Analysis of ERI-1" by Stephanie Eckhardt, Kassel University, March 2006.

6.2.14. *in vitro* binding and cleavage assays for recombinant ERL1

For *in vitro* assays to determine ERL1 binding and cleavage specificities, approximately 50 fmol of radiolabelled synthetic siRNAs or *in vitro*-transcribed small ribosomal RNAs were incubated with different amounts of recombinant ERL1 protein in ERI-1 *in vitro* assay buffer [10 mM Tris (pH 8), 27 mM KCl, 0.5 mM $MgCl_2$, 0.5 % glycerol (Iida et al., 2006)] at room temperature. Suitable incubation times had to be determined empirically, and after incubation the samples were run on 6-20 % PAA gels (depending on the respective experimental requirements). Finished gels were fixed with acetic acid, sealed in plastic bags, and directly exposed to X-Ray films.
This work was performed by Stephanie Eckhardt and Ioannis Vlatakis as part of their Master projects. For additional details please refer to the Master Thesis "Functional Analysis of ERI-1" by Stephanie Eckhardt, Kassel University, March 2006.

6.3. Supplementary results

The following summarised results should be considered as preliminary data derived from *in vitro* assays with the aim to elucidate specifities of ERL1 for binding and cleavage of a variety of substrates. These results have been obtained by Stephanie

Eckhardt and Ioannis Vlatakis during their Master projects at the Institute of Molecular Biology & Biotechnology in Heraklion, Greece. For detailed descriptions of these results please refer to the Master Thesis "Functional Analysis of ERI-1" by Stephanie Eckhardt, Kassel University (March 2006) and the Master Thesis "*In vitro* μελετη της AtEri: καθαρισμός, απομόνωση και προσπάθεια ανεύρεσης του φυσικού υποστώματος της" by Ioannis Vlatakis, University of Crete, (June 2009).

6.3.1. Recombinant ERL1 fails to bind and process siRNAs and ribosomal RNAs *in vitro*

A variety of experiments have been performed with the aim to characterise biochemical properties of recombinant ERL1 protein in small RNA binding and cleavage. To this end electrophoretic mobility shift assays have been performed with synthetic siRNAs and *in vitro*-transcribed small ribosomal RNAs as substrates. Specifically, increasing amounts of recombinant ERL1 protein were incubated with radiolabelled 21 nt siRNAs, mature versions of 5.8S, 5S, and 4.5S rRNAs, as well as known 3'-elongated processing intermediates of 5S and 4.5S rRNAs. Under the conditions tested neither full-length nor mature (*i.e.* chloroplast leader-less) ERL1 were able to bind and shift any of the respective substrates.

Similarly, no processing activity could be observed upon incubation of increasing amounts of recombinant full-length or mature ERL1 with the abovementioned substrates.

Thus far it could not be determined, whether the cause for the unability of recombinant ERL1 to bind or process the tested substrates are unsuitable reaction conditions or non-functional recombinant protein due to technical reasons arising from the purification procedure. It also cannot be excluded that ERL1 requires the presence of a protein partner for functionality or specific co-localisations. Determining conditions for ERL1 that reconstitute its physiological functionality *in vitro* is one of the major challenges that is likely to yield interesting future insights into the biochemical properties of this versatile 3'-5' exonuclease.

6. Supplements

6.4. Supplementary references

Höfgen, R., and Willmitzer, L. (1988). Storage of competent cells for *Agrobacterium* transformation. Nucleic Acids Res **16,** 9877.

Iida, T., Kawaguchi, R., and Nakayama, J. (2006). Conserved ribonuclease, Eri1, negatively regulates heterochromatin assembly in fission yeast. Curr Biol **16,** 1459-1464.

Inoue, H., Nojima, H., and Okayama, H. (1990). High efficiency transformation of *Escherichia coli* with plasmids. Gene **96,** 23-28.

Sambrook, J., and Russel, D.W. (2001). Molecular Cloning - A Laboratory Manual. (New York: Cold Spring Harbor Laboratory Press).

Künstlers Abendlied

Ach, daß die inn're Schöpfungskraft
Durch meinen Sinn erschölle!
Daß eine Bildung voller Saft
Aus meinen Fingern quölle!

Ich zittre nur, ich stottre nur
Und kann es doch nicht lassen;
Ich fühl', ich kenne dich, Natur,
Und so muß ich dich fassen.

Bedenk' ich dann, wie manches Jahr
Sich schon mein Sinn erschließet,
Wie er, wo dürre Heide war,
Nun Freudenquell genießet:

Wie sehn' ich mich, Natur, nach dir,
Dich treu und lieb zu fühlen!
Ein lust'ger Springbrunn, wirst du mir
Aus tausend Röhren spielen.

Wirst alle meine Kräfte mir
In meinem Sinn erheitern,
Und dieses enge Dasein hier
Zur Ewigkeit erweitern.

Johann Wolfgang v. Goethe

In guter Erinnerung